Ca' Foscari
University
of Venice

Master's Degree programme

in **Environmental Sciences**

Final Thesis

Obtaining added-value products through ammonium nitrogen recovery with gas-permeable membrane and chain elongation bioprocesses

Supervisor
Ch. Prof. Francesco Valentino

Assistant supervisor
Ch. Prof. Joan Dosta
Ch. Prof. Marco Gottardo

Graduand
Vittorio Pelizzaro
Matriculation Number 879937

Academic Year
2023 / 2024

UNIVERSITAT DE BARCELONA

This thesis was developed in partnership with the University of Barcelona as part of Erasmus+ internship programme.

Index

1. Introduction

The 2030 Agenda of the United Nations is a keystone for achieving the goal of a sustainable development. The integration of sustainable development goals (SDGs) into the European Union policies with the European Green Deal has defined a bright vision towards an ecological transition and the implementation of a circular economy. Become crucial expand the current perspective by considering approaches that take into account the entire life of products and substances, closing usage cycles, maximising the value of materials and eliminating waste.

Closing the carbon and nitrogen element cycles is part of a systemic thinking that starts with improving the regeneration of resources in a sustainable way. The conscientious utilization of the biomass become a priority to implement an holistic way of thinking (UN 2030 Agenda, 2015).

Carbon and nitrogen are an essential element for all living organisms due to its role in the vital functions meanwhile nitrogen and carbon pollution has become a critical environmental issue that arises primarily from the anthropic activities (IEA Emissions Factors, 2023). In this view, the production of carbon-biobased platform molecules and the recovery of nitrogen fertilisers is then an integral part of a circular approach.

Nowadays most carbon-based substances are produced from non-renewable sources, with high global greenhouse gas emissions and, very often, upper energy consumption that contributed roughly 70% of their carbon footprint (Vom Berg et al., 2022). Likewise, the main production of nitrogen-based fertilizers is through Haber-Bosch process, which is energy-intensive and environmentally unfriendly since it represents 1% of the world's energy consumption and 2% of carbon dioxide global emissions (Bartels et al., 2008).

Various carbon compounds contribute significantly as greenhouse gas (CO_2, CH_4) to rising global temperatures and many derivatives cause problems such as contamination, toxicity and non-biocompatibility (Bertasini et al., 2023). Nitrogen compounds, especially ammonia (NH_3) and ammonium ions (NH_4^+), are significant pollutants in aquatic systems, causing eutrophication, which leads to excessive growth of aquatic plants, deterioration of water quality, and threats to aquatic biodiversity (Pyra et al., 2023).

Wasted carbon and nitrogen is accumulated in wastewater being the main sink of this nutrient (Shrestha et al., 2015). An important dissipation of these two elements is notable in the organic

waste generated in urban areas that is considered a high-quality resource due to its biodegradability and potential substance recovery (Zhang et al., 2022).

The implementation of circular economy schemes in the urban-agro-industrial sector requires technologies that allow combined production of biomolecules and the recovering of ammonium nitrogen, rather than removing it. The use of these sources through chemical-engineering processes could represent a solution to mitigate impact in the environment and obtain products while contributing to meet the growing demand for platform-molecules and fertilizers (Zhang et al., 2021).

As an alternative to current treatments for different kinds of organic waste, anaerobic digestion (AD) and fermentation processes coupled with ammonium recovery allow biomass to be valorised by achieving ammonium recovery and simultaneous obtain value products such as volatile fatty acids (VFAs) (Peña-Picola et al., 2024). The ammonium recovery from waste streams plays a central role, as it enables ammonium sulphate ($(NH_4)_2SO_4$) based fertilisers to be obtained while obtaining a liquid effluent rich in VFAs and with high C/N ratio, useable in subsequent processes. The gas-permeable membrane (GPM) technology has gained increasing interest to recover total ammonia nitrogen (TAN) from waste streams due to its simple operability, little energy consumption and the generation of a valuable fertiliser product (Serra-Toro et al., 2022).

Biological VFAs are short-chain fatty acids (SCFAs) and are considered the “building blocks” to produce multiple bio-based products, such as medium-chain fatty acids (MCFAs), that have a wide range of applications such as in the production of bioplastics and biopolymers, bioenergy, pharmaceutical, petrochemical and chemical industries (Wu et al., 2021). One promising biological process to synthetize MCFAs is “chain elongation”, an anaerobic pathway in the fermentation process with the presence of an electron donor, usually ethanol or lactic acid from biological origin, where VFAs are converted into longer fatty acids (Battista et al., 2024).

The focus of this study is to conceptualise an integrated process for obtaining high-value commercial products with ammonium removal and $(NH_4)_2SO_4$ fertiliser recovery from different wastewaters, in tandem with liquid concentration. VFAs in the liquids could be subsequently used to produce high-value MCFAs, particularly caproic acid, via chain elongation in a fed-batch process. The suitability of this integrated process for resource recovery (carbon-based products and ammonium nitrogen valorisation) as an alternative to traditional processes, mainly focused on organic matter and nitrogen removal, will be investigated in this study.

1.1 Ammoniacal nitrogen recovery

Various methods have been developed to remove or recover nitrogen from waste streams, including biological nitrification in combination with denitrification (N/DN) and physico-chemical methods (Xiang et al., 2020). Other methods include ammonia capture via carbon-based and mineral adsorbents (Perdigão-Lima et al., 2024), struvite precipitation (Astals et al., 2021), ammonia stripping (Chen et al., 2023), electrodialysis and microbial electrolysis cells (Ye et al., 2021), membrane distillation (Zarebska et al., 2014), membrane concentration and ion exchange (Sheikh et al., 2023) and gas-permeable membrane (GPM) technology (Riaño et al., 2021).

Biological N/DN process, where ammonia is converted into inert nitrogen (N_2), require high hydraulic and solids retention times and nitrification needs abundant supply of oxygen (O_2) by addition of air which represents an energy-consuming process. Greenhouse gas emissions (NO_x) and dissipation of nitrogen in the atmosphere results in large footprints. These processes do not allow the recovery of nitrogen in a usable form, and they represent a loss of ammonia, a valuable building block for the fertiliser and chemical industry (Ronan et al., 2021).

Physicochemical methods offer a range of alternatives with several efficiency and practicality. Ammonia stripping is technique that involves the extraction of free ammonia at high pH levels, followed by its capture in an acidic solution to produce an ammonium salt. This method boasts high recovery efficiency but is hindered by significant reagent consumption and space requirements (Noriega-Hevia et al., 2023). Struvite crystallization is another method that recovers nitrogen by precipitating it with magnesium and phosphate to form magnesium ammonium phosphate. This process requires the equimolar presence of all reactants, which could limit its economic feasibility (Aguilar-Pozo et al., 2023). Ion exchange processes, which replace ammonium ions in wastewater with other ions, are also used but often involve high operational costs and complexity (Sheikh et al., 2023). Accordingly, there is an urgent need to develop new technologies that enable the recovery of TAN whilst preventing the presence of other contaminants that may compromise their quality.

Selective membranes represent an emerging technology to recover TAN due to its capacity to operate effectively under various operating conditions and the opportunity of generation of valuable product (Darestani et al., 2017). Numerous strategies for membrane technology are being researched, among them, gas-permeable membrane (GPM) contactors stand out for simple employment, little energy requirements and high efficiency and selectivity (Serra-Toro et al., 2024).

GPM facilitate the transfer of ammonia gas through a hydrophobic membrane to an acidic solution located on the other side of the membrane, enabling the recovery of nitrogen in a usable form such as ammonium salt, usually $(NH_4)_2SO_4$. This method can operate at ambient conditions and offers an attractive solution with low energy demands and high product quality (Darestani et al., 2017).

A multicriteria-based analysis of some of the principal technologies, concluded that GPM is the most suitable technology to recover TAN from several liquids tested (Delanka-Pedige et al., 2021). High nitrogen recovery efficiencies have been obtained using GPM for the treatment of waste streams including municipal wastewaters, municipal organic wastes and agricultural or farming effluents (Beckinghausen et al., 2020; Noriega-Hevia et al., 2023; Serra-Toro et al., 2024).

However, some challenges such as membrane fouling, wetting or water passage, and the consumption of chemical additives to maintain pH levels during the process remain significant obstacles to the widespread adoption of GPM technology (Licon Bernal et al., 2016). Despite these challenges, continuous advancements in membrane materials and process optimization hold promise for overcoming these barriers and enhancing the efficiency and economic feasibility of GPM for nitrogen recovery.

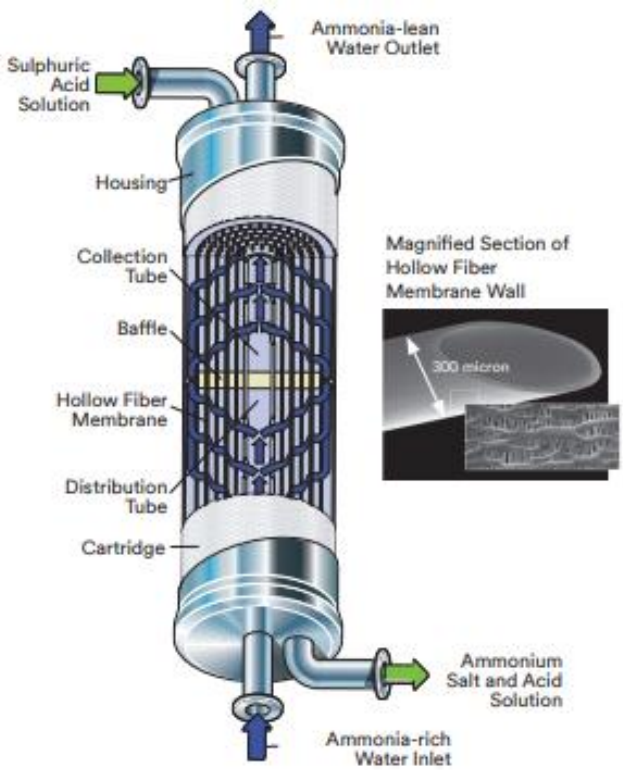

Figure 1: Scheme of a gas-permeable membrane unit for nitrogen recovery.

1.2 Gas-permeable membrane (GPM)

The GPM process for nitrogen recovery consists of circulating nitrogen-rich effluent (feed solution) through one side of a selective membrane whilst circulating an acidic trapping solution (diluted H_2SO_4) on the other side of the membrane. Membranes are typically micro-perforated or nano-perforated designed to facilitate the diffusion of free NH_3 and other neutral and non-hydrated species while limiting the diffusion of charged species, including NH_4^+ ion (He et al., 2020).

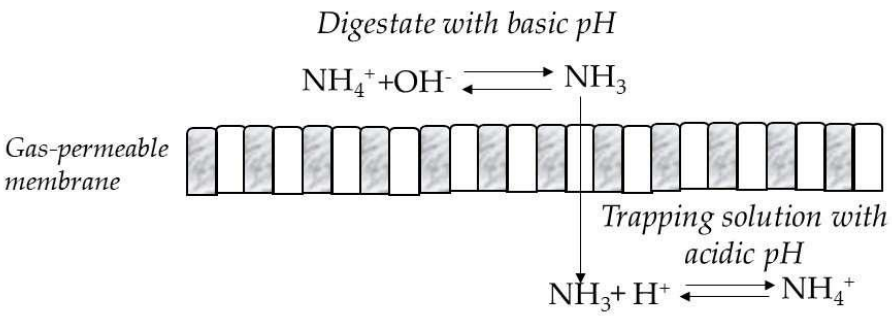

Figure 2: Diffusion of free NH_3 on gas-permeable membrane.

An engineering important factor is quantifying the mass transfer between the two phases formed on the surface of the membrane: immiscible liquid phases - outside the membrane - and miscible (partially) liquid pashes - inside the membrane - (Liu et al., 2024). Mass transfer values allow to estimate what will happen in real life situations and design equipment based on these specific requirements. To evaluate the ammonia flux through the GPM the most widely parameter is the mass transfer coefficient (K_m) that represent the diffusion rate constant that relates the mass transfer rate, mass transfer area, and concentration change as driving force (Vecino et al., 2019). The K_m parameter expressed in terms of metres per second (m/s) allow to quantify the ammonia transfer under specific conditions.

To determine the K_m a physicochemical calculation model can be used, considering that:

- the hydrophobic membrane is only permeable to NH_3;
- the pH is constant and the acid-base equilibrium is maintained for feed and trapping;
- NH_3 losses by volatilisation are negligible;
- the volumes of the feed solution (V_f) and the trapping solution (V_t) remains constant.

NH_3 transport is described by Fick's law that considers previous point of ideal diluted solution for and no interferences amongst solution components. The driving force for ammonia mass transfer is the concentration gradient of unionised ammonia between the feed and the trapping solution (Al-Juboori et al., 2023). Water diffusion through the membrane should not be observable but as when high differences in the water vapour pressure on both sides of the hydrophobic membrane takes place, the initial and final volume of both solutions may not remain constant during the operation due to osmotic distillation.

1.2.1 Membrane contactor operational conditions

In contrast to other membrane systems, GPM are more susceptible to certain physicochemical factors and some operating parameters. Most relevant operating parameters include pH and temperature that have a significant effect on ammoniacal nitrogen speciation and impact the efficiency of the entire process (Noriega-Hevia et al., 2023).

Recovering ammoniacal nitrogen using GPM requires to operate at a feed solution pH above pKa of the NH_4^+/NH_3 equilibrium so is needed to increase the feed pH up to values to displace this acid-base equilibrium. This pH control is important to maintain the driving force across the membrane and can be accomplished either through the inclusion of an alkaline reagent or by aeration. An acidic solution (usually at pH ≤ 2) on the other side of the membrane captures the NH_3 in the form of NH_4^+ (i.e. ammonium sulphate), which could be valorised as fertiliser (Serra-Toro et al., 2024).

Without pH regulation, TAN recoveries between 57-66% have been reported for slurry (Garcia-González et al., 2015). Nevertheless, from literature it is suggested a moderate alkaline pH values (above 9.0) to prevent inorganic fouling by precipitates on the membrane and to have lower reagent consumption per mole of TAN (Serra-Toro et al., 2022).

However, other operating parameters could also impact the efficiency of the process. One operating parameter, which is a subject of this study, is the volume of trapping solution required to treat a certain volume of feed solution and its replacement frequency (Rizzioli et al., 2023). It is critical to obtain a solution with a significant amount of nitrogen salt, without compromising attention to gradient concentration, to achieve better marketability and market price. Despite the successful results reported in literature, further research, like this one, is required to optimise GPM technology operating conditions and control strategies to find a compromise solution between transfer rates, reagent consumption, and membrane lifespan.

1.2.2 Fouling, wetting and water transfer

Membrane fouling is caused by the deposition of suspended particles or colloids, organic macromolecules, sparingly soluble inorganic compounds, microorganisms, or their mixtures on or inside the membrane (She et al., 2016). Membrane fouling not only reduces the permeate water flux, liquid recovery, permeate quality, but also causes shortened membrane life and increased operating cost (Dutta et al., 2022). Fouling can take place at different locations of the membrane and could be divided into external and internal fouling (see Fig. 3). Depending on orientation, the external fouling is related to the deposition of flocs/particles onto the membrane surface and formation of a "cake layer". When the flocs have a relatively small size, they could enter the membrane pores, be adsorbed on the pore walls or be retained. The deposit on the back side leads to "pore plugging". Internal fouling scenario can be observed when flocs will continue to deposit on the outer surface of the porous support in addition to internal pore clogging. If the feed water contains a mixture of foulants with different sizes, both external fouling and internal fouling may occur (She et al., 2016).

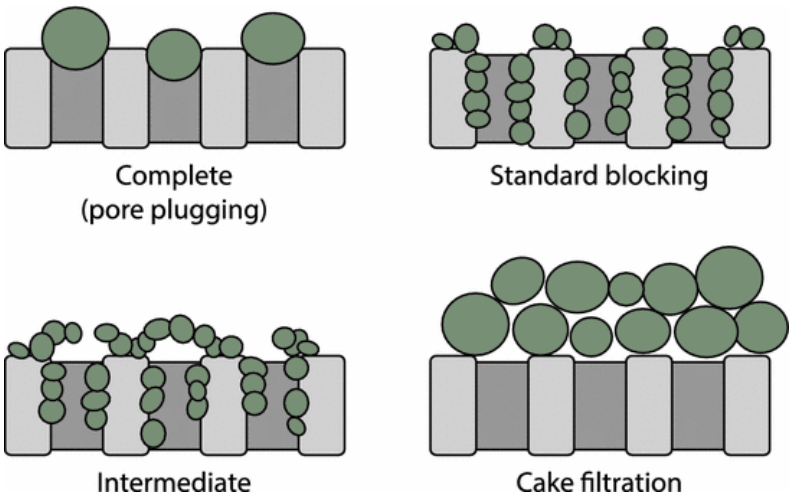

Figure 3: Different types of fouling that may arise on the surface of the membrane.

The main effects of fouling on gas permeable membranes are the decrease in the K_m and the trapping solution contamination (Ladewig et al., 2017). Also fouling obstructs the nanopores reducing the hydrophobicity, which hinders ammonia transport and limits the process scalability.

Clogging problem is mainly related to the type of flowing liquid, so more exhaustive pre-treatment of the effluent is required (filtration and centrifugation) to remove suspended solids. Not to involve in industrially complex treatments (liquid-liquid or solid-liquid separations) should be consider. An

internal physical or physical/chemical clean-up could be adopted. Physical backflushing with water and reversing the flow remove reversible fouling (cake layer from OFWSM supernatant and fermented). Physico-chemical cleaning protocols using chemical reagents, such as bases (NaOH or KOH) and acids (HCl) and a constant flushing are used to remove hard fouling (pore plugging from ABPs liquid). Chemical agents used together physical means improve effectiveness and reduce chemical loading (Z. Wang et al., 2014). The chosen method was that do not cause membrane degradation/damage while maintaining efficiency.

Membrane pore wetting involves a complex physical and chemical interactions. The non-wetting liquid facing the hydrophobic membrane forms a fixed interface at the pore. High surface tension (capillary pressure effect) not allow liquid to enter (Rezaei et al., 2018). When the surface tension decreases by the entry of air, pressures balance is overwhelmed, and the liquid begins penetrating the pores (Ladewig et al., 2017). Once wetting takes place, the membrane starts to lose its hydrophobicity locally, leading to continuous water bridging.

The main effects on membranes are the decrease in the K_m, small molecules diffusion and trapping solution dilution (Rongwong et al., 2020). A clean-up and minimise the concentration gradient between both solutions is adopted to easily bypass this problem.

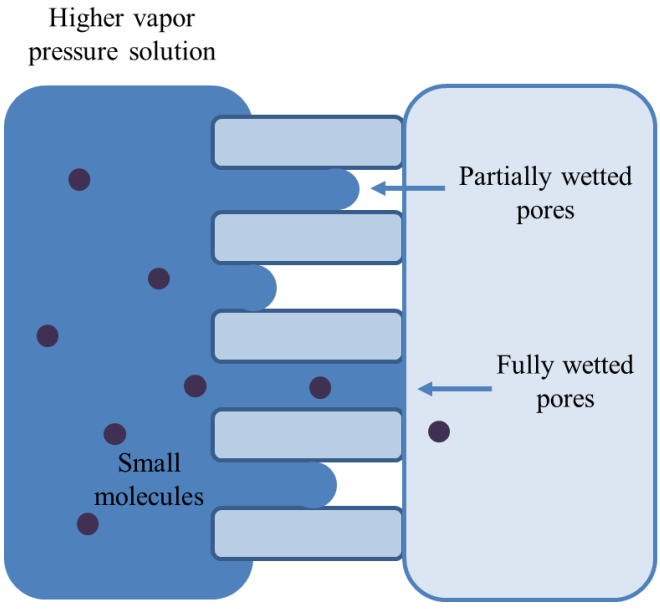

Figure 4: Wetting effect that may arise on the surface of the membrane.

Water passage occurs when some water can penetrate a portion of the membrane, diffuse through the pores and adds a mass transfer resistance from the wetted phase to the membrane inside. This

phenomenon occurs due to the capillary condensation of water or other volatile species, or the high vapor pressure difference between the wastewater and stripping fluid has exceeded a value, known as the penetration pressure (Rezaei et al., 2018).

The main effects on membranes are the water molecules diffusion and the dilution of the trapping solution. The solutions adopted are increase the hydrophobicity of the membrane and minimise the concentration gradient between both solutions. However, both present difficulties. Increasing the hydrophobicity involves a technical modification of the chemical-physical properties of the membrane, which is currently not available on the market. Decreasing the gradient difference between the two solutions has the disadvantage that the solution concentration in the trapping is too dilute and therefore not commercially viable (Yao et al., 2020). This problem is critical and is one of the subjects of these studies.

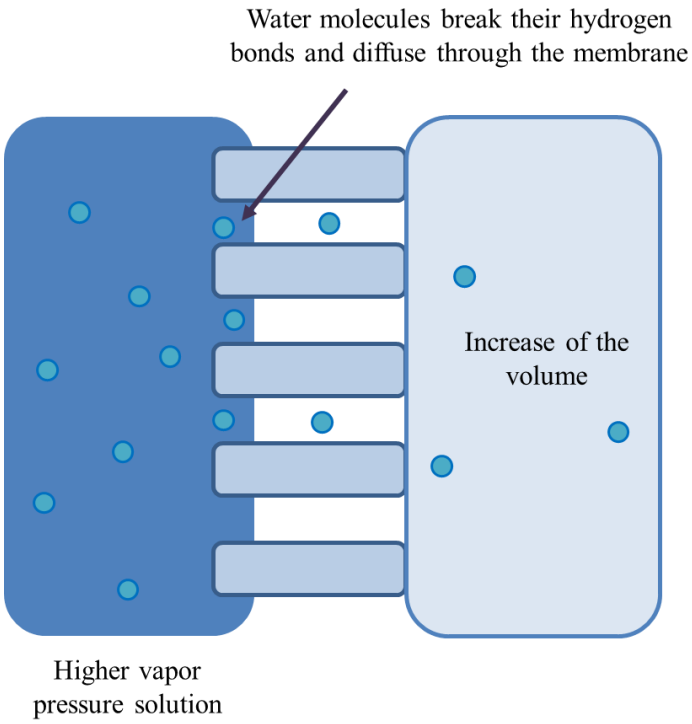

Figure 5: Water transfer effect that may arise on the surface of the membrane.

1.3 Forward osmosis membrane (FO)

Membrane filtration technology is an effective and compact system used in sewage treatment to treat water for numerous reuse or recovery applications. Different kinds of membranes and methods

have been investigated. Microfiltration (MF) and ultrafiltration (UF) in aerobic and anaerobic membrane bioreactors (MBRs) have been employed for sludge separation and pressure-driven membrane processes such as reverse osmosis (RO) and nanofiltration (NF) have been used for tertiary treatment (Blandin et al., 2020).

Forward osmosis (FO), led by the osmotic pressure gradient throughout the membrane, has received interest for desalination as it is lower power consuming than RO. Important issues such as water scarcity provide reason to sewage reuse and FO membrane allow to shift focus into integrated wastewater treatment with important advantages (Morrow et al., 2018). This application enables in organic effluents the bioproducts concentration (such as VFAs) meantime obtains clear water. The process requires the use of a divalent salt that could be regenerated to produce water and reconcentrate the new salt solution. VFAs concentration as saleable by-products and water recovery provide interesting income-generating opportunities (Singh et al., 2019).

FO operability is given by a physical-chemical mechanism where the solute concentration gradient (or osmotic pressure differential $\Delta\pi$) is the driving force between liquids divided by a selectively permeable membrane. Suspended solids, mainly dissolved molecules or ions, cannot pass through the membrane and concentrate in the feed solution. Water permeates through the membrane from the lowest solute concentration (feed solution) to the highest solute concentration (draw solution) (Blandin et al., 2019). Considerable interest had been shown for aquaporin biomimetic membrane type to investigate the FO of sewage using a divalent salt solute as the draw solution.

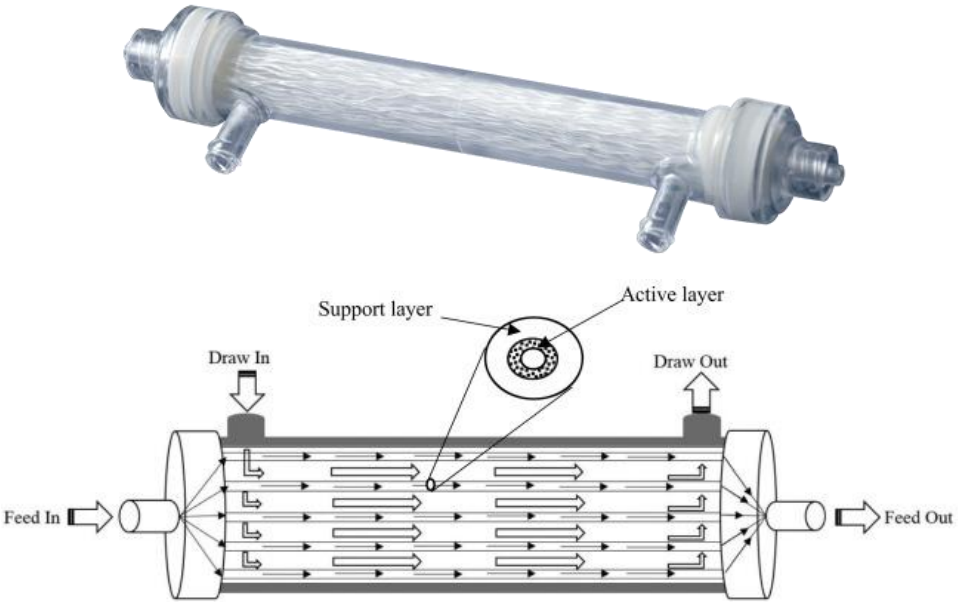

Figure 6: Forward osmosis membrane image and scheme of the inner membrane layers.

The choice on the type of divalent salt for the draw solution is given by the consideration of the osmotic pressure affecting the efficiency of the process and execution time. At the same concentration, the widely used salt sodium chloride (NaCl) has lower osmotic pressure than magnesium chloride ($MgCl_2$) or other types of divalent salts. Compared to most other salts used to prepare draw solutions, $MgCl_2$ is cheaper in the global market and industrial grade $MgCl_2$ is available at a low cost (Singh et al., 2019). Furthermore, the use of $MgCl_2$ as a draw solution could be advantageous because, since the reverse saline flow leading to increase salinity in the feed cannot be completely avoided, it would combine with the nutrients in the concentrated slurry to form the fertiliser magnesium ammonium phosphate (struvite). This technology provides an important dual source: salt in diluted form $MgCl_2$ in water recovered from the effluent (draw solution) or $MgCl_2$ fertilizer in struvite from in the concentrated sewage (feed solution).

Depleted $MgCl_2$ brine could be regenerated by RO to obtain clean water and reconcentrate salt, reusable in the FO process. At the same concentration of other salts, with $MgCl_2$ lower pressure for RO (higher compared to salts) are used (Piadeh et al., 2024). The main limitations of this technology are mass transfer limitations, membrane developments, fouling, rejection of trace organic contaminants, optimized draw solutions, energy aspects and potential applications (Blandin et al., 2020). Despite significant advances in membrane and modules designs and operation, applications of osmotic processes mostly remained on a pilot scale. Future research should focus on answering these challenges and consider adopting this technology in an integrated approach together with other wastewater treatments.

1.4 Anaerobic digestion and fermentation

A well-established technology for biological residues treatment, to obtain energy bioproducts (mainly CH_4 and CO_2) as well as, in some cases, fertilizers from organic waste feedstock is anaerobic digestion (AD) (Piadeh et al., 2024). AD can be divided into two metabolic phases, characterized by different microbial groups and operational conditions.

The first step is characterised by an initial biopolymers hydrolysis of polysaccharides, lipids and proteins into monosaccharides, fatty acids and amino acids (Lee et al., 2014). The presence of complex bow structures and hard cell walls make it a limiting step in the entire AD process. After molecules breaking there is the acidogenic fermentation step, with principally synthesis of organic

acids (OAs) and hydrogen accumulation. Acidogenesis phase, namely dark fermentation (DF), transform smaller organic molecules mainly into SCFAs (i.e. acetic acid, propionic acid, butyric acid, valeric acid, and caproic acid), alcohols (ethanol and methanol) and gas (CO_2 and H_2) by anaerobes bacteria activity. The final step is acetogenesis where ethanol and SCFAs are combined into CO_2, H_2, and acetate. Acetogenesis bacteria live in symbiosis with methanogenic bacteria.

The last phase is the methanogenesis (digestion) where obligate anaerobes make the conversion of acetic acid, H_2 and CO_2 into bio-methane (CH_4) and CO_2 (Micolucci et al., 2020). The stages of AD and AF (DF) are summarized in Fig. 7.

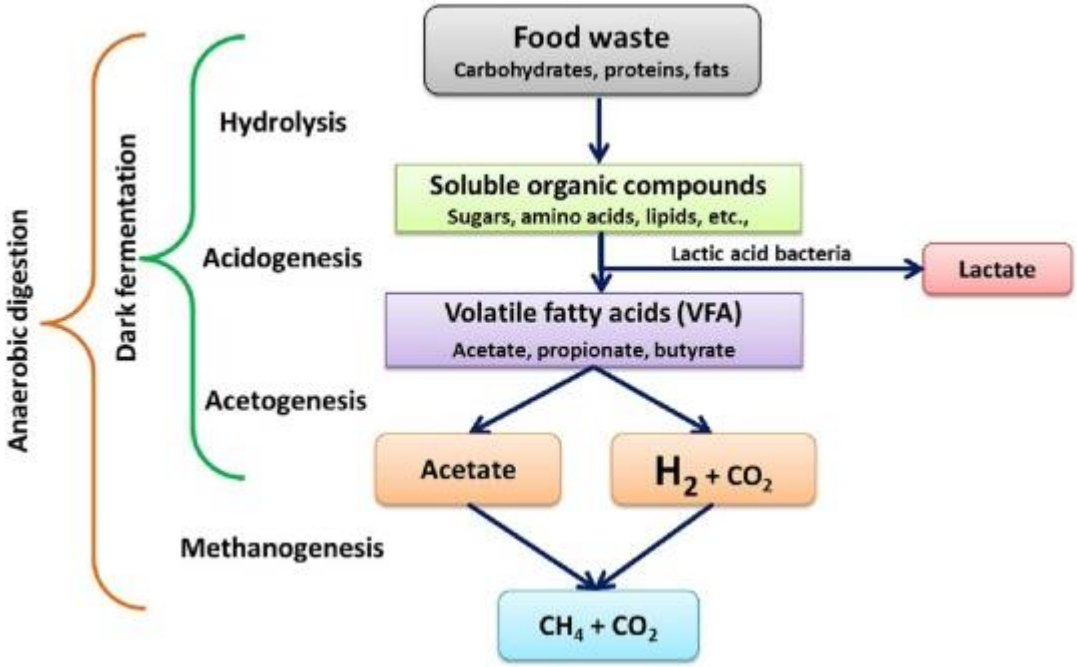

Figure 7: Anaerobic digestion and anaerobic fermentation processes.

Nowadays, AD full-scale plants are mostly focused in performing the entire digestion process for methanation and energy recovery, which however generates low revenues given by complexity and difficult operating conditions to keep. However, many other valuable products can be obtained due to the interaction of different microorganisms with distinct biochemical sign-pathways. As a result, anaerobic fermentation (AF), also known as dark fermentation (DF), process is gaining attention due to its potential of recovering more valuable products, like H_2 and VFAs (Gottardo et al., 2023).

VFAs are platform chemicals employed as building blocks for the chemical industry or precursors of chemicals in conventional organic chemistry and can be obtained via AF from the exploitation of renewable bioresources at relatively low-cost. Approximately 90% of the actual VFAs market

demand is covered by petroleum-based feedstock, with a resulting high environmental impact and costs (Ramos-Suarez et al., 2021).

For this reason, biological VFAs production form AF are becoming a trend topic in the biorefinery field investigation. The main drawback of this process, especially when thermophilic conditions are adopted, is the requirement to maintain stable conditions during the acidogenic fermentation step, keeping a pH higher than 5.0 to promote fermentation activity, but preferably lower than 7.0 to avoid the proliferation of methanogens (Gottardo et al., 2024). Various pH control strategies have been evaluated but, especially with highly putrescible feedstock like OFMSW, some weak points are shown and among these is notable the possible accumulation of ammonia (above 1.0 g/L) which negatively affected the VFAs production (Wei et al., 2021).

TAN recovery from fermentation liquids enables a better AF processing, resulting in a liquid rich in VFAs with low TAN content, which could be advantageous for several downstream processes. Few investigations have currently been focused to obtain high-value commercial products through an initial TAN recovery into fertiliser in tandem with FO to concentrate VFAs liquid output and then through chain elongation in fed-batch bioprocess produce high-value MCFAs fatty acids, particularly caproic acid.

1.5 Chain elongation bioprocess (CE)

Biological VFAs are short-chain fatty acids (SCFAs) that are considered the “building blocks” to produce multiple bio-based products, such as Medium-Chain Fatty Acids (MCFAs). MCFAs are carboxylic fatty acids with a carbon chain ranging from 6 to 12 atoms (Narisetty et al., 2023). One important MCFA is the caproic acid whose economic revenue is estimated to grow up more in near future (Research and Markets, 2023). MCFAs have a wide range of applications such as in the production of bioplastics and biopolymers, bioenergy, pharmaceutical, petrochemical and chemical industries. A promising biological process to synthetize MCFAs is the “chain elongation” (CE).

This process is an anaerobic pathway in the fermentation process with the presence of compatible electron donor, usually ethanol or lactic acid of biological origin, SCFAs are converted into longer chain carboxylic fatty acids (Wang et al., 2022).

The CE mechanism is the reverse β-oxidation, a cyclic reaction elongates by adding two carbon atoms (form acetyl-CoA molecule) per cycle to the original carbon chain while consuming reducing power.

Acetyl-CoA and the reducing power are provided suitable electron donor compounds, such as ethanol or lactate (Tarasava et al., 2022). The end products depend on the precursor VFAs: acetate [C_2] is converted to n-butyrate [C_4] and n-butyrate to n-caproate [C_6] and so on.

Ethanol is an essential reagent/substrate necessary for chain elongation that can be produced from organic waste through a biochemical conversion process or can also be converted itself into SCFAs (Roghair et al., 2018). So, in a circular economy perspective the use of ethanol, either added from other waste or already available in ethanol-containing waste stream, are fundamental to reduce the costs and the environmental impacts.

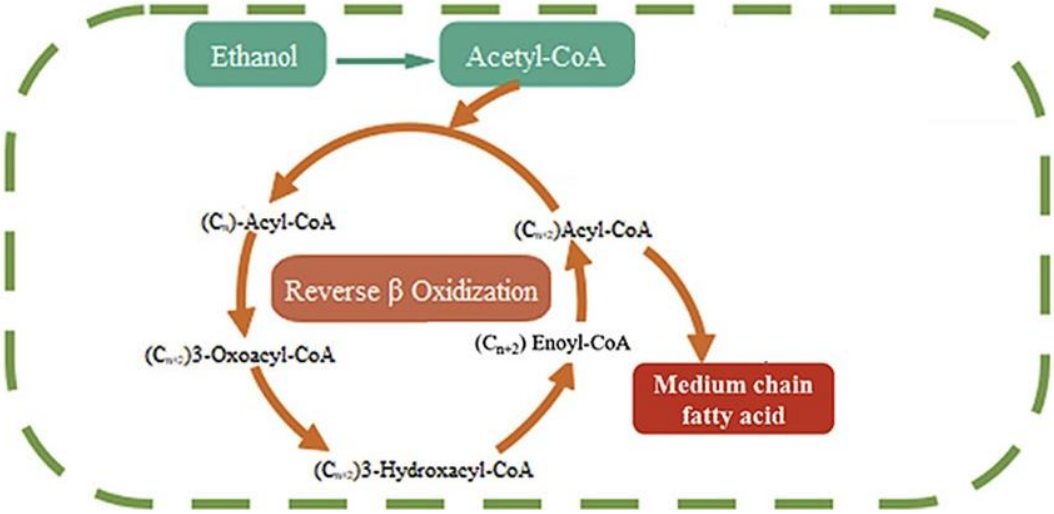

Figure 8: Chain elongation bioprocess - reverse β oxidation.

In CE bioprocess the most influencing parameter is represented by the molar ratio between the electron-donor compounds and the acetic acid (Battista et al., 2024). Adding ethanol to the mixed culture fermentation improve the process but high concentrations of ethanol inhibit the acid producing microorganisms resulting in low biomass conversions while a low concentration of ethanol reduces the yield because the substrate is not available (Quintela et al., 2024). Several works emphasized how large is this range of the optimal ethanol:acetate molar ratio. In literature, the minimum ratio between ethanol and acetic was 1:2 (Coma et al., 2016) and the maximum reported ratio between ethanol and acetic was 1:10 and sometimes higher (Spirito et al., 2018).

The pH is another important parameter affecting the CE bioprocess. Some works indicated the optimal pH range at 5.0-5.5, meaning slightly acid conditions (Candry et al., 2020), but other works indicated pH range at 6.0-7.0, close neutral conditions (Gehring et al., 2020).

The CE is likewise aided by the kind of pretreatments (alkaline, acidic, deacetylation or thermal), which are indispensable in the presence of complex substrates not available to the biosystem (Gottardo et al., 2024). Other parameters, for example the inorganic carbon concentrations, have been shown to affect the CE process (San-Valero et al., 2020). The duration of the tests (indicated as the Hydraulic Retention Time (HRT)) and the operational temperature linked to the adaptation of the microbial mass emerged as an affecting factor (Grootscholten et al., 2013). The HRT equal to 25 days emerged in a previous study as the minimal time for starting the chain elongation reactions in CSTR reactor. The best operational temperature for CE promotion was both thermophilic (~55°C) and mesophilic conditions (~35°C) mainly performed in anaerobic condition (Ren et al., 2024).

The advantage of using CE is to overcome the limitation of primary fermentation processes in VFAs extraction, because are synthetise longer chains, more apolar and consequently more hydrophobic, making separation from the fermentation broth easier (Wang et al., 2022).

In literature not many works dealing with the conversion of organic wastes into MCFA, shift the biological pathways from the mere acidogenic fermentation into chain elongation bioprocess. Focusing on the conditions and operational parameters unstudied is one possible research gap. Most CE research employed various types of biotechnological reactors (Fernando-Foncillas et al., 2021). Among these the fed-batch reactor enables an operational technique where one or more nutrients (substrates) are fed (supplied) to the bioreactor during cultivation and in which the products remain in the bioreactor until the end of the run (Lidén, 2002).

This reactor is also a type of semi-batch culture. The advantage of the fed-batch reactor is that it is possible control the concentration of fed-substrate in the culture liquid at arbitrarily desired levels (mainly at low levels). Fed-batch culture, generally, is superior to conventional batch culture when controlling nutrients affects the yield or productivity of the desired metabolite.

Despite these advantages, no fed-batch reactor had been tested so far for CE reactions. According to this scenario the present work optimizes the CE process productivity and conditions using real organic waste in fed-batch tests. Different real substrates batch were performed by identifying the best acetate-ethanol molar ratio, pH, HRT and yield in terms of MCFA.

2. Thesis objective

The main objective of this study was obtaining added-value commercial products from different wastewater through ammonium nitrogen recovery with gas-permeable membrane and chain elongation bioprocesses.

The research focused on ammonium removal and $(NH_4)_2SO_4$ fertiliser recovery from effluents using a GPM membrane at different operation strategies, to optimise the performance of technology at 35°C. Process efficiency was determined in terms TAN recovery, nitrogen mass transfer constant (K_m), and reagents consumption. Several factors were studied, including the pH control, VFAs change, volume ratio modification related to water transfer and the impact in the trapping solution concentration were controlled. The commercial quality of concentrated $(NH_4)_2SO_4$ trapping solution obtained was also evaluated. The possibility of a concentration step of the VFAs solution through a biomimetic forward osmosis (FO) membrane with a draw $MgCl_2$ solution was then studied. Effect of draw solution concentration, optimising the technology and obtaining high-value product was researched due to development of several parameters.

The second part of this study was to achieve chain elongation (CE) by investigating the effect of reverse β oxidation on high organic content sludge. Ethanol was used as electron donor on SCFAs to and boost the MCFAs production, especially bioproducts caproic acid with high economic value. Of interest was provide experimental information for different series of fed-batch tests, carried out involving fermented liquid and diluted synthetic ethanol. The fed-batch test was evaluated by assessing the concentration and composition of VFAs modified by ethanol acting to elongate.

The outlook of these three phases is design an integrated process to obtain added-value commercial by TAN removal with GMP and $(NH_4)_2SO_4$ fertiliser recovery, concentrate rich VFAs liquid by FO membrane and water-$MgCl_2$ recovery and produce high-value MCFAs fatty acids through CE in fed-batch bioprocess.

3. Materials and methods

3.1 Wastewaters substrate liquids composition and origin

Synthetic feed solution, supernatant from anaerobic digestion (AD) of the organic fraction of municipal solid waste (OFMSW), OFMSW fermentation liquid, and a wastewater from animal by-products not aimed for human consumption (ABPs), were used in this study for the TAN recovery. A second OFMSW fermented liquid was used for the CE bioprocess in this study.

A. Synthetic feed solution

Synthetic wastewater was initially used to assess the performance of the GPM contactor under different operational conditions. This wastewater consisted of deionised water with NH_4Cl to reach the desired nitrogen concentration and 5.0 g/L of acetic acid (AcOH). Acetic acid was selected to determine the maximum diffusion of VFAs through the membrane since this is the VFAs with the lowest molecular weight. The pH of the synthetic solution was adjusted throughout the experiment since an alkaline pH is needed to ensure ammonium recovery.

B. OFMSW AD supernatant

The OFMSW was collected from a mechanical-biological treatment (MBT) plant of the Barcelona Metropolitan Area (Spain) that treats about 50,000 t per year. The OFMSW was taken after the anaerobic digester treatment and subsequent centrifugation. The OFMSW supernatant was then sieved in the laboratory (0.2 mm mesh size) and centrifuged (12000 xg, 10 min) as a previous step to its treatment in the GPM. Table 1 summarises the final physical-chemical features of the OFMSW AD supernatant.

Table 1: Characterization OFMSW AD supernatant before and after centrifugation.

Parameters	Units	Collected supernatant of OFMSW AD	Centrifuged supernatant of OFMSW AD
pH	-	8.0 ± 0.1	8.2 ± 0.1
Conductivity	mS/cm	50.2 ± 0.2	50.6 ± 0.2
TS	g TS/kg	35.3 ± 0.0	24.2 ± 0.7
VS	g VS/kg	15.4 ± 0.8	12.1 ± 0.2

VS/TS	%	43.9 ± 0.8	50.0 ± 0.8
COD total	g COD/L	46.9 ± 0.4	24.2 ± 1.8
COD soluble	g COD/L	19.4 ± 1.9	19.4 ± 1.9
Total Alkalinity	g $CaCO_3$/L	24.0 ± 0.5	20.7 ± 0.5
TAN	g NH_4^+-N/L	5.6 ± 0.1	5.6 ± 0.1
VFAs	g COD/L	0.62 ± 0.00	0.62 ± 0.00
Acetic acid	g COD/L	0.49 ± 0.00	0.49 ± 0.00
Propionic acid	g COD/L	0.06 ± 0.00	0.06 ± 0.00
Butyric acid	g COD/L	0.03 ± 0.01	0.03 ± 0.01
Valeric acid	g COD/L	0.04 ± 0.00	0.04 ± 0.00
Caproic acid	g COD/L	0.00 ± 0.00	0.00 ± 0.00

C. OFMSW fermented liquid

The OFMSW fermented liquid was obtained using a sample of OFMSW collected in the same MBT plant before its feeding to the anaerobic digesters (AD). The anaerobic fermentation process was conducted in 40-L steel batch reactor equipped with a thermostatic jacket at 35°C for the T control and a mechanical stirrer. The entire fermentation process was followed for 7 days and characterised (*see section 4.1 OFMSW fermentation process*). The OFMSW fermentation liquid was then sieved in the laboratory (0.2 mm mesh size) and centrifuged (12000 xg, 10 min) obtaining the fermented liquid of OFMSW. Table 2 summarises the main characteristics of the collected OFMSW and the produced OFMSW fermented liquid, where an increase in the VFAs and TAN content are observed.

Table 2: Characterization OFMSW fermented liquid before and after the fermentation.

Parameters	**Units**	**Collected supernatant of OFMSW**	**Centrifuged fermented of OFMSW**
pH	-	6.2 ± 0.1	6.3 ± 0.1
Conductivity	mS/cm	41.5 ± 0.2	48.5 ± 0.2
TS	g TS/kg	94.6 ± 3.9	44.2 ± 4.7
VS	g VS/kg	19.3 ± 0.2	13.0 ± 0.0
VS/TS	%	20.4 ± 3.9	29.4 ± 4.7
COD total	g COD/L	119.2 ± 2.4	95.8 ± 6.7
COD soluble	g COD/L	54.6 ± 1.5	65.8 ± 0.8
Total Alkalinity	g $CaCO_3$/L	14.7 ± 0.5	12.5 ± 0.5

TAN	g NH_4^+-N/L	3.7 ± 0.0	5.9 ± 0.1
VFAs	g COD/L	30.85 ± 0.50	39.83 ± 1.26
Acetic acid	g COD/L	8.2 ± 0.10	10.82 ± 0.51
Propionic acid	g COD/L	11.48 ± 0.29	10.57 ± 0.40
Butyric acid	g COD/L	10.33 ± 0.37	10.76 ± 0.43
Valeric acid	g COD/L	0.42 ± 0.02	3.21 ± 0.13
Caproic acid	g COD/L	0.19 ± 0.01	4.48 ± 0.21

D. ABPs wastewater

The animal by-products (ABPs) are products of animal origin that people do not consume. In this study the ABPs included were sorted into the Category 3 (*Cat3*) as material with a low risk and they are usually employed as feed for food producing animals (ABPs Regulation EU Parliament, 2009). The ABPs was collected in a chicken farm in Sant Esteve d'en Bas (Spain) and referred as VTK3 effluent. The ABPs wastewater was obtained after a pre-treatment (mechanical shredding and laboratory sieving) and centrifugation (12000 xg, 10 min) of the collected effluent. Table 3 summarises the main characteristics of the ABPs wastewater, where it is observed the high VFAs content, TAN concentration and salinity of this residual stream.

Table 3: Characterization ABPs wastewater after centrifugation.

Parameters	**Units**	**Centrifugated supernatant of ABPs**
pH	-	7.3 ± 0.1
Conductivity	mS/cm	57.0 ± 0.2
TS	g TS/kg	51.9 ± 0.8
VS	g VS/kg	3.3 ± 0.1
SV/ST	%	6.6 ± 0.5
COD total	g COD/L	141.5 ± 2.2
COD soluble	g COD/L	81.1 ± 4.7
Total Alkalinity	g $CaCO_3$/L	25.1 ± 0.3
TAN	g NH_4^+-N/L	11.9 ± 0.6
VFAs	g COD/L	76.70 ± 2.10
Acetic acid	g COD/L	29.17 ± 0.90
Propionic acid	g COD/L	9.70 ± 0.20

Butyric acid	g COD/L	12.50 ± 0.70
Valeric acid	g COD/L	6.10 ± 0.20
Caproic acid	g COD/L	1.20 ± 0.02

E. *OFMSW fermented liquid for CE*

For the CE process, the OFMSW came from the separate collection (in 50 districts of Treviso municipality; northeast Italy) and subjected to inert removal and organic matter homogenization (with the screw-press technique). To be used as inoculum (source of fermentative bacteria), an anaerobic fermentation process was conducted in 5.0 L borosilicate glass CSTR, equipped with a thermostatic jacket for the temperature control and a mechanical stirrer. The reactor was manually fed with the OFMSW on daily basis. The desired amount of the effluent has been extracted and centrifuged (*Heraeus Megafuge 40 with a Swinging Bucket Rotor, Thermo Fisher Scientific*) for 15 min at 4500 rpm to obtain the supernatant for the analysis (mainly VFAs). To be used as inoculum for CE process, the centrifugation step was avoided. The main initial physical-chemical features of the OFMSW liquid, useful to understand the CE process, are reported in Table 4:

Table 4: Characterization OFMSW fermented liquid for CE.

Parameters	**Units**	**Centrifuged fermented of OFMSW *T1***	**Centrifuged fermented of OFMSW *T2***	**Centrifuged fermented of OFMSW *T3***
pH	-	4.7 ± 0.1	5.5 ± 0.1	5.3 ± 0.1
TS	g TS/kg	39.7 ± 2.8	41.9 ± 2.3	40.6 ± 1.9
VS	g VS/kg	19.3 ± 1.5	21.3 ± 1.1	20.5 ± 0.9
SV/ST	%	48.6 ± 0.5	50.8 ± 0.5	50.5 ± 0.5
Inoculum HRT	day	4	4	4
OLR	Kg VS/m^3	12.5	12.5	22.5
VFAs	g COD/L	4.35 ± 2.10	18.26 ± 2.10	34.10 ± 4.62
Acetic acid	g COD/L	2.30 ± 0.90	8.08 ± 0.90	10.98 ± 0.90
Propionic acid	g COD/L	-	-	-
Butyric acid	g COD/L	0.25 ± 0.70	4.61 ± 0.70	15.33 ± 0.70
Valeric acid	g COD/L	-	-	-
Caproic acid	g COD/L	1.80 ± 0.02	4.75 ± 0.02	7.79 ± 0.02

3.2 Experimental set-up

3.2.1 Acidogenic fermenter

To produce the OFMSW fermented liquid a 40-L fermenter was used at mesophilic conditions (35°C). The fermenter was equipped with a mechanical stirrer (*Triam, 75040*), a pH controller (*Crison, pH 28*), a heating system (*AS, Electric Heating Jacket*) and a set of valves located at the top of the fermenter to avoid overpressure. 15 L of OFMSW were fed to the reactor without adding external inoculum nor external chemicals since it was considered that the anaerobic digestion supernatant recirculation provided enough fermentative bacteria and alkalinity (Fernández-Domínguez et al., 2020). The fermentation batch lasted 7 days, when the VFAs concentration reached its maximum value. The fermentation liquid used in the membrane contactor was obtained after sieving (0.2 mm mesh size) and centrifuging (16600 ×g, 10 min) the fermentation broth to prevent membrane clogging. The resulting fermented liquid was stored at 4°C until use.

3.2.2 Gas-permeable membrane contractor

The experimental set up consisted of two sealed glass tanks and a microporous hollow-fibre polypropylene (PP) membrane contactor with an active surface area of 0.50 m^2. A 3-L jacketed tank was used for the trapping solution (H_2SO_4 0.1 M) and a 5-L jacketed tank was used for the feed solution. The feed and trapping solutions were pumped using a peristaltic pump (*Masterflex L/S*) in a closed loop to the membrane module (*3M, 1.7 × 5.5 MiniModule*). The flow rate for the feed solution was 15 L/h and for the trapping solution was 5 L/h. The operational temperature was maintained at 35°C by circulating water from a heated water bath (*Thermo Scientific HAAKE DC30*) through the jacket surrounding each of the tanks. To minimise the free NH_3 losses by volatilisation, both chambers were completely sealed using a lid, gum and parafilm.

Each reactor was equipped with a magnetic stirrer (agitation velocity of 180 rpm) and a pH control system. The pH control system consisted of two pH electrodes (*Crison, code 53-35*), two pH controllers (*Crison, pH 28*), two peristaltic pump (*Ismatec, type ISM827*) and two graduated cylinders. The pH was controlled through peristaltic pumps that added an acid solution (H_2SO_4 25%) and a basic solution (NaOH 8 M) to the feed and trapping solution, respectively. The pH controller switched on the peristaltic pump connected to the tank to control the pH within a defined pH setpoint. The consumption of reagents for pH control was also monitored to account for volume

changes due to water diffusion. The feed solution was recirculated through the membrane shell side, and the trapping solution was recirculated internally in the lumen side. This circulation way has been reported in the literature as the most suitable choice to higher TAN recovery efficiencies and to minimize fouling issues to the membrane (Serra-Toro et al., 2022).

Experiments were monitored by collecting multiple samples from both the feed and trapping solutions over the course of 54 h. Samples were taken hourly for the first 8 h, with two samples collected during the first hour every 30 min. Experiments running overnight were sampled after 12 h and subsequently samples were then taken every 4 h. In each sampling 4 mL were extracted from for both solutions, which was then stored at 4 °C until TAN analysis. This method has been adopted to minimise its impact in the results of the trapping solution characterisation. The volume was determined using a pre-calibrated mark correlated liquid height with volume in each tank.

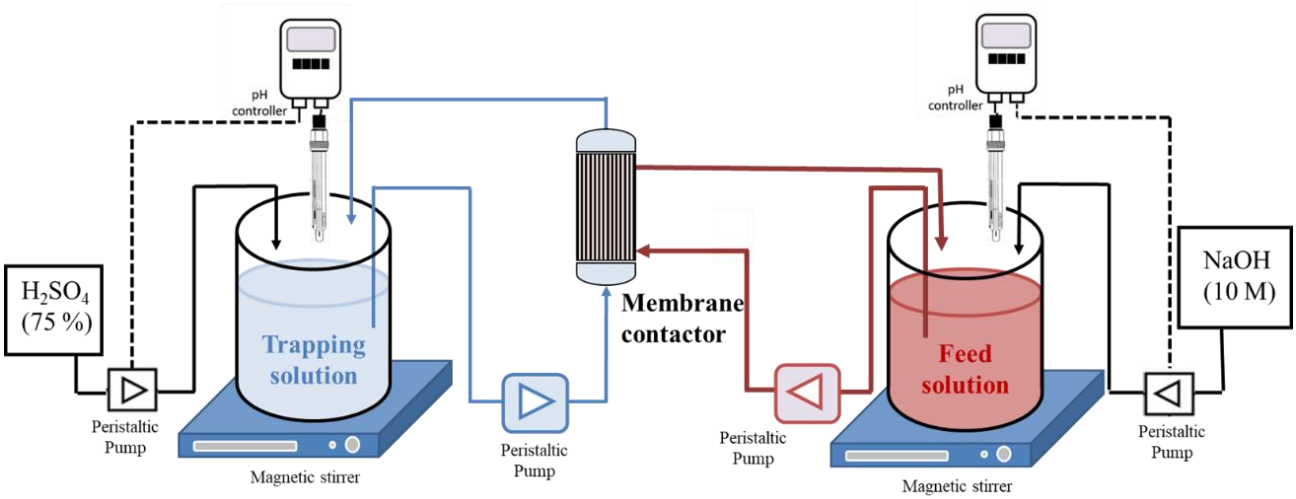

Figure 9: Experimental set-up for the gas permeable membrane contactor.

3.2.3 Forward osmosis membrane system

The FO experimental set up consisted of a membrane module connected through piping and pump at two glass tanks, one for draw solution (2.0 L) and another for feed solution (0.50 L), as Fig. 10 schematize. FO membrane was composed by Aquaporin Inside (*HFFO2 module - Aquaporin A/s, Denmark*) and an acrylic cell. Aquaporin membrane was a biomimetic hollow fibre with an active layer of polyamide composite and a membrane area of 2.30 m^2. This membrane is fitted with several polyamide-based selective flat sheet mimics the outside of a cells. This incorporate aquaporin water channels leading to high permeate flow water filtration.

Two peristaltic pumps (*Masterflex L/S*) with maximum flow rate of 15 L/h were used for feed and draw solutions circulation in the module. The test was conducted at room temperature. The draw and the feed solution were continuously stirred using a magnetic stirrer (agitation velocity of 180 rpm). The change in the volume was measured using a pre-calibrated mark that correlated the liquid height with the volume in each tank. The optimal cross flow velocity of at 0.38 cm/sec and draw solution concentration were reported in literature. The process performance was monitored by taking samples initially every 1 min and then every 5 min until no change in volume was observed. Industrial grade magnesium chloride hexahydrate ($MgCl_2 \cdot 6H_2O$ > 99.4% purity) was used to prepare the draw solution with DI water. 1 M $MgCl_2 \cdot 6H_2O$ solution was used to get an osmotic pressure of 150 bar, capable of removing water. The feed solutions were the previous OFMSW digestate and OFMSW fermented that had been subjected to the TAN removal.

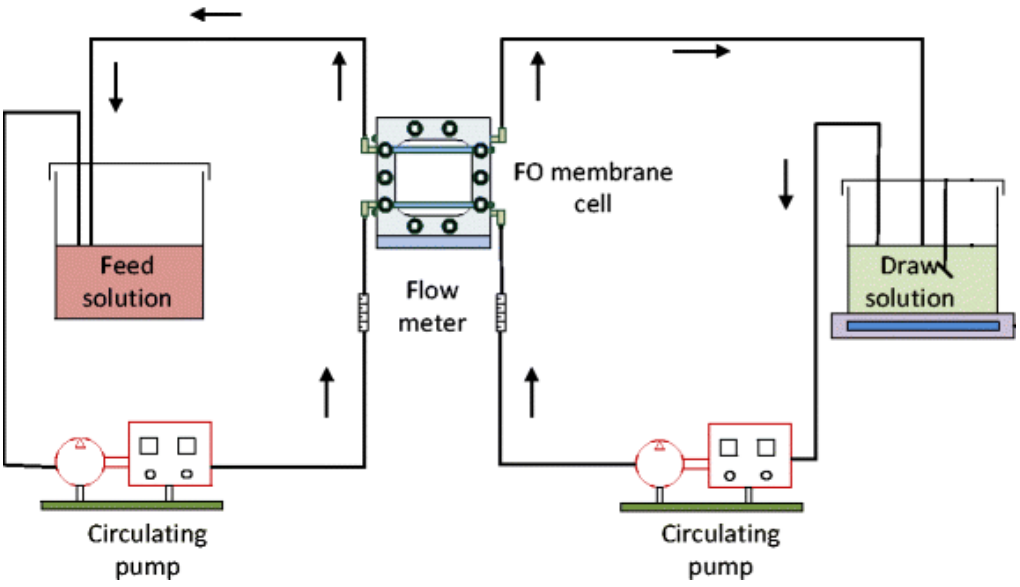

Figure 10: Experimental set-up for the forward osmosis membrane system.

3.2.4 Chain elongation fed-batch reactors

The experimental set up for the CE process consisted in two duplicated tests performed using a polypropylene (PP) 0.5-L reactors (*Nautilus*) equipped with a mechanic plastic stirrer (agitation velocity of 180 rpm) as depicted in Fig. 11. The chosen reactors were among a set and the operational temperature was maintained at 55°C (thermophilic condition) by keeping it in a water heated bath (*Thermo Scientific HAAKE DC30*) sealed by a plastic cap to not allow water evaporation.

The fed-batch system was provided by a peristatic pump (*Kamoer 42-88 ml/min KAS*) for each tank pumping a predefined set flow rate of diluted ethanol, according to experimental concerns.

The activation of the pumps was automatic and pre-set through the use of a time-controlled electrical plug (*Perry - 1IO 0053*). Peristatic pumps activated for 15 min in 12 h to provide the pre-defined ethanol flow rate. Fermented OFMSW was taken, and 500 mL was added at the beginning of the experiment and left for 2-3 days to allow the mixed biomass to adapt and stabilise.

An initial amount of ethanol (100, 250 or 500 gCOD/L) was added, and the remaining ethanol was gradually injected. The experiment was maintained until a certain amount of ethanol was reached, but never more than 0.8 L as total volume. A second pipe ensured the release of any gases as not to put the biosystem under pressure. Multiple samples, approximately of 4 mL, were taken every two days at the same time to monitor the experiment. This method has been adopted to minimise the loss of relevant volumes and its impact in the results of VFAs characterisation.

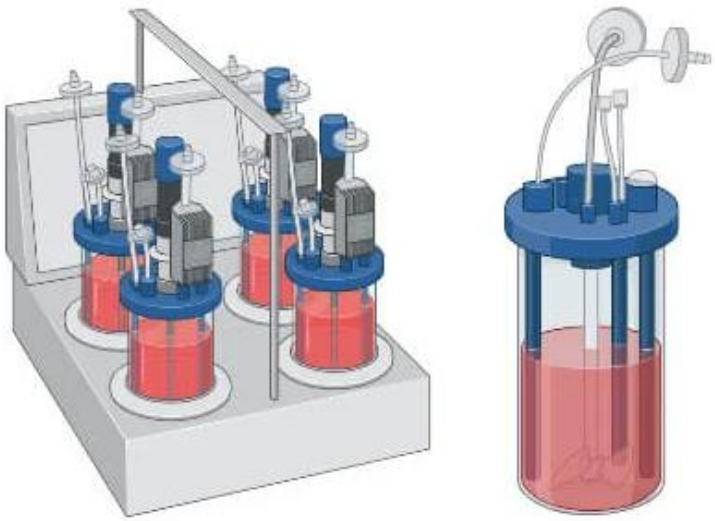

Figure 11: Experimental set-up for the chain elongation fed-batch reactors.

3.3 Experiments methodology

3.3.1 Fermentation process methodology

During the OFMSW fermentation test carried out under mesophilic conditions (35°C), samples were daily withdrawn to analyse the evolution of pH, VFAs concentration and profile, soluble COD (sCOD)

and TAN. Samples were immediately centrifuged after withdrawal and stored at 4°C until analysis. pH was constantly monitored and initially a slight increase of pH was detected, then started to decrease, due to VFAs production and the process was stopped.

These conditions, according to the literature (Valentino et al., 2021) ensured the start of anaerobic fermentation phases. The idea of this process configuration enables VFAs-rich mass flow produced from the anaerobic system, to be used for other purposes. This provided, after the steady state was reached, a fermentation batch in 7^{th} days with a fermented liquid with appealing industrial features.

3.3.2 TAN recovery methodology

For the TAN recovery, Table 5 summarises the experiments carried out in this study to analyse the potential and limitations of the gas permeable membrane (GPM). The results of the process were evaluated by quantifying:

- TAN removal and recovery rates for the different wastewaters tested.
- The dynamics of ammonia passage by assessing of the ammonia mass transfer constant (K_m).
- Consumption of alkalinity (NaOH) and acid (H_2SO_4) to keep the pH of each solution constant.
- Water transfer across the GPM and to describe these phenomena, a possible physical chemical model was proposed.

Experiments S1-S11 were carried out with synthetic wastewater (feed solution) to understand the behaviour of the GPM at a certain initial TAN value. The aim was to simulate the possible behaviour of real highly ammonium loaded effluents in the process (2.5-10 g NH_4^+-N/L) and to study the removal and recovery efficiency and the TAN transfer rate under different volume ratios (2:1 and 10:1) between the feed and the trapping solution ($\omega = V_{feed}/V_{trapping}$), while maintaining an optimal pH in both solutions. The interest was to maintain a volumetric ratio that makes it possible to obtain concentrations of ammonium sulphate in the trapping solution with commercial interest (it is required to reach a 20 wt.% of $(NH_4)_2SO_4$). Moreover, a model was also proposed to understand and predict both ammonia and water transfer, which is to be intended as a tool to optimise operating conditions and control the dilution effect that reduces the quality of capture solutions.

Experiments D1-D3, F1-F2, A1-A2 were performed to determine the TAN removal and recovery efficiency and the TAN transfer rate under different volume ratios between the feed and the trapping

solution ($\omega = V_{feed}/V_{trapping}$) from real effluents, namely AD OFMSW supernatant, OFMSW fermentation liquid and ABPs wastewater.

Two replicates were carried out for each condition studied. For the experiments with a volume ratio ω=10, an operational time of 54 h was set to assess the ultimate recovery efficiency and to study the possible transfer of water that is particularly marked during long operation time. The experiments with a volume ratio ω=2 were conducted for 24 h as a proper ammonium removal and a lower volumetric change due to waster diffusion were observed. The experiments with ABPs wastewater were conducted for 24 h as a high-water passage did not allow continuation for test A1.

For all test the Km was analysed before water diffusion was observed as required by the formula.

Table 5: Operational conditions of the TAN recovery experiments carried out in this study.

Feed Solution	Test	Vf/Vt (ω)	Operational Time (h)	Temperature (°C)	pH Feed (-)	pH Trapping (-)
Syntetic wastewater	S1	2:1	24	35	9.0	1.5
	S2	2:1	24	35	9.0	1.5
	S3	2:1	24	35	9.0	1.5
	S4	10:1	54	35	9.0	1.5
	S5	10:1	54	35	9.0	1.5
	S6	10:1	54	35	9.0	1.5
	S7	10:1	54	35	9.0	1.5
	S8	10:1	54	35	9.0	1.5
	S9	10:1	54	35	9.0	1.5
	S10	10:1	54	35	9.0	1.5
	S11	10:1	54	35	9.0	1.5
AD OFMSW	D1	2:1	24	35	9.0	1.5
supernatant	D2	10:1	54	35	9.0	1.5
	D3	10:1	54	35	9.0	1.5
OFMSW fermented	F1	2:1	24	35	9.0	1.5
liquid	F2	10:1	54	35	9.0	1.5
ABPs wastewater	A1	2:1	24	35	9.0	1.5
	A2	5:1	24	35	9.0	1.5

In all experiments the initial volume of the feed solution was 5 L. For all the experiments performed, the pH of the trapping solution was set at 1.0-1.5 while the pH for the feed was set at 9.0-9.5 (Serra-Toro et al., 2024). The trapping solution must be kept at pH below 2, sufficiently acidic to retain diffused NH_3 as NH_4^+ since charged species cannot diffuse through the membrane. Instead, the feed solution must be kept alkaline at pH around 9, to shift the TAN equilibrium towards NH_3 which is the uncharged species that can diffuse across the membrane (Serra-Toro et al., 2024).

The temperature was selected to keep the mesophilic conditions (35°C) that are used to ferment OFMSW and to mimic industrial reaction conditions (Valentino et al., 2021). When treating industrial effluents, the resulting trapping solution was exhaustively analysed to determine the presence of contaminants such as metals, ions and total organic carbon (TOC) that could compromise its commercial value (Vecino et al., 2019).

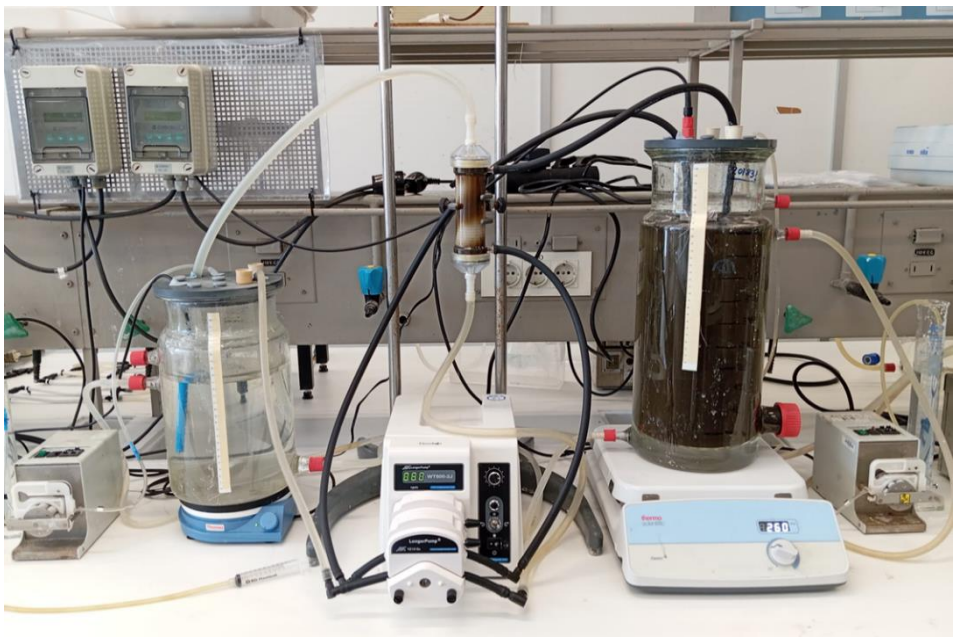

Figure 12: Technical features of TAN recovery reactors.

3.3.3 FO methodology

For the FO, two tests with different wastewater after GPM treatment, were conducted in order to increase the VFAs concentration of the OFMSW 30% gCOD/L, based on observations collected during initial tests (VFAs analysis). The implemented operating conditions were chosen to reach a water concentration factor (WCF) leading to a VFAs concentration >70 gCOD/L. The results of the process were evaluated by quantifying:

- The decrease in volume in the feed solution and the increase in volume in the draw solution.
- VFAs concentration in both the feed and the draw solution.
- Measuring the conductivity to understand the driving force for water permeation between the two solutions.

The aim was to concentrate the industrial effluents previously treated using a GPM (for example, to obtain a VFAs fermentation liquid with high VFAs/N ratio that could be useful for multiple downstream applications) and a diluted $MgCl_2$ solution that could be potentially regenerated. For each test, the OFMSW effluents were taken out of the fridge few hours before filtration so to start the filtration at constant temperature (20 °C). The test finished when the volumes of the feed and the draw solution remained constant and was generally around 50 min. In all experiments the initial volume was 2 L for the feed and 2 L for the draw solution. Fouling-related issues, even if no visible, were avoided by a membrane cleaning before each experiment.
Volume variation linked to water permeation was also evaluated by measuring reactor height over time to calculate the final WCF. Several samples were taken every minute for pH and conductivity analysis, two very important parameters indicating the reaching of osmotic equilibrium. VFAs concentration was systematically analysed during the filtration test both on the feed and draw solutions.

3.3.4 CE methodology

For the chain elongation bioprocess, two replicas of three tests with different initial ethanol concentration were conducted as summarised in Table 6. The characterised OFMSW fermented was added together with a specified quantity of synthetic solution of ethanol until the desired molar ratio ethanol:acetic was reached. A flow rate of ethanol was added until a molar ratio of 1:10 was reached. The results of the process were evaluated by quantifying:

- The production and composition of VFAs during the fed-batch process.
- The optimal ethanol:acetic molar ratio to shift the biological pathway from acidogenic fermentation towards the reverse β-oxidation reactions (chain elongation).
- The trend in caproic acid production in relation to the fed-batch reactor characterised by VFAs production and consumption.

Table 6: Operational conditions of the experiments carried out in this study.

Test	EtOH/AcOH initial molar ratio (-)	EtOH added (g COD/L)	Initial EtOH added (mL)	Operational Time (d)	Temperature (°C)	pH (-)
T1	1:2	100	25	25	55	4.7
T1’	1:2	100	25	25	55	4.7
T2	1:2	250	50	20	55	5.5
T2’	1:2	250	50	20	55	5.5
T3	1:2	500	57	11	55	5.3
T3’	1:4	500	114	11	55	5.3

The initial stoichiometric ethanol:acetic molar ratio to start up CE has been set at 1:2. This initial ratio was reached by the initial addition and then the ethanol flow rate was calculated to added ethanol each time to achieve a ratio of 1:10. This results in an incremental range of added ethanol which gives information on the best ratio for evolves CE process and how this develops over time in a fed-batch reactor.

In the fed-batch tests carried, the fermented was discharged and renovated only after completing a test. OFMSW fermented liquid was collected on different days, so every initial composition of VFAs were analysed and reported. The test’s working volume was 0.50 L, under anaerobic conditions at operational temperature of 55°C, temperature selected to maintain the characteristics of the fermented product. The reactor was maintained also considering the maximum volume of 0.80 L.

Figure 13: Technical features of CE fed-batch reactors.

The pH of all the trials was monitored and result around pH 5 in all samples. This value given by the reaction conditions and the ethanol addition emerged as the best condition for tests. The Hydraulic Retention Time (HRT) at first was set up at 25 d but after the results obtained and the considerations made, it was reduced to 10 d, which emerged in a previous study as the minimal time for starting the chain elongation reactions (Grootscholten et al., 2013).

3.4 Analytical methods

For the measurement of ammonia nitrogen, a selective ammonium electrode (*Thermo Fisher Scientific, Orion 9512HPBNWP*) was used following the Standard Method 4500-NH3D (APHA Standard Methods, 2017) procedure. Calibration of the electrode was performed with 5 standard solutions of known concentration (10, 25, 50, 100 and 150 mgNH_4^+-N/L) prior to the sample measurement, that was also repeated at the end of the sample's measurement.

Total solids (TS) and volatile solids (VS) were measured following the Standard Method 2540G procedure (APHA Standard Methods, 2017) by volatilisation in the stove and then in muffle.

Total and soluble chemical oxygen demand (COD) were determined according to Standard Method 5220C (APHA Standard Methods, 2017). 10 mL vials were taken for COD digestions and 2.5 mL of sample (or diluted sample) were added to the vials. Then 1.5 mL of potassium dichromate ($K_2Cr_2O_7$) digestant solution, 3.5 mL of a solution of sulphuric acid (H_2SO_4) and silver sulphate (Ag_2SO_4; 10 g/L) was added. The vials were placed in a digestion block at 150 °C for 2 h. COD was determined by measuring the absorbance at 600 nm in a spectrophotometer (*JP-Selecta V-1100D*). For the measurement of soluble COD every liquid was centrifuged (16,000 × g, 8 min; *Sigma 1-14 microcentrifuge*) and filtered (1.2-µm cellulose filters) prior to its analysis.

The pH measurements were carried out with a glass pH electrode for liquids (*METRIA*) connected to a multimeter (*Crison MM 41*) calibrated with 3 standard solutions of pH 4.10, 7.00 and 9.21. Conductivity measurements were carried out using a conductivity cell with platinum electrodes and glass body (*HACH CAT 5070*). Alkalinity was determined following the Standard Method 2320B procedure (APHA Standard Methods, 2017) using an automatic titrator (*Crison, pH 24*) with a 0.1 M HCl solution and a pH end point of 5.75 for partial alkalinity and 4.75 for the total one.

Volatile fatty acids (VFAs) (i.e. acetic, propionic, butyric, butyric, valeric, caproic and heptanoic acids) were analysed using a gas chromatograph (*Shimadzu GC-2010 plus*) equipped with an Agilent DB-FFAP capillary column and a flame ionisation detector. Before GC analysis, each sample was centrifuged (16.000 × g, 8 min; *Sigma 1-14 microcentrifuge*) and filtered (1.2-µm cellulose filters). The VFAs were converted to COD equivalents using the theoretical value (mgCOD/mgVFAs): 1.07 for acetic acid, 1.51 for propionic acid, 1.82 for butyric acid, 2.04 for valeric acid, 2.21 for caproic acid and 2.34 for heptanoic acid.

The concentration of heavy metals (As, Zn, Pb, Cd, Hg, Cu, Mn, and Li) and other elements (S, K, Mg, Ca, Na, Fe, and P) were determined using a coupled plasma mass spectrometry ICP-MS (*Perkin Elmer Nexion 350D*). Total Carbon (TC) was determined using a *Multi N/C 3100 Analytik Jena* by a catalytic combustion process where the resulting CO_2 is quantified by an infrared detector. Inorganic carbon (IC) analysis is carried out by the injection of the sample to a phosphoric acid and quantifying the CO_2. TOC was the difference between TC and IC.

For the second part of the research (CE experiments), VFAs and ethanol were analysed according to the standard method (APHA Standard Methods, 2017), by N-gas chromatograph (*Agilent 6890 GC*) equipped with Agilent J&W DB-WAX fused silica capillary column and a flame ionization detector. The method operated with a ramp temperature from 40°C to 160°C and a split ratio of 20:1 was maintained for the inlet. Before GC analysis, each sample was centrifuged (16.000 × g, 10 min; *Heraeus Megafuge 40, Thermo Fisher*) and filtered (0.2-µm cellulose filters). The VFAs were converted to COD equivalents using the theoretical value (mgCOD/mgVFAs). The pH measurements were carried out with a portable probe (Eutech pH 700) calibrated with 3 standard solutions of pH 4.00, 7.00 and 9.21.

3.5 Calculations and statistical analysis

The TAN removal and recovery efficiencies were determined using Eq. 1 and 2, respectively (Serra-Toro et al., 2024). The TAN mass [g] is the following: $TAN_f(0)$ for the feed solution at the beginning, $TAN_f(t)$ for the feed solution at a specific time, $TAN_t(0)$ for the trapping solution at the beginning and $TAN_t(t)$ for trapping solution at a specific time. The volume [L] is the following: $V_f(0)$ for the volume feed at the beginning, $V_f(t)$ for the volume feed at a specific time, $V_t(0)$ for the volume trapping at

the beginning and $V_t(t)$ for volume trapping at a specific time. The difference between TAN removal and recovery is associated with TAN losses.

$$\% \text{ TAN removal (t)} = \frac{\mathrm{TAN}f(0)\cdot \mathrm{V}f(0) - \mathrm{TAN}f(\mathrm{t})\cdot \mathrm{V}f(\mathrm{t})}{\mathrm{TAN}f(0)\cdot \mathrm{V}f(0)} \cdot 100 \qquad \text{(Eq. 1)}$$

$$\% \text{ TAN recovery (t)} = \frac{\mathrm{TAN}t(\mathrm{t})\cdot \mathrm{V}t(0) - \mathrm{TAN}t(0)\cdot \mathrm{V}t(\mathrm{t})}{\mathrm{TAN}f(0)\cdot \mathrm{V}f(0)} \cdot 100 \qquad \text{(Eq. 2)}$$

The ammonia mass transfer constant (K_m) was used to evaluate the ammonia flux through the membrane (Serra-Toro et al., 2022). This parameter quantifies the ammonia transfer under specific conditions. Eq. 3 determines the K_m value [m/s] from experimental concentration data if the NH_3/NH_4^+ equilibrium is fulfilled during the operation.

In Eq. 3, $c_{TAN,f}(t)$ is the concentration of TAN in the feed solution at any time [gNH_4^+-N/L], $_{CTAN,f}(0)$ is the initial concentration of TAN in the feed solution [gNH_4^+-N/L], A is the area of the membrane [m^2], V_f is the volume of the feed solution [m^3] and t is the time [s]. The K_m depends on the pH and temperature of the feed solution, amongst other operating factors.

$$\frac{C\ \mathrm{TAN}f(\mathrm{t})}{C\ \mathrm{TAN}f(0)} = \exp\left[\frac{-Km\mathrm{A}}{\mathrm{V}f} \cdot t\right] \qquad \text{(Eq. 3)}$$

For the K_m determination this equation model was coded in Python using the curve fit function of the SciPy and the Levenberg-Marquardt algorithm to perform non-linear least squares estimates. The algorithm estimates the K_m and its standard deviation by fitting the TAN concentration of the feed and trapping solution in the tanks.

The reagent consumption was calculated in moles of reagent (NaOH and H_2SO_4) per mole of TAN recovered to facilitate tests comparison. The total consumption accounted for the total amount of reagent added throughout the test, whereas the consumption to control the pH did not consider the initial addition to reach the pH set point.

To evaluate the FO membrane performance, dedicated indicators were used with regards to achievable concentration and associated filtration time. The used indicator is the WCF (Blandin et al., 2019) that represents the concentration of the feed solution over time and is calculated using the following equation:

$$\text{WCF} = \frac{V(t)}{V(0)} \qquad \text{(Eq. 4)}$$

With V_0 the feed initial volume and V(t) the feed volume at any time [min] during the filtration. Was especially of interest the WCF at the end of the filtration (when osmotic equilibrium was reached). All batches were performed to reach a minimum requirement of WCF = 3 to concentrate the VFAs to this factor. WCF was also used as a comparative filtration indicator.

CE molar ratio between acetic acid (AcOH) and ethanol (EtOh) was calculated using Eq. 5 and Eq. 6. Initial AcOH(i) concentration [mol/L] is the following: AcOH in gCOD/L multiplied by 1.07 (COD grams conversion value to grams) on AcOH molecular weight in g/mol. To calculate the value of EtOH to be added, the result of the Eq.5, AcOH(i) in mol/L is multiplied by the desired molar ratio (from 2 to 10) minus the EtOH(0) initial in mol/L and multiplied by the EtOH molecular weight in g/mol.

$$\mathrm{AcOH(i)} = \frac{\mathrm{AcOH}\,\frac{\mathrm{gCOD}}{\mathrm{L}} \cdot 1{,}07}{\mathrm{PM\ AcOH}} \qquad \text{(Eq. 5)}$$

$$\mathrm{EtOH} = [\mathrm{AcOH(i)} \cdot \frac{\mathrm{AcOH}}{\mathrm{EtOH}} - \mathrm{EtOH(0)}] \cdot \mathrm{PM\ EtOH} \qquad \text{(Eq. 6)}$$

4. Results and discussion

4.1 OFMSW fermentation process

The performance of the OFMSW fermentation test is summarised in Fig. 14 (VFAs evolution), Fig. 15 (sCOD and COD evolution) and Fig. 16 (TAN and pH evolution).

As stated in Fig. 14, the concentration of VFAs increased from 30.85 gCOD/L reaching a maximum concentration of 47.25 gCOD/L (day 4). The VFAs yield was slightly higher than the fermentation yield from the same MBT plant reported in literature (Peña-Picola et al., 2024; Serra-Toro et al., 2022). The VFAs profile was dominated by acetic (36 % COD basis), propionic (27 % COD basis) and butyric (23 % COD basis) acids. During fermentation the proportion of valeric and caproic acids increased due to the processing of butyric acid. The maximum amount of VFAs was recorded at day 4, and the OFMSW fermented liquid composition was 5.55 gCOD/L acetic, 2.71 gCOD/L propionic, 2.912 gCOD/L butyric, 0.82 gCOD/L valeric, 0.90 gCOD/L caproic and 0.12 gCOD/L heptanoic. At the end of the batch test (day 8 and 9) it was observed an overall VFAs concentration decrease.

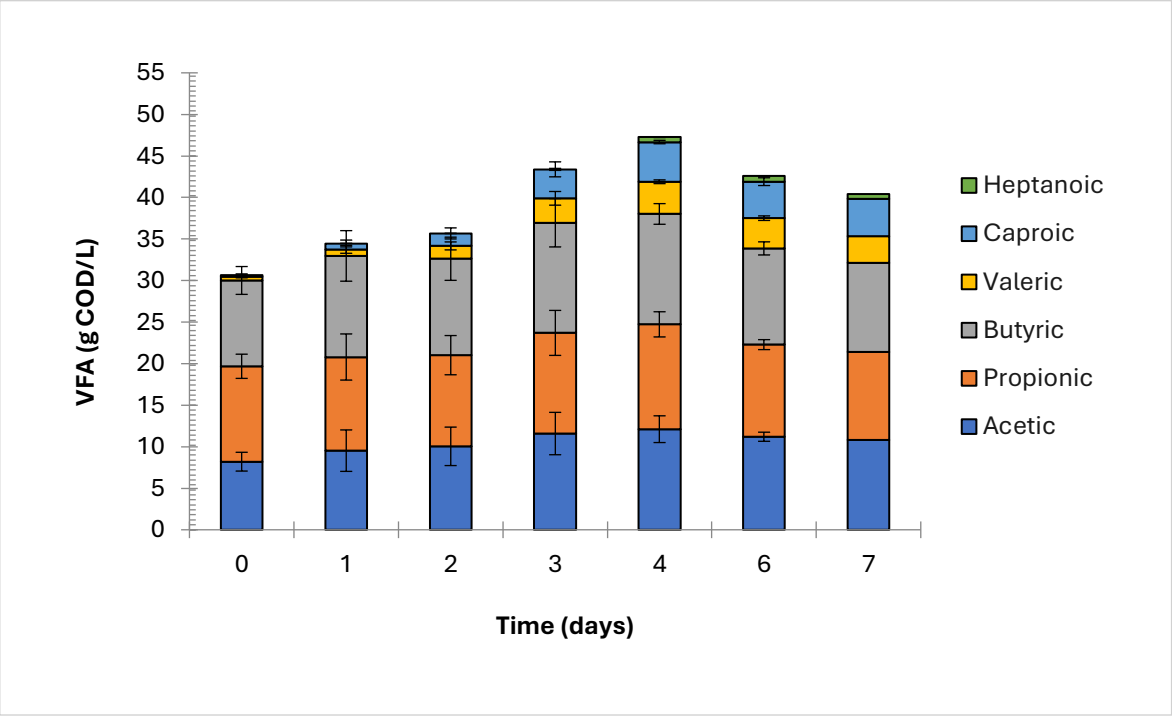

Figure 14: Evolution of the VFAs concentration during OFMSW fermentation performance.

In the Fig. 15 the COD_{VFA}/sCOD ratio increased over time reaching a final value of 0.69 ± 0.40 g COD_{VFA}/g sCOD indicating that most of the sCOD was in the form of VFAs. This COD_{VFA}/sCOD ratio turn out to be very similar compared by previously reported results (Peña-Picola et al., 2024), for the same type of biomass treatment. Changes in feedstock physical and chemical properties due to seasonal variation could affect the concomitant VFAs production and profile. The high COD_{VFA}/sCOD value may be related to the batch operation, the high biodegradability of source-sorted OFMSW and the wastewater characteristics given by the pre-treatment implemented in the MBT.

The high acidification efficiency (percentage of sCOD as COD_{VFA}) reached in this study is a positive feature for the proposed biorefinery. The fermented broth with a low concentration of non-VFA soluble COD is preferable for biomolecule (polyhydroxyalkanoates PHA) production. On the other hand, the low concentration of non-VFA sCOD implies that the organic matter that has not been converted to VFAs could be diverted to the anaerobic digester for biogas production. Such high concentration of non-VFA soluble COD result is hence preferable.

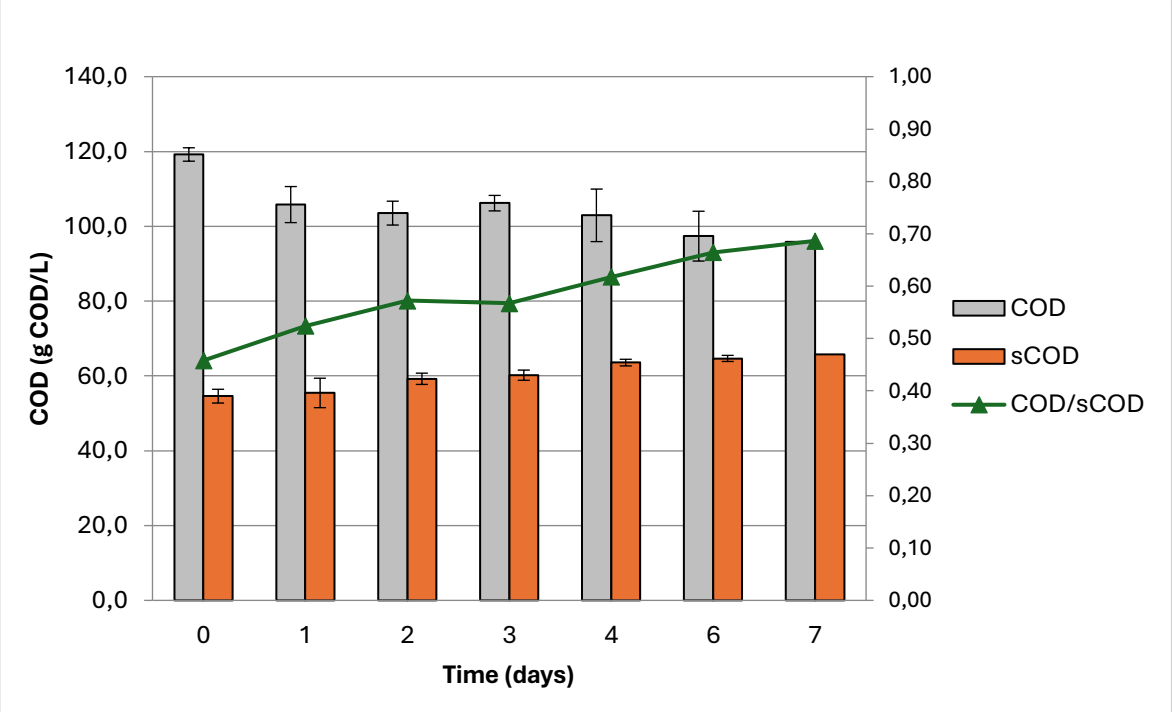

Figure 15: Monitoring of soluble COD, total COD and the COD_{VFA}/sCOD ratio during OFMSW fermentation performance.

In Fig. 16, the TAN concentration increased from 3.8 to 5.9 gNH_4^+-N/L due to protein hydrolysis and ammonification of organic nitrogen. The resulting TAN/COD_{VFA} ratio is 0.10 gNH_4^+-N/COD, which is unfavourable to produce PHA (Peña-Picola et al., 2024), thus the recovery of TAN from this

fermentation liquid will then be studied to improve the potential downstream application of the fermentation liquid. At the beginning of the batch, the pH decreased from 6.45 to 6.30, due to the accumulation of VFAs followed by a slight rise in pH on the 7th day, which usually occurs when the VFAs concentration stabilises. The slightly acidic pH (6.6 ± 0.2) provided a reduced risk of inhibition from acidic environment. This favourable pH value is a result of the high buffering capacity of the OFMSW influent. Having a pH stability inherent in the influent is ideal for acidogenic fermentation, as pH plays a critical role in ensuring consistent performance during the fermentation process (Peña-Picola et al., 2024). Finally, a slight increase in the conductivity up to 48.5 ± 0.2 mS/cm was related to the solubilisation of particulate matter and a slight decrease in the total alkalinity (12.5 ± 0.5 $gCaCO_3/L$) was related to VFAs production.

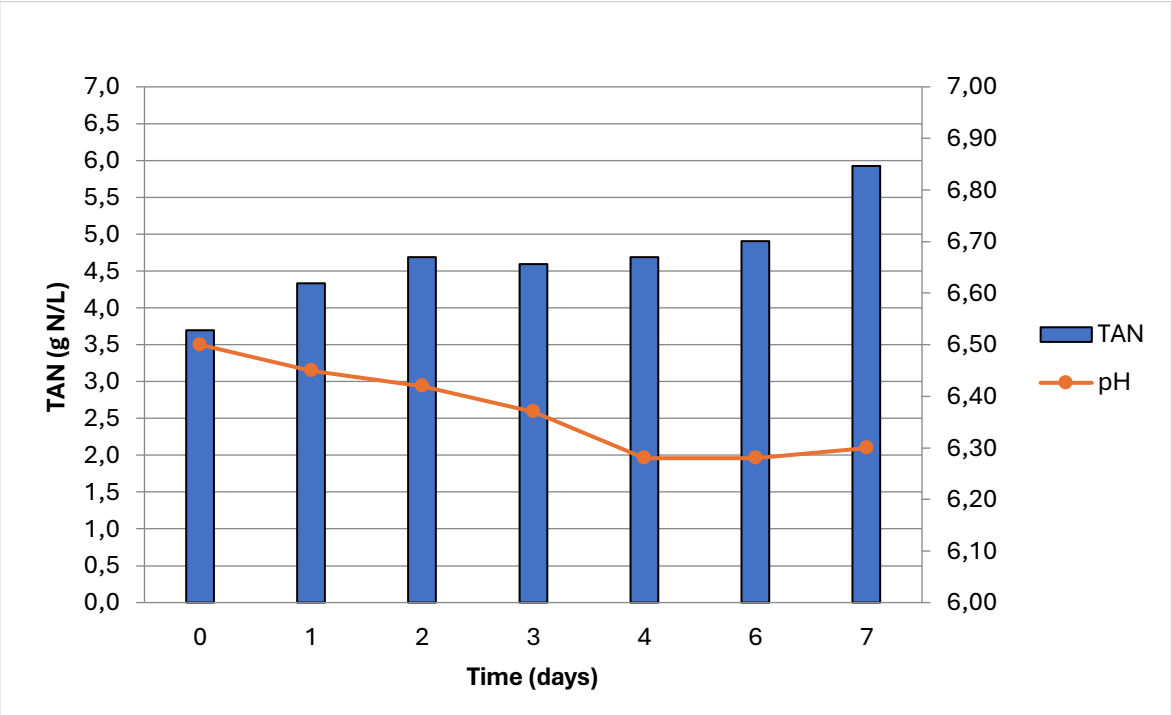

Figure 16: OFMSW fermentation performance in TAN and pH.

4.2 TAN recovery for synthetic feed solution

In this section, the results related to TAN valorisation from highly ammonium loaded (2.5-10 gNH_4^+-N/L) synthetic wastewaters using a GPM are discussed. Table 7 summarises the main results of TAN removal and recovery efficiencies for the synthetic wastewaters tested at different volume ratios. The experimental results show that the performance of the GPM process is stable and effective for

all the studied cases. The parameters evaluated TAN removal and recovery rate, K_m, the ratio mol NaOH/mol TAN recovered and the ratio mol H_2SO_4/mol TAN recovered maintained similar values.

The TAN recovery for tests conducted over 24 h (S1-S3) are slightly lower than those conducted over 54 h (S4-S11), an indication that the process can also be conducted in a shorter timeframe.

The K_m values of the GPM remain uniform for the experiments performed, since it is highly dependent on the wastewater matrix and the working pH and temperature, which is the same for all the experiments carried out. The results between the tests S1-S3 and S4-S11 are comparable as volume ratio does not consider in the statistical calculation of the K_m. Other references reported similar K_m values when operating the same membrane module under similar conditions ($(2.99 \pm 0.04)\cdot10^{-7}$ m/s (Serra-Toro et al., 2024)).

The total reagent consumption per mole of TAN recovered for both NaOH and H_2SO_4 was statistically similar for all tests conducted and very close to the theoretical values (1 mol NaOH/mol N recovered and 0.5 mol H_2SO_4/mol N recovered). These parameters, related to the pH values maintained, ensure the gradient difference and greater performance of the membrane. Higher pH can be directly related to the higher amount of NH_3 in the solution due to the displacement of the NH_4^+/NH_3 equilibrium. The superior performance of NH_3 membrane contactors at pH 9.0 is in accordance with the results reported (Noriega-Hevia et al., 2023).

Table 7: Performance parameters in experiments using synthetic feed solution.

Test	ω (Vf/Vt)	gN/L initial	TAN removal (%)	TAN recovery (%)	K_m (m/s)	mol NaOH/ mol TAN	mol H2SO4/ mol TAN
S1	2	2.35	99.67	99.68	$(1.43 \pm 0.04)\cdot10^{-6}$	1.12	0.52
S2	2	2.35	98.77	98.73	$(1.32 \pm 0.07)\cdot10^{-6}$	1.17	0.51
S3	2	10.0	92.45	91.22	$(1.65 \pm 0.23)\cdot10^{-7}$	1.75	0.68
S4	10	2.35	99.91	99.96	$(8.67 \pm 0.34)\cdot10^{-7}$	1.36	0.66
S5	10	2.35	99.99	99.99	$(1.10 \pm 0.05)\cdot10^{-6}$	1.24	0.62
S6	10	5.5	99.96	99.96	$(5.14 \pm 0.11)\cdot10^{-7}$	0.90	0.57
S7	10	5.5	99.98	99.98	$(6.50 \pm 0.34)\cdot10^{-7}$	1.03	0.57
S8	10	7.0	99.97	99.97	$(5.53 \pm 0.01)\cdot10^{-7}$	0.99	0.53
S9	10	7.0	99.96	99.96	$(4.67 \pm 0.21)\cdot10^{-7}$	0.92	0.56
S10	10	10.0	99.98	99.98	$(8.96 \pm 0.58)\cdot10^{-7}$	1.01	0.47
S11	10	10.0	99.96	99.96	$(5.01 \pm 0.07)\cdot10^{-7}$	1.08	0.52

The NH_3 diffusion through the GPM was not affected by the presence of acetic acid based to literature reports (Peña-Picola et al., 2024). Acetic acid concentration in the feed solution (samples taken at 0 h, 6 h, 24 h and 54 h) remained nearly constant during all the experiments (Table 8).

Slight increase is observed due to the decrease in the volume of the feed is observed (related to water diffusion). Moreover, acetic acid concentration in the trapping solution was below the detection limit for all experiments (<10 mg/L). The retention of acetic acid allows to assume that VFAs with higher molecular weight (e.g. propionic acid, butyric acid, …) would not diffuse across the membrane and would not affect the nitrogen recovery efficiency under the tested operating conditions. These results are in line with the literature results (Riaño et al., 2021) reporting a minimal transfer of soluble organic matter (5-20 mgCOD/L·day) and cations (0-20 mg/L·day).

The amount in g $(NH_4)_2SO_4$/L of final ammonium sulphate recovery and its percentage by weight was also calculated using the stoichiometric equation. This value increases as the initial TAN concentration in the solution is increased, and it is possible to achieve high quantities suitable for industrial use. In the following section the issue of volumes variation in these experiments, due to water diffusion, will be discussed.

Table 8: Performance parameters in experiments using synthetic feed solution.

Test	ω (Vf/Vt)	Feed solution						Trapping solution	
		Initial TAN (gN/L)	Final TAN (gN/L)	AcOH 0h (gCOD/L)	AcOH 6h (gCOD/L)	AcOH 24h (gCOD/L)	AcOH 54h (gCOD/L)	Final TAN (gN/L)	$(NH_4)_2SO_4$ (% w/w)
S1	2	2.35	4.77	4.56	4.88	4.94	-	22.49	2.25
S2	2	2.35	4.79	4.61	4.85	4.98	-	22.59	2.26
S3	2	10.0	15.27	4.78	4.88	4.94	-	72.05	7.21
S4	10	2.35	11.87	4,72	4.87	5.09	5.49	56.01	5.60
S5	10	2.35	11.18	4,68	4.80	5.36	5.54	52.77	5.28
S6	10	5.5	18.22	4.04	4.62	5.19	5.55	86.01	8.60
S7	10	5.5	17.55	4.36	5.05	5.00	5.11	82.84	8.28
S8	10	7.0	22.58	4.99	4.97	5.02	4.93	106.58	10.66
S9	10	7.0	22.74	4.67	4.50	4.80	5.39	107.32	10.73
S10	10	10.0	27.17	4.26	4.51	4.75	5.48	128.21	12.82
S11	10	10.0	26.98	4.89	4.81	5.04	5.48	127.34	12.73

4.2.1 TAN recovery for synthetic feed solution with volume ratio (ω) 2

The TAN value (in gNH_4^+-N/L) removed from the feed solution and recovered in the trapping solution, has been evaluated for the experiments carried out with synthetic feed solution with a volume ratio ω=2 and over 24 h. Fig. 17 and Fig. 18 show the results, respectively, with an initial TAN concentration of 2.35 gNH_4^+-N/L (S1 and S2) and 10.00 gNH_4^+-N/L (S3).

Slight deviations in the measurement of the initial concentration are observed, but they are in the calculated deviation and can be attributed to possible experimental errors. In S1 and S2 tests no significant volume changes were observed. In S3 test from an initial trapping volume of 2.5 L a volume of 3.54 L was reached at the end of the test, limiting the recovered TAN in this acidic solution. From an initial concentration of 2.35 gNH_4^+-N/L and with the final volume of tapping half the feed, if it remained constant, the expected value of final TAN in the tapping should be 4.70 gNH_4^+-N/L (namely the double). Similarly, from an initial concentration of 10.00 gNH_4^+-N/L and with the final volume of trapping half the feed, if it remained constant, the expected value of final TAN in the tapping should be 20.00 gNH_4^+-N/L (namely the double). The final TAN value recovered for the two tests S1 and S2 (4.77 and 4.79 gNH_4^+-N/L) corresponds to what was expected (4.70 gNH_4^+-N/L) while for the test S3 the value (15.25 gNH_4^+-N/L) does not correspond to what was expected (20.00 gNH_4^+-N/L). This happened because the volume of the trapping solution increased.

The results obtained indicate that under these operating conditions the removal and recovery efficiency is elevated already within 24 h of process (but not complete). In S3 test not all TAN was removed at 24 h. This is noted in removal rate for S1 TAN removal % is 99.67 and 99.68 for S2 TAN removal % is 98.77 and 98.73 while for S3 TAN removal % 92.45 and 91.22. This diminution in S3 recovery/removal is related to the incomplete process in 24 h and water-related phenomena that limited the ammonia transfer. It is therefore necessary to conduct the experiment for more than 24 h to guarantee the maximum recovery of TAN.

The K_m values for S1 and S2 $(1.43 \pm 0.04)\cdot10^{-6}$ m/s and $(1.32 \pm 0.07)\cdot10^{-6}$ m/s are higher in comparison with the value of the test S3 $(1.65 \pm 0.23)\cdot10^{-7}$ m/s. This K_m and volume results indicates that the highest difference in concentration gradient promotes wetting and water passage phenomena. This decreases the efficiency of the entire system.

Despite the significant efficiency of the TAN removed obtained, the final ammonium sulphate concentration was too low to guarantee a quantity useful for large-scale use. Therefore, it is necessary to work with a lower trapping volume trying to achieve the same removal efficiency.

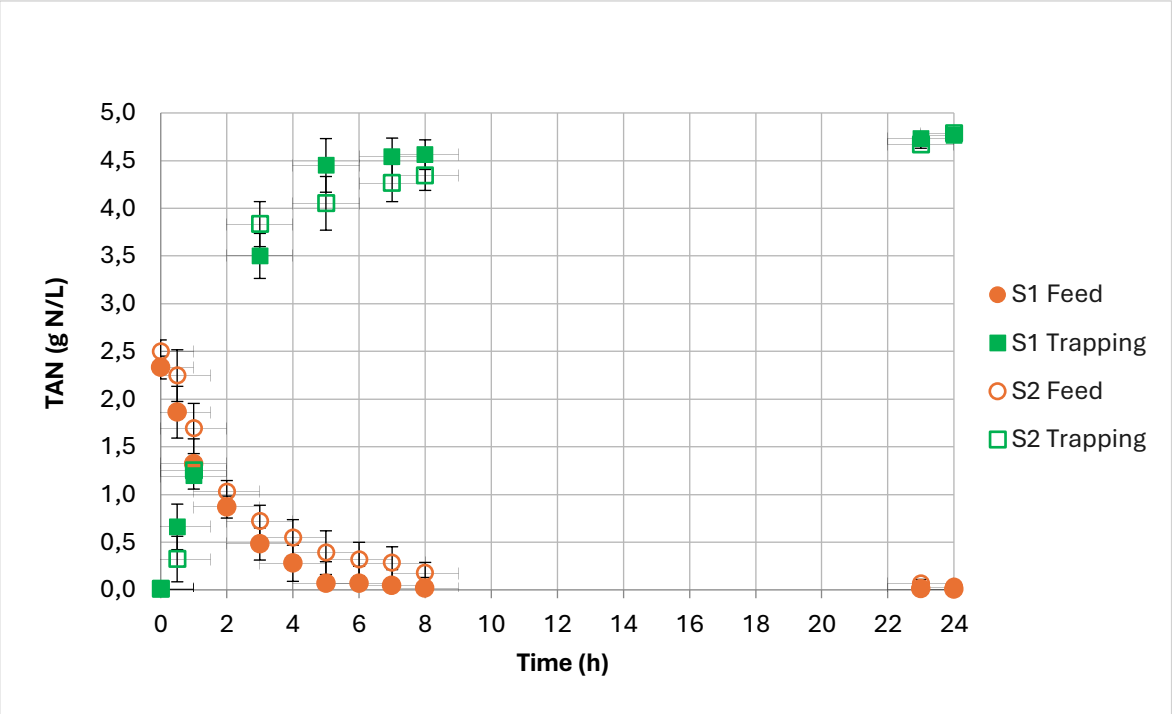

Figure 17: TAN of the synthetic feed and trapping solution over time for two tests (S1-S2) with volume ratio ω=2 and initial TAN of 2.35 gNH_4^+-N/L. Error bars represent the standard deviation between the two tests.

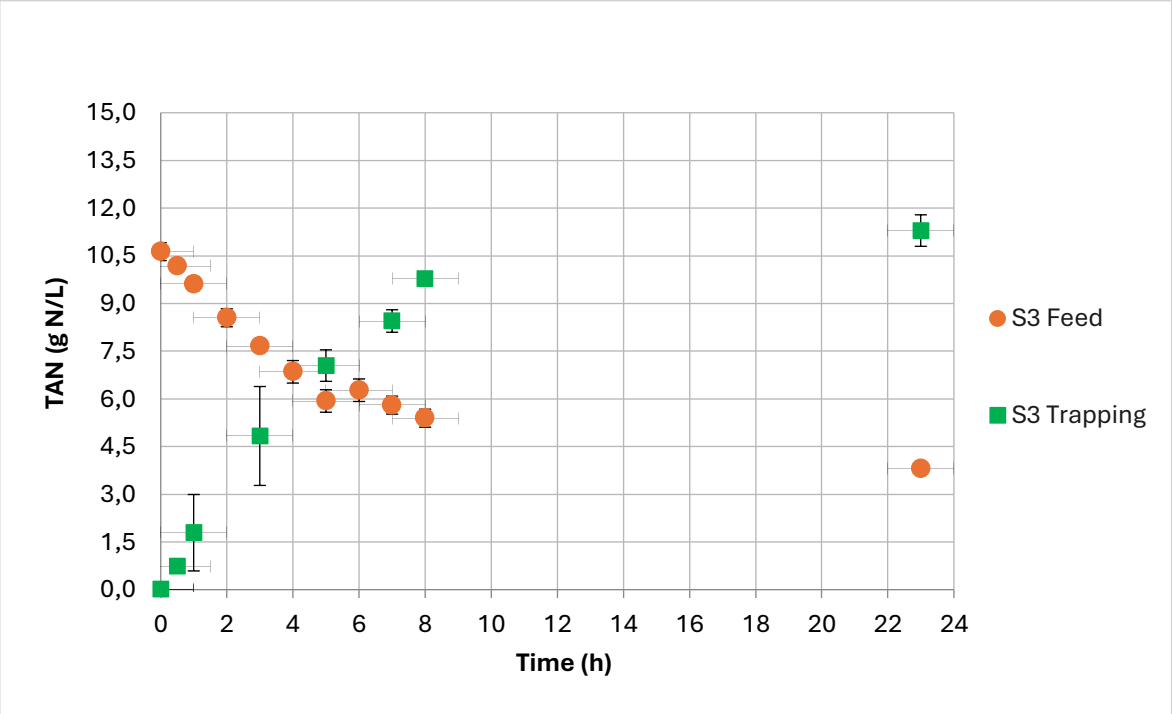

Figure 18: TAN of the synthetic feed and trapping solution over time for one test (S3) with volume ratio ω=2 and initial TAN of 10.0 gNH_4^+-N/L. Error bars represent the standard deviation of the single tests.

4.2.2 TAN removal for synthetic feed solution with volume ratio (ω) 10

The TAN value (in gNH_4^+-N/L) removed from the feed solution and recovered in the trapping solution, has been evaluated for the experiments carried out with synthetic wastewaters with a volume ratio ω=10 and over 54 h. The results obtained working with synthetic wastewaters with an initial TAN concentration of 2.35 gNH_4^+-N/L, 5.50 gNH_4^+-N/L, 7.00 gNH_4^+-N/L. and 10.00 gNH_4^+-N/L are shown in Fig. 19, Fig. 20, Fig. 21 and Fig. 22, respectively. A large experimental error is seen in test S10 and S11 due to difficulties in analysing the elevated TAN at high dilutions.

The results obtained indicate that with these operating conditions the removal and recovery efficiency is maximum already within 8 h of process. However, it was decided to continue the test in order to observe the main limitation of the technology, which is the transfer of water that dilutes the final ammonium concentration of the trapping solution.

The maximum TAN value for the two tests S4 and S5 with an initial concentration of 2.35 gNH_4^+-N/L reached the recovery of 19.03 and 17.46 gNH_4^+-N /L, values very close to what was expected (23.50 gNH_4^+-N /L). The maximum TAN value for the two tests S6 and S7 with an initial concentration of 5.50 gNH_4^+-N /L reached the recovery of 28.67 and 29.42 g NH_4^+-N/L, values with significant difference to what would expect if no water diffusion occurred (55.00 gNH_4^+-N /L). The maximum TAN value for the two tests S8 and S9 with an initial concentration of 7.00 gNH_4^+-N /L reach the recovery of 51.48 and 52.68 gNH_4^+-N/L, values with a significant difference to what would be expected without water diffusion (70.00 gNH_4^+-N/L). Finally, the maximum TAN value for the two tests S10 and S11 with an initial concentration of 10.00 gNH_4^+-N/L reached the recovery of 72.18 and 61.29 gNH_4^+-N/L, values significantly different to what would be achieved with no water diffusion (100.00 gNH_4^+-N/L). The recovery and removal rate are high (close to 99% in most tests) indication that the recovery process is complete in 54 h.

The K_m values for S4 and S5 $(8.67 \pm 0.34)\cdot10^{-7}$ m/s and $(1.10 \pm 0.05)\cdot10^{-6}$ m/s are higher compared to K_m for S10 and S11 $(8.96 \pm 0.58)\cdot10^{-7}$ m/s and $(5.01 \pm 0.07)\cdot10^{-7}$ m/s. This indicates to us a decrease in the efficiency of mass transportation. This K_m and volume increasing in trapping indicates that the highest difference in concentration gradient promotes wetting and water passage phenomena.

For synthetic feed solution fouling effect was not present but wetting and water transfer caused a strong variation in volume. The final ammonium sulphate ($(NH_4)_2SO_4$) concentration obtain in S11 was one of the highest (12.73 %w/w) very close to guarantee a quantity useful for large-scale use. It is necessary to work with a lower trapping volume trying to achieve the same removal efficiency.

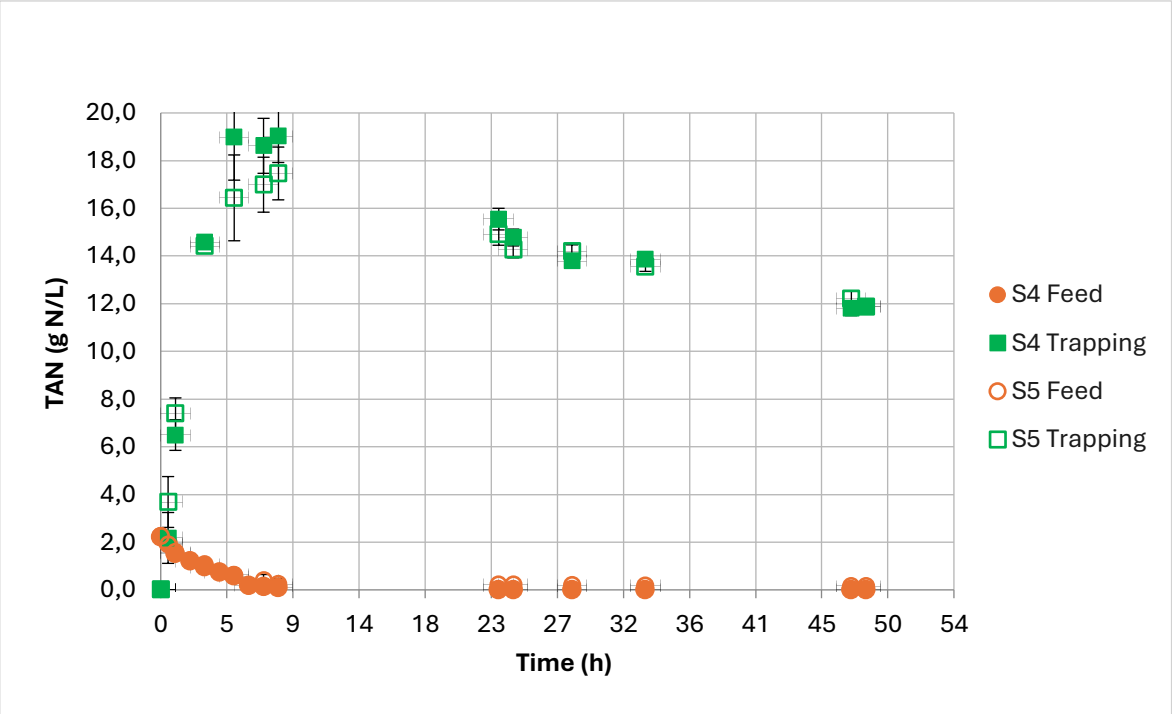

Figure 19: TAN of the synthetic feed and trapping solution over time for two tests (S4-S5) with volume ratio ω=10 and initial TAN of 2.35 gNH_4^+-N/L. Error bars represent the standard deviation between the two tests.

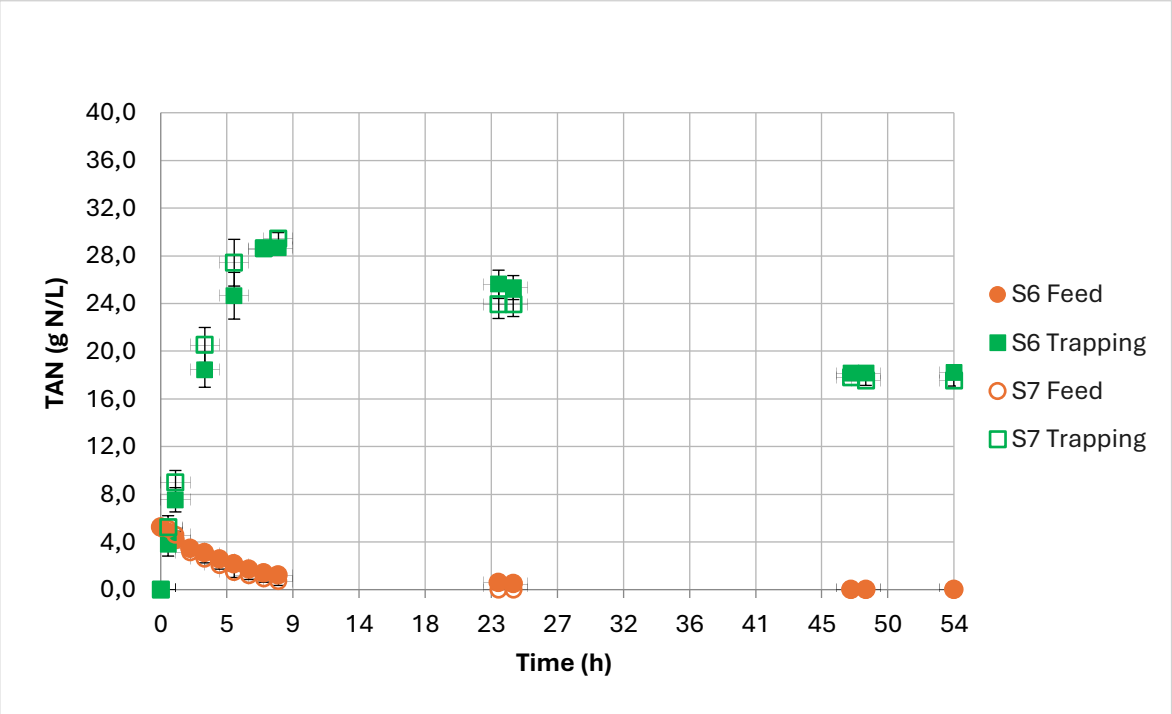

Figure 20: TAN of the synthetic feed and trapping solution over time for two tests (S6-S7) with volume ratio ω=10 and initial TAN of 5.5 gNH_4^+-N/L. Error bars represent the standard deviation between the two tests.

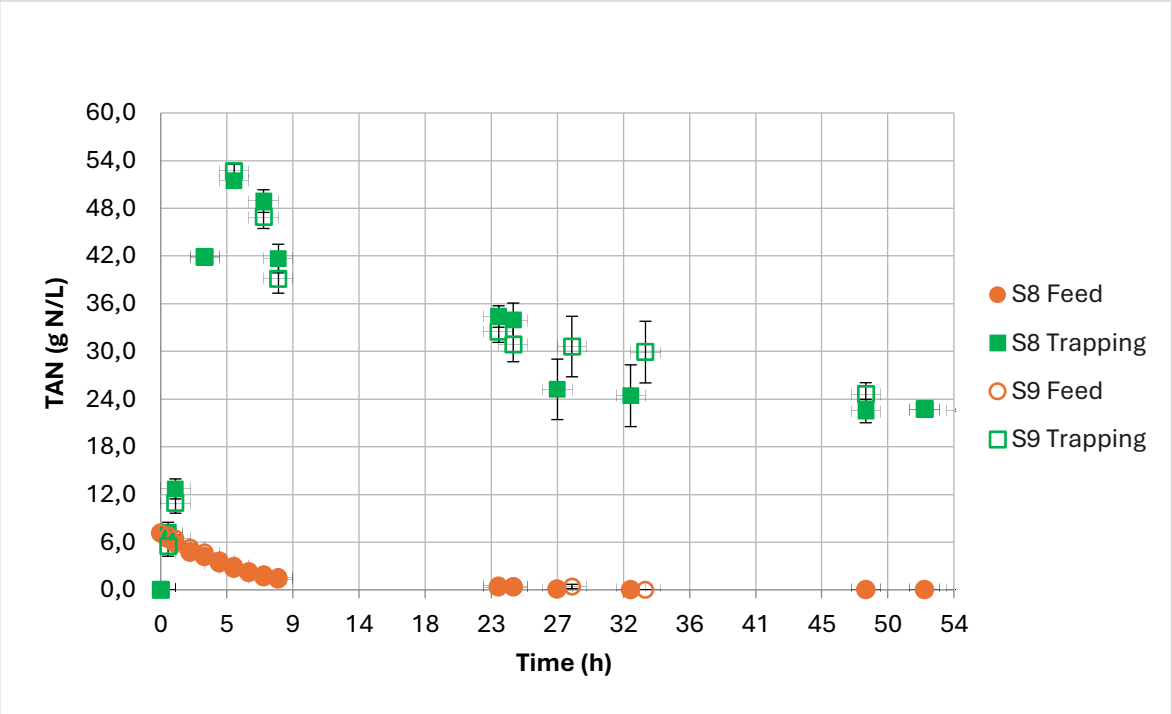

Figure 21: TAN of the synthetic feed and trapping solution over time for two tests (S8-S9) with volume ratio ω=10 and initial TAN of 7.0 gNH_4^+-N/L. Error bars represent the standard deviation between the two tests.

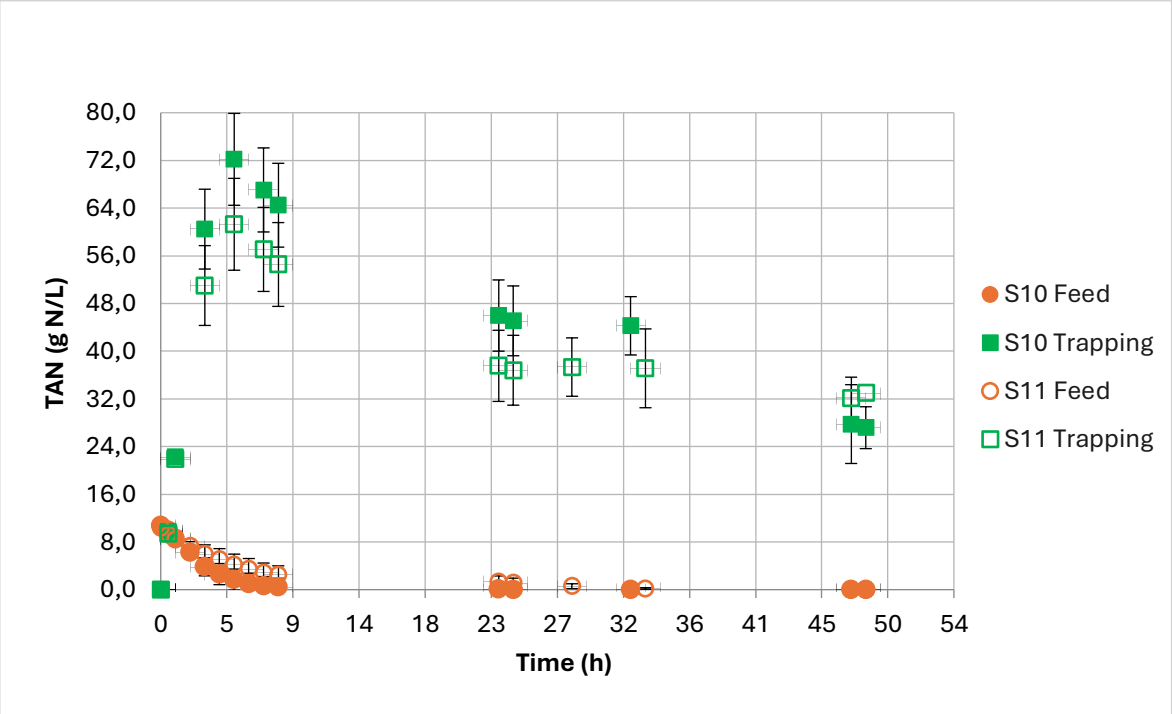

Figure 22: TAN of the synthetic feed and trapping solution over time for two tests (S10-S11) with volume ratio ω=10 and initial TAN of 10.0 gNH_4^+-N/L. Error bars represent standard deviation between the two tests.

In Fig. 23, in the experiments carried out with synthetic wastewater using a volume ratio ω=10 (S4-S11), a pronounced decrease of the volume of the feed was observed. From an initial feed value of 5.00 L it initially increased due to the addition of diluted NaOH (8 M) and then went down significantly over 24 h and subsequently over 54 h reaching 4.24 - 4.57 L. The initial increase in volume is more marked in tests in which the initial TAN concentration is higher (i.e. S11) due to the need to use more NaOH to maintain the pH at 9 and promote the presence of free ammonia. The subsequent decrease in the feed volume was different for those experiments conducted with a lower initial TAN (i.e. S4), this is because must be consider the smaller amount of NaOH that was previously added.

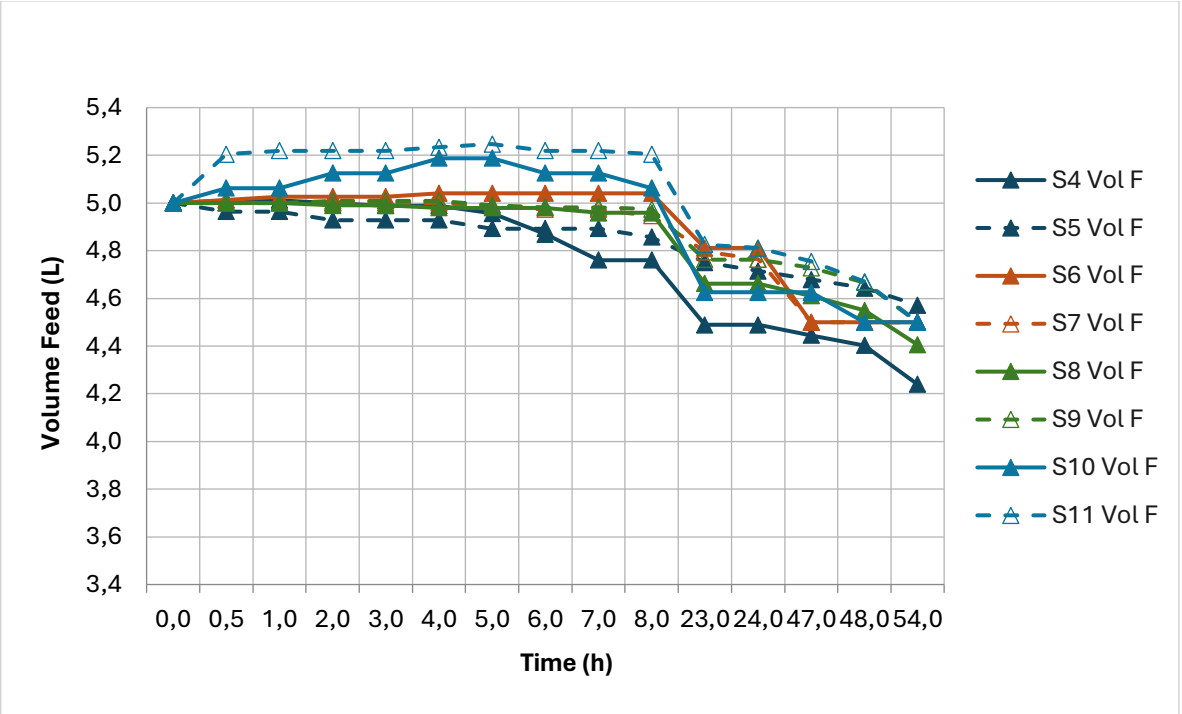

Figure 23: Experimental synthetic feed volume over time for all the test (S4-S11) carried out with a volume ratio of ω=10.

In Fig. 24, in the experiments carried out with synthetic wastewater under a volume ratio of ω=10 (S4-S11), the volume of the trapping solution showed a pronounced increase. For all the tests from an initial feed value of 0.50 L, trapping rises progressively due to the addition of diluted H_2SO_4 (25 %) and then sharp increase over 24 h and subsequently over 54 h reaching 1.25 - 1.81 L.

The volumes of Fig. 23 and Fig. 24 include the volumes of diluted NaOH (8M) and H_2SO_4 (25 %) to control the pH at both sides of the membrane, that contributed to increase the volume in both the feed and trapping solution tanks, but did not significantly affect the membrane performance.

Changes in volume due to the working temperature in both tanks (35°C) were discarded, since both tanks were sealed to avoid evaporation losses. Water diffusion is therefore related to the different water vapour pressure at both sides of the membranes. This water driving force becomes more important when the trapping solution is more concentrated in ammonium sulphate.

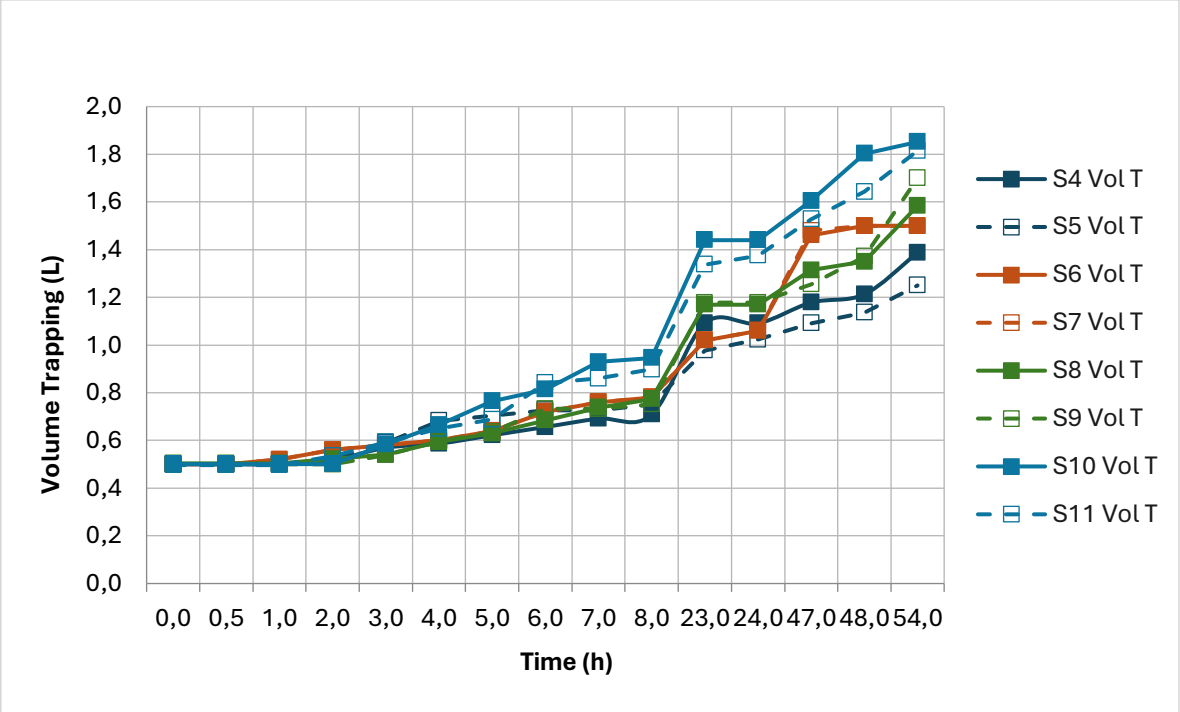

Figure 24: Experimental trapping volume over time for all the test (S4-S11) carried out with a volume ratio of ω=10.

Water passage phenomena had a majoritarian impact in the changes of volumes and trapping dilution. So become important describe this phenomenon and related the water diffusion at higher initial TAN concentration (different osmotic pressure).

A possible model for the transport of TAN and water flux could be described using the mass balance for each tank or cell, feed or trapping (see Fig. 25). This balance assumes that the volume is variable, resulting in four mass balances: two for modelling nitrogen transport and two for modelling water transport between cells. For the TAN transport, an equation (Eq. 7) could be formulated with the driving force being the difference in ammoniacal nitrogen concentrations based on first Fick's Law (Sheikh et al., 2023).

$$\frac{d([TAN]_f \cdot V_f)}{dt} = -K_m \cdot A \cdot \left([N_{NH_3}]_f - [N_{NH_3}]_t\right) \qquad \text{(Eq. 7)}$$

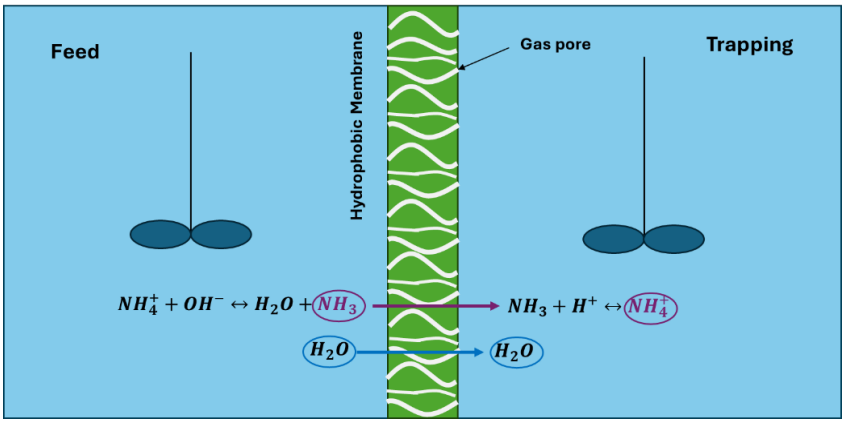

Figure 25: Model diagram of membrane contactor considering the water passage.

Water transport between cells might be modeled with another mass balance, where the driving force is assumed to be the difference in osmotic pressure between the cells. Although the development of the model does not fall within the objectives of this study, it is important to bring the attention of the authors as there is no literature that has dealt with this aspect when working with high ammonium loaded wastewaters (up to 10 gNH_4^+-N/L).

In Fig. 26 the trapping-feed ratio (in gNH_4^+-N/L) was evaluated and pictured. It is possible to describe a decreasing ratio between TAN recovery in trapping and initial TAN concentration increases.

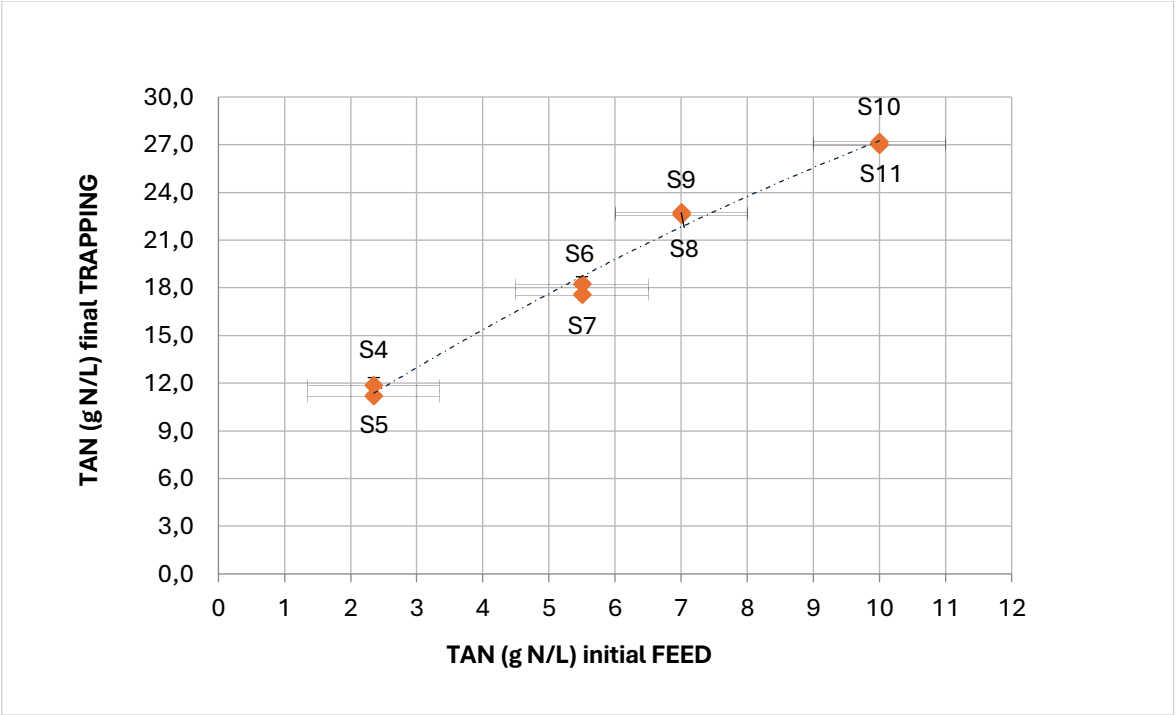

Figure 26: Final TAN in trapping respect to the initial TAN in feed for synthetic wastewater working with a volume ratio ω=10. Error bars represent the standard deviation between the two tests.

This reduction is mainly for the exponential increase in volume, as already noted, related to the effects of wetting and water passage due to large difference in concentration gradient. Synthetic feed solution values provide us with an idea of the potential ammonium recovery (theoretical) that should be achieved for real wastewaters. Hardly a quantity of ammonium salt [$(NH_4)_2SO_4$ 20% w/w] will be achieved in real water, where other factors such as salinity, ionic strength and vapour pressures are involved.

4.3 TAN recovery from different wastewaters

The TAN removal and recovery efficiencies using a GPM were also evaluated for the experiments carried out with OFMSW AD supernatant, OFMSW fermentation liquid and animal by-products ABPs wastewater as reported in Table 9.

The experimental results show that the performance of the GPM process is stable and effective throughout all the experiments. The parameters evaluated were TAN removal and recovery, K_m, the ratio mol NaOH/mol TAN recovered and the ratio mol H_2SO_4/mol TAN recovered.

Animal by-products ABPs wastewater significantly diverged comparing the other test parameters. The test A1 failed due to a rise in the volume of the feed reactor greater than the maximum containable volume. The explanation for this phenomenon is related to the high salinity content of this real effluent and will be addressed later and therefore this test will no longer be compared.

The TAN recovery values for tests conducted over 24 h (D1-F1) are similar than those conducted over 54 h (D2-D3-F2-A2), which is an indication that the process can also be conducted in a shorter timeframe.

Table 9: Performance parameters in experiments using different wastewater.

Test	ω (Vf/Vt)	gN/L initial	TAN removal (%)	TAN recovery (%)	K_m (m/s)	mol NaOH/ mol TAN	mol H_2SO_4/ mol TAN
D1	2	5.61	95.96	95.78	$(2.56 \pm 0.08)\cdot10^{-7}$	1.04	0.55
F1	2	6.20	99.51	99.25	$(3.40 \pm 0.18)\cdot10^{-7}$	1.36	0.73
A1	2	10.46	17.90	6.08	$(4.63 \pm 0.78)\cdot10^{-8}$	-	-
D2	10	5.43	98.65	98.44	$(4.38 \pm 0.21)\cdot10^{-7}$	0.97	0.66
D3	10	5.50	99.88	99.89	$(4.88 \pm 0.36)\cdot10^{-7}$	0.83	0.62
F2	10	5.91	97.42	96.89	$(4.33 \pm 0.26)\cdot10^{-7}$	1.20	0.61
A2	5	9.90	99.67	99.67	$(1.23 \pm 0.04)\cdot10^{-6}$	0.99	0.37

The K_m values remained uniform for the experiments performed. The results between the tests conducted at a volume ratio ω=2 for 24 h (D1-F1-A1) and at a volume ratio ω=10 for 54 h (D2-D3-F2-A2) were comparable as this volume ratio does not affect the K_m (Serra-Toro et al., 2024). Similar K_m values ($5.9 \cdot 10^{-7}$ m/s and $8.8 \cdot 10^{-7}$ m/s) operating with the same membrane module under similar conditions is reported (Serra-Toro et al., 2022; Vecino et al., 2019) for AD OFMSW supernatant and OFMSW fermentation broths. (Serra-Toro et al., 2024).

Consumption of reagents in the feed solution and in the trapping solution is also considered. The total reagent consumption per mole of TAN recovered for both NaOH and H_2SO_4 was statistically similar for all tests conducted and in good agreement with those reported by (Serra-Toro et al., (2024)). Slightly higher values are noted for the test OFMSW fermented liquid (F1 and F2) and can be attributed to the lower pH and high TAN concentration.

The NH_3 recovery using the GPM process did not affect the concentration and composition of VFAs (Table 10). It is important to highlight that at the beginning of each GPM assay, the initial VFAs concentration for OFMSW AD supernatant and OFMSW fermentation liquid could be slightly lower due to a VFAs loss during sample post-treatment (i.e., filtration and centrifugation).

However, during the GPM treatment no significant losses of VFAs were observed. A slight decrease (22% and 11%-22% on COD basis) noticeable for OFMSW AD supernatant is and could be attributed to biological aerobic degradation of these compounds. This decrease could be related to the possible composition of the effluent characterised by more volatile acids and a higher volatile fraction.

Table 10: Performance parameters in experiments using different wastewater.

Test	ω (Vf/Vt)	Feed solution						Trapping solution	
		Initial TAN (gN/L)	Final TAN (gN/L)	VFAs 0h (gCOD/L)	VFAs 6h (gCOD/L)	VFAs 24h (gCOD/L)	VFAs 54h (gCOD/L)	Final TAN (gN/L)	$(NH_4)_2SO_4$ (% w/w)
D1	2	5.61	9.32	0.57	0.72	0.44	-	43.98	4.40
F1	2	6.20	8.79	40.12	39.27	39.05	-	41.47	4.15
A1	2	10.46	0.07	-	-	-	-	0.34	0.03
D2	10	5.43	19.16	0.65	0.60	0.48	0.58	90.42	9.04
D3	10	5.50	21.28	0.77	0.65	0.45	0.42	100.42	10.04
F2	10	5.91	18.36	40.77	39.34	38.49	38.86	86.66	8.67
A2	5	9.90	28.06	-	-	-	-	132.40	13.24

In all feed solution tests VFAs concentration (samples taken at 0 h, 6 h, 24 h and 54 h) remained similar during all the experiments. Accordingly, loss of VFAs is not related to their passage through the GPM since in the trapping solution VFAs value was below the detection limit for all experiments (<10 mg/L). No increase in ions concentration (i.e. Ca^{2+}, Mg^{2+}, K^{+}, Na^{+}, Cl^{-}) was detected in the trapping solution (detection limit of 0.5 mg/L). This demonstrates that VFAs and ions are unable to diffuse across the membrane under the tested short-term conditions.

The final ammonium sulphate recovery amount in $g(NH_4)_2SO_4/L$ and its percentage by weight was also calculated using the stoichiometric equation. For ω=10, the values related to OFMSW fermented liquid (86.7 $g(NH_4)_2SO_4/L$) and OFMSW AD supernatant (90.4-100.4 $g(NH_4)_2SO_4/L$) were lower than that obtained with ABP (132.4 $g(NH_4)_2SO_4/L$). This was attributed to a lower water passage thanks to the high salinity of the feed (57 mS/cm).

4.3.1 TAN recovery for OFMSW AD supernatant

The evolution of TAN concentration (in gNH_4^+-N/L) removed from the feed and recovered in trapping, has been evaluated for the experiments carried out with OFMSW AD supernatant (5.60 gNH_4^+-N/L). Fig. 27 and Fig. 28 show the results when working with a volume ratio of ω=2 and ω=10, respectively.

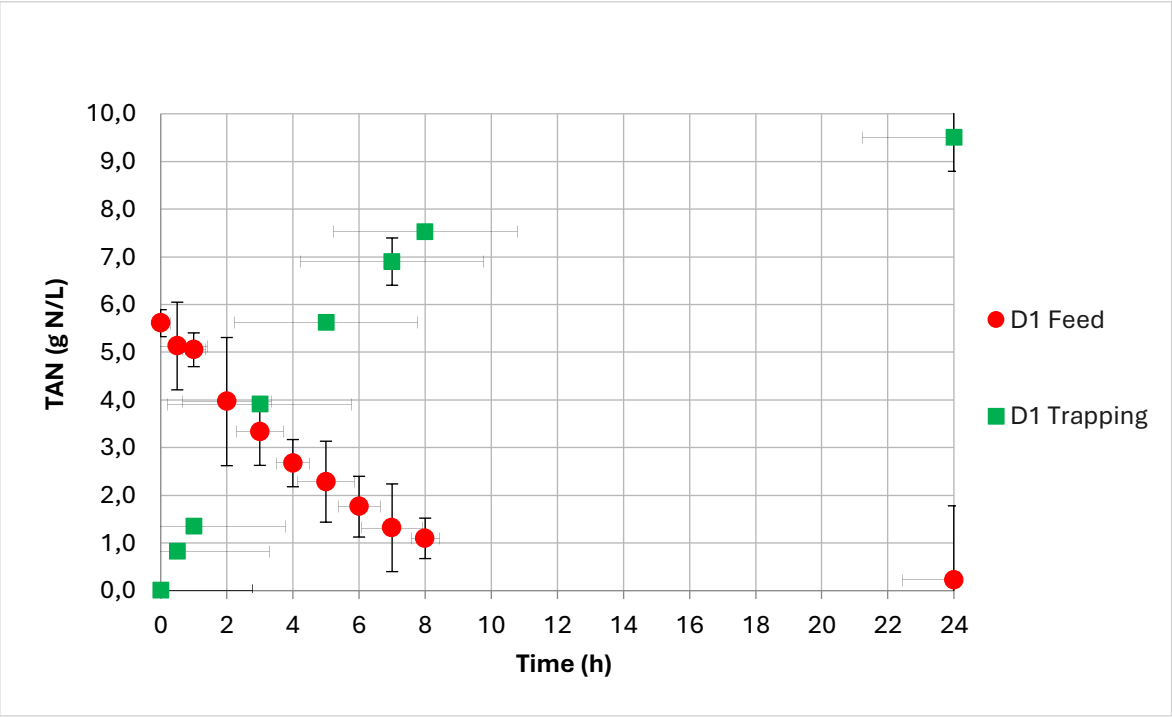

Figure 27: TAN of the OMFSW AD supernatant feed and trapping solution over time for one test (D1) with volume ratio ω=2. Error bars represent the standard deviation of the single tests.

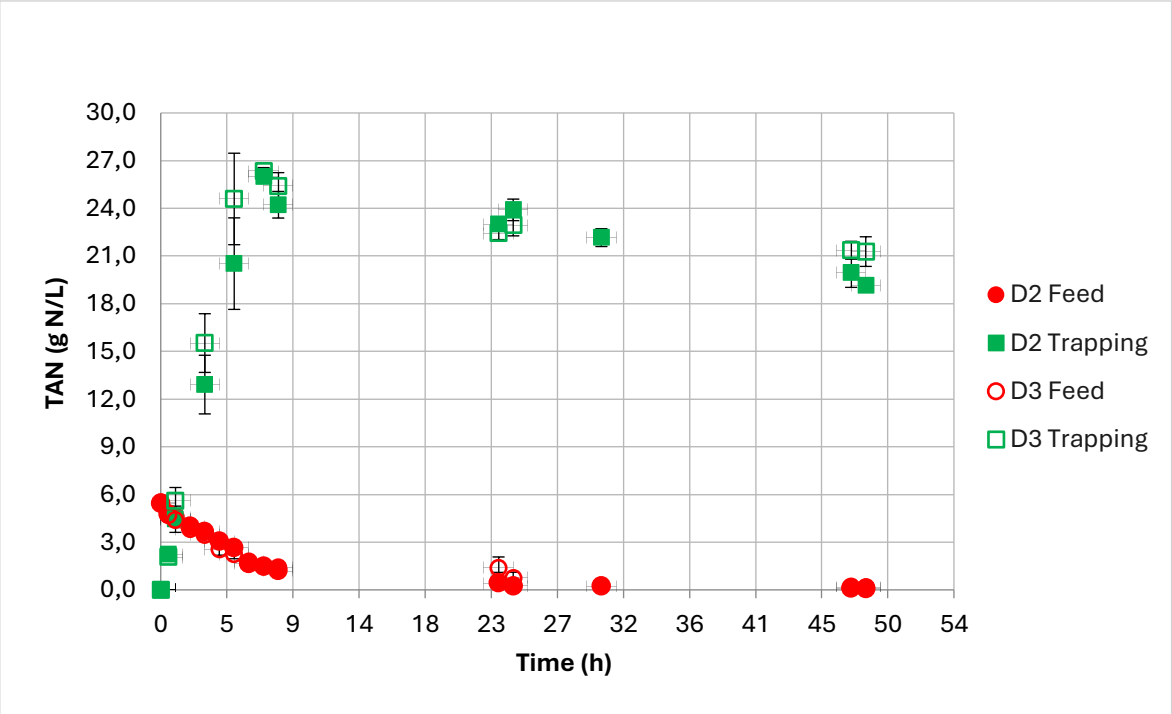

Figure 28: TAN of the OMFSW AD supernatant feed and trapping solution over time for two tests (D2-D3) with volume ratio ω=10. Error bars represent the standard deviation between the two tests.

The higher TAN fluxes gained in these experiments could be attributed to higher initial TAN concentration of the OFMSW AD supernatant (higher driving force due to the concentration gradient). A high recovery and removal rate was achieved.

Since K_m does not depend on the operation time, initial TAN concentration, volumes of feed and trapping solution or molar acid/basic ratio, will be the parameters used to compare results. The K_m values obtained with OFMSW AD supernatant (Table 8) showed the same synthetic solution trend. The K_m values fall within the range previously recorded: at ω=2 was $(2.56 \pm 0.08)\cdot10^{-7}$ m/s and at ω=10 were $(4.38 \pm 0.21)\cdot10^{-7}$ m/s and $(4.88 \pm 0.36)\cdot10^{-7}$ m/s; while the equivalent K_m for the synthetic feed solution at ω=10 were $(5.14 \pm 0.11)\cdot10^{-7}$ m/s and $(6.50 \pm 0.34)\cdot10^{-7}$ m/s.

The slightly lower performance of the GPM contactor using the OFMSW AD supernatant might be related to the more complex matrix of industrial wastewaters that could also impact on membrane fouling. However, the fouling effect is nevertheless limited, since a regular cleaning was carried out and tests with industrial wastewaters were alternated with synthetic solution test. The low fouling observed in these experiments could be attributed to the low fouling propensity of PP membranes compared with other membranes such as PTFE membranes (Zarebska et al., 2014). Accordingly, the loss of performance could be related to the interference (e.g., ionic interaction) of other species and the complex matrix of the fermentation liquid.

The total NaOH and H_2SO_4 consumption in the OFMSW AD supernatant experiments (Table 8) was almost the same than the consumption in the synthetic feed experiments (Table 6). The NaOH required to adjust the pH at the beginning of the experiment was higher, but the amount of NaOH required to keep the pH at the set point was noticeably lower. This behaviour can be explained by the total alkalinity of the OFMSW AD supernatant (20.7 ± 0.5 $gCaCO_3$/L) that acted as a buffer making the pH of the feed solution harder to raise, but also harder to decrease during the operation.

The total consumption of H_2SO_4 was similar to synthetic feed solution experiments, but its addition during the experiment was slightly higher, probably only caused by the excess of acid in the trapping solution at the end of the test due to the limited accuracy of the dosing pump controlling the trapping solution pH.

4.3.2 TAN recovery for OFMSW fermented liquid

The evolution of TAN concentration (in gNH_4^+-N/L) removed from the feed and recovered in trapping, has been evaluated for the experiments carried out with OFMSW fermented liquid (5.90 gNH_4^+-N/L). Fig. 29 and Fig. 30 show the results when working with a volume ratio of ω=2 and ω=10, respectively.

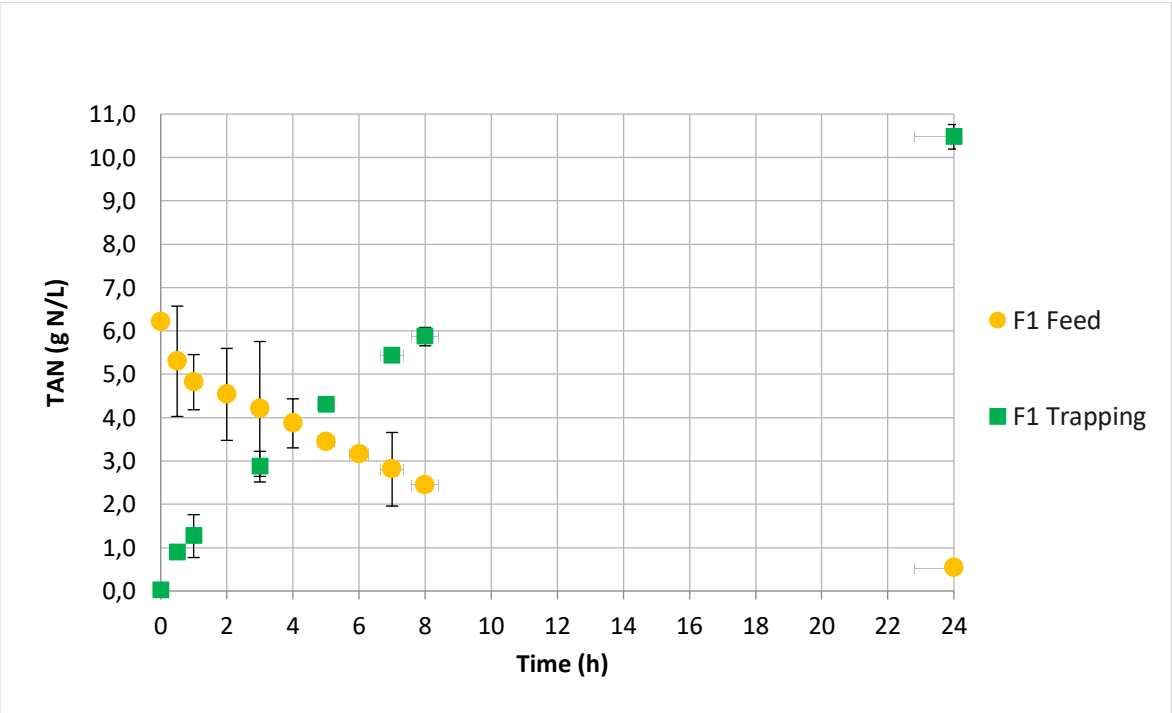

Figure 29: TAN of the OFMSW fermented feed and trapping solution over time for one test (F1) with volume ratio ω=2. Error bars represent the standard deviation of the single tests.

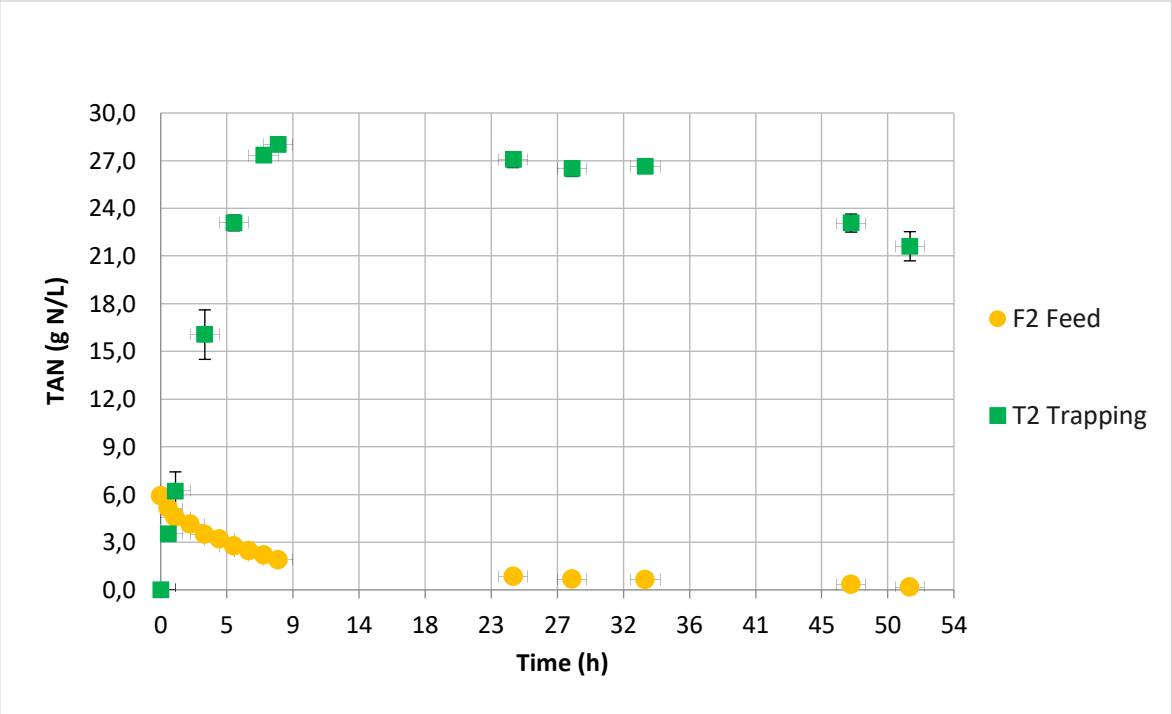

Figure 30: TAN of the OFMSW fermented feed and trapping solution over time for one test (F2) with volume ratio ω=10. Error bars represent the standard deviation of the single tests.

For the test conducted with ω=2 the removal of TAN was similar to the tests conducted with synthetic wastewater, where an increase to twice the initial concentration was observed in 24 h.

For the test conducted with ω=10 the results obtained indicate that, under these operating conditions, the TAN concentration in the trapping solution reached 28 gNH_4^+-N/L within 8 h of process performance. However, a progressive decrease in TAN concentration of trapping solution was observed up to 54 h due to the water diffusion from the feed tank to the trapping solution. These results are in line with those obtained for the synthetic feed solution.

TAN fluxes were higher in the first hours of operation, which can be attributed to a higher TAN concentration gradient on both sides of the membrane. However, the percentage of TAN recovery was slightly lower than that obtained when using OFMSW AD supernatant, which could be related to the characteristics of this wastewater (e.g. salinity, VFA content, …) or to membrane layer effects. K_m, because of its parameter independence, will be the used to compare these results with others.

The tests using OFMSW fermented liquid (Table 8) showed the same trend observed in the experiments carried out synthetic wastewater: higher NH_3 mass transfer as the feed-trapping volume ratio increases. However, the K_m values calculated were slightly lower than those obtained using synthetic wastewaters, because of its more complex matrix.

Namely, the K_m values at ω=2 was (3.40 ± 0.18)·10^{-7} m/s and at ω=10 was (4.33 ± 0.26)·10^{-7}, while the equivalent K_m for the synthetic feed solution at ω=10 were (5.14 ± 0.11)·10^{-7} m/s and (6.50 ± 0.34)·10^{-7} m/s. The lower performance using the OFMSW fermented liquid might be related to other species interference (e.g., ionic interaction) and the complex fermented liquid matrix.

The total NaOH and H_2SO_4 consumption in the OFMSW fermented liquid experiments (Table 8) was almost the same than the consumption in the synthetic feed experiments (Table 6). The NaOH required to adjust the pH at the beginning of the experiment was higher, but the amount of NaOH required to keep the pH at the set point was noticeably lower. This behaviour can be explained by the total alkalinity of the OFMSW fermented liquid (12.5 ± 0.5 g $CaCO_3$/L) that acted as a buffer making the pH of the feed solution harder to raise, but also harder to decrease during the operation.

4.3.3 TAN recovery for ABPs wastewater

The evolution of TAN removed (in gNH_4^+-N/L) from the feed solution and recovered in trapping, has been evaluated for the experiments carried out with ABPs wastewater (11.90 gNH_4^+-N/L). Fig. 31 and Fig. 32 show the results when a volume ratio of ω=2 and ω=10 was applied, respectively.

In Fig. 31, the test conducted with ω=2 failed because a water passage from the trapping solution to the feed solution occurred. The transfer of water in 6 h completely filled the feed reactor to the maximum (7 litres), although a volume was taken from it to allow TAN recovery to continue. This unusual result did not allow for the measurement of some parameters. The VFAs and NaOH - H_2SO_4 consumption in this ABPs experiments (Table 8 and Table 9) were not possible to measure (the amount in mL of acid and base added is negligible).

Up to 6 h a constant remove of TAN in the feed and TAN recovery in the trapping solution can be observed. This trend is in line with previous liquids but diverge in recovery time: TAN recovered in trapping exceeds the TAN retained in the feed already after 4 h for synthetic feed solution and wastewater. Higher TAN fluxes are associated with higher initial TAN concentration and consequently higher concentration gradient.

The K_m values obtained for this ABPs wastewater test (Table 8) was lower than that obtained when using synthetic wastewater: the K_m values at ω=2 was (4.63 ± 0.78)·10^{-8} m/s while the equivalent K_m for the synthetic feed solution at ω=2 were (1.65 ± 0.23)·10^{-7} m/s.

These two considerations lead to assume that the TAN recovery process took place, but a second process of water passage took place simultaneously that limited the good performance of the

process. The high salinity of the wastewater tested promoted the water diffusion from the trapping solution to the feed tank, which also hindered TAN recovery. This event might be related to the characteristics of the waste stream and vapor pressure decreased with the increase in ammonia concentration (mass transfer rate reduction). This phenomenon has been also discussed in other works (Ferby et al., 2024; Sürmeli et al., 2018), although it is important to underline that further investigations are necessary.

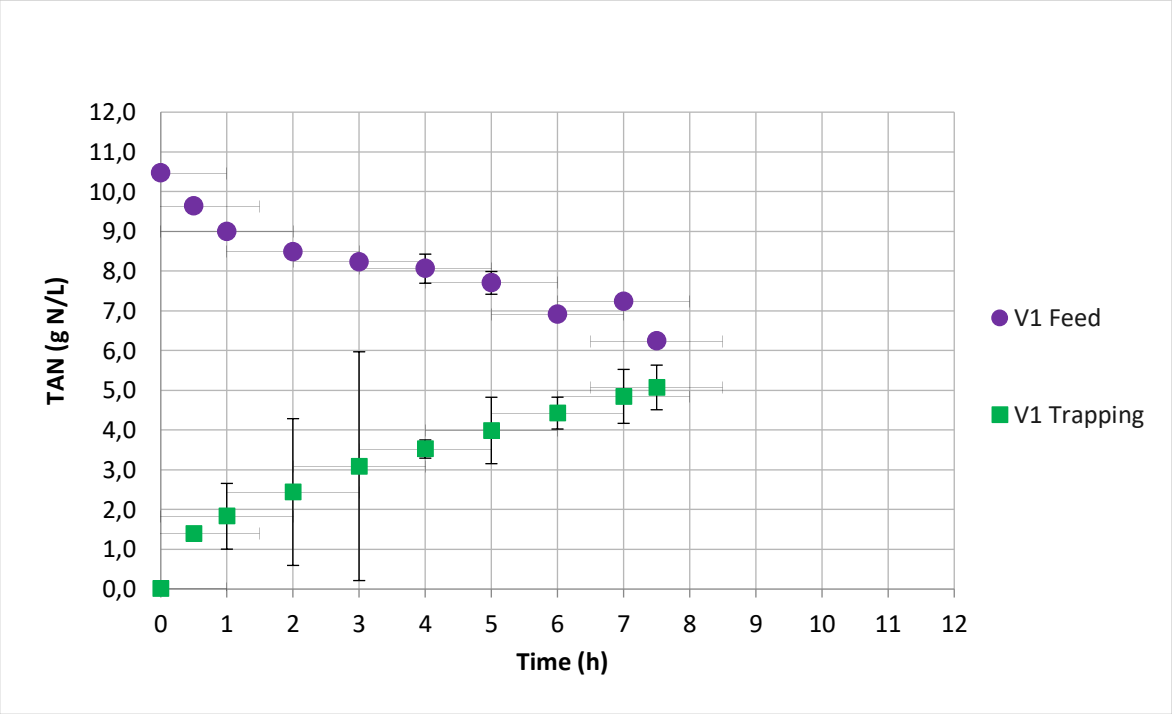

Figure 31: TAN of the ABPs wastewater feed and trapping solution over time for one test (A1) with volume ratio ω=2. Error bars represent the standard deviation of the single tests.

In Fig. 32, the test conducted with ω=5 is in line with those obtained for the synthetic feed solution. In contrast to the test carried out at ω=2, at the beginning of the test water passage from the trapping to the feed solution occurs but as it get concentrated, water passage goes from the feed to the trapping solution. This phenomena has been also reported in some recent research (Ferby et al., 2024). So, this phenomenon didn't compromise the performance of the experiment.

The results obtained indicate that under these operating conditions the nitrogen was almost completely recovered after 8 h of operation. However, TAN concentration in the trapping solution decreased because water diffusion was promoted thanks to the water vapour pressure difference between both sides of the membrane.

The maximum TAN concentration recorded in the trapping solution for the test A2 was 34.6 gNH_4^+-N/L (7.5h of operation). Although this TAN concentration was higher than others reported in the literature when treating other ABP wastewaters using GPM (~25 gNH_4^+-N/L (Garcia-González et al., 2015; Serra-Toro et al., 2022; Sürmeli et al., 2018), this value was significantly lower than the expected value without the osmotic distillation phenomena (99.0 gNH_4^+-N/L).

The high TAN fluxes recorded could be attributed to the high initial TAN concentration of the ABP wastewater, which lead to a high driving force for ammonia recovery.

The K_m values at ω=5 was $(1.23 \pm 0.04)\cdot10^{-6}$ m/s while the equivalent K_m for the synthetic feed solution at ω=10 was $(5.14 \pm 0.11)\cdot10^{-7}$ m/s. The total NaOH consumption (Table 8) was almost the same than the consumption in the synthetic feed experiments (Table 6). The NaOH required to adjust the pH at the beginning of the experiment was higher, but the amount of NaOH required to keep the pH at the set point was noticeably lower. This behaviour can be explained by the total alkalinity of the ABPs wastewater (25.1 ± 0.3 g $CaCO_3$/L) that acted as a buffer making the pH of the feed solution harder to raise, but also harder to decrease during the operation. H_2SO_4 is inferior to the others.

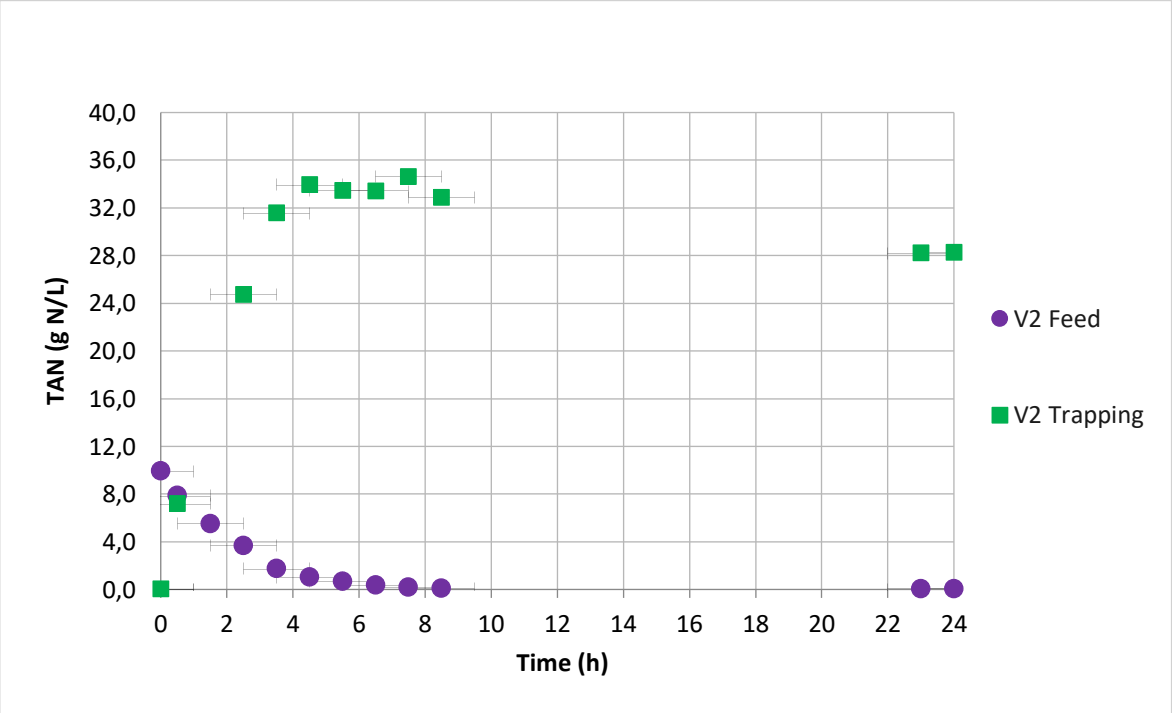

Figure 32: TAN of the ABPs wastewater feed and trapping solution over time for one test (A2) with volume ratio ω=5. Error bars represent the standard deviation of the single tests.

The lower performance using the ABPs fermented wastewater might be related to interference (e.g., ionic interaction) of other species and the complex matrix of the fermentation liquid.

The water transfer occurred between the feed towards trapping but to a much lesser extent than the synthetic feed solution. This agree with what was reported in the test earlier (A1) where ammonia removal efficiency seem independent of feed ammonia concentration. In this case the ionic gradient given by the ionic species in the trapping volume granitised a correct process. Viscosity may affect the ammonia transfer rate by changing ammonia concentrations (Darestani et al., 2017). Salinity (e.g., ionic interaction) could be involved in interference of other species and the complex matrix of the ABPs wastewater. The VFAs in this ABPs experiments (Table 8 and Table 9) were not possible to measure.

4.3.4 TAN recovery comparison between various wastewaters

The ratio between the final TAN concentration in the trapping on the initial TAN concentration in feed was evaluated. Fig. 33 highlight that similar values of TAN recovery ratio between synthetic wastewater and real wastewater are observed.

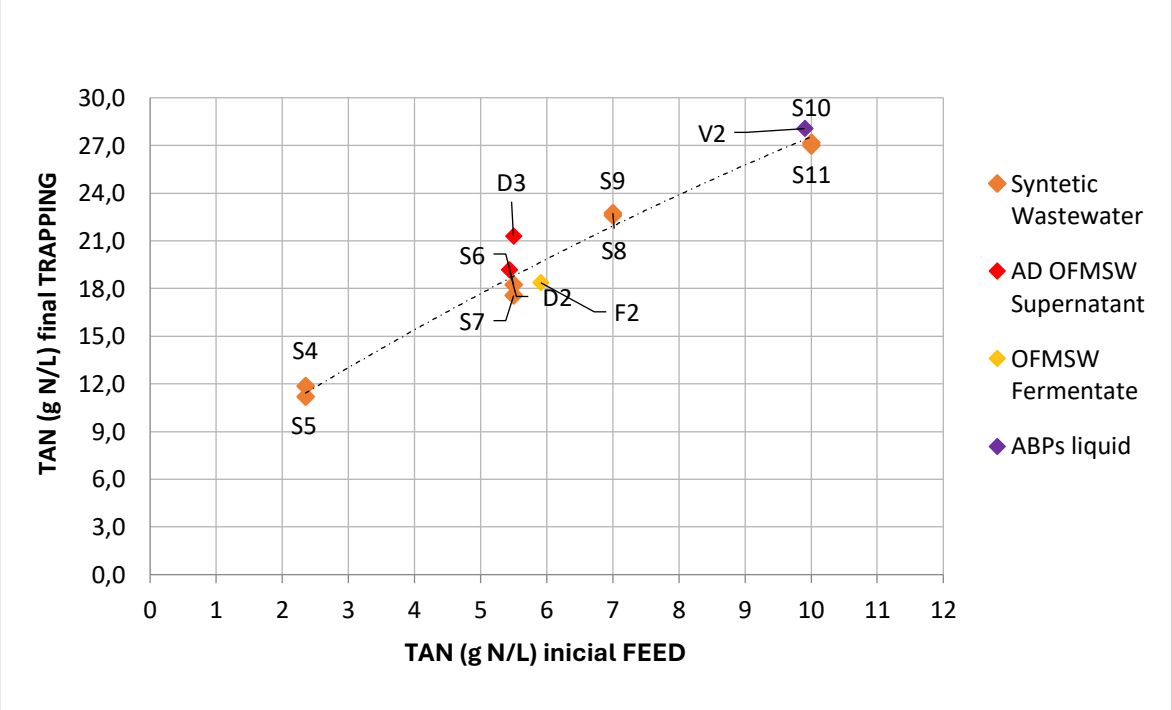

Figure 33: Final trapping TAN recover vs initial TAN removed in synthetic wastewater, OFMSW AD supernatant and OFMSW fermented liquid ratio for the experiment with volume ratio ω=10 carried out. Error bars represent the standard deviation between the two coupled tests.

In all the cases studied, the recovery is related to the mass of TAN in the trapping solution with respect to the initial TAN mass. While another aspect is the maximum TAN concentration potentially reach in the trapping solution. In fact, a constant decrease happens in maximum TAN final concentration as the initial increases. This is mainly due to the exponential increase in volume.

The values obtained provide us with an idea of the potential ammonium sulphate that should be achieved for other wastewaters, where, however, other factors such as salinity, ionic strength and vapour pressures are involved. Ammonium sulphate could be commercialised in the chemical industry at concentrations around 20 ± 0.5 wt.% in weight (Serra-Toro et al., 2024). The maximum obtained concentration (ABPs) of 34.63 g N/L represents a concentration of $(NH_4)_2SO_4$ of 13.7 wt.%. These results imply that GPM contactors need to be improved to produce solution useful at commercial scale without needing further concentration processes.

Moreover, the ammonium sulphate solution obtained from the GPM process had a very low concentration of contaminants, including metals and organic compounds. All the analysed metals were not detected in the trapping solution (detection limit of 100 ppb). The concentration of K, Ca, Mg, Fe, and P ions in the trapping solution was also below the detection limit (3 mg/L).

TOC analysis showed that some organic molecules diffused across the membrane were detected in the trapping solution after 16 h of operation. It is hypothesised that TOC diffusion provided a pale-yellow tone to the trapping solution, which occurred at the very end of the experiment based on visual observation. IC analyses showed that inorganic carbon did not diffuse across the membrane.

To sum up, for almost complete TAN recovery of wastewater at 35 °C, the results of this study suggest as preferred working conditions a pH control around 9.00 in the feed tank and the selection of a feed-to-trapping volume ratio that promotes 20 wt.% of $(NH_4)_2SO_4$ in the trapping solution. These operating conditions would not only lead to high TAN recovery efficiencies, but also to the production of a concentrated $(NH_4)_2SO_4$ with high purity.

In this case where real wastewater are used, several other chemical and physical factors must be taken into account, including salinity and ionic gradient. The salinity of the feed due to its characteristics allows less water to pass through and yet a less pronounced change in volume. These factors buffer the problem of water passage and make TAN recovery technology more attractive.

Methodological procedures adopted have overcome the problem of fouling and wetting. To avoid the fouling phenomenon, filtration and centrifugation were used to obtain the supernatant. This procedure is simple and can also be used on an industrial scale. Among the tests, a simple cleaning

procedure with recirculating water led to the regeneration of the membrane layer. A corrected gradient was used to avoid the phenomenon of wetting.

4.4 Forward osmosis (FO) for VFAs concentration

FO membranes for VFAs concentration and clear water recovery water was investigated. The impact of draw solution concentration (1.25 M $MgCl_2$) and the salinity of the tested wastewaters on permeation flux and achievable WCF were systematically studied. WCF were experimentally obtained when no water permeation flux was observed (i.e. osmotic equilibrium was reached), as a consequence of the dilution of the draw solution over time and salts concentration in the feed.

The efficiency of the FO membrane was measured by monitoring the decrease in volume shown in Fig. 34 for the OFMSW AD supernatant and Fig. 35 for the OFMSW fermented liquid. The final WCF for OFMSW AD supernatant was 3.6 and for the OFMSW fermented liquid was 2.7. This factor indicates that the feed solution has been concentrated more than 2.5 times for both liquids. These values are close to the desired values for these effluents and with a draw solution of 60 g/L.

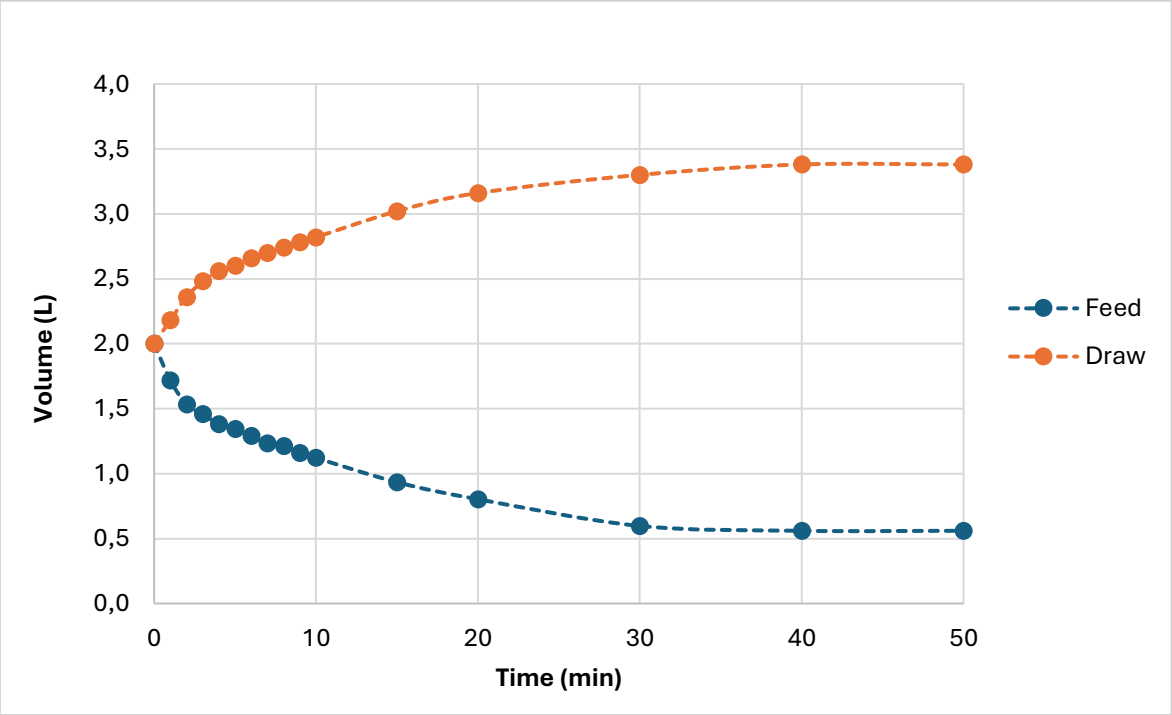

Figure 34: Volume of OFMSW AD supernatant and volume of draw solution over time.

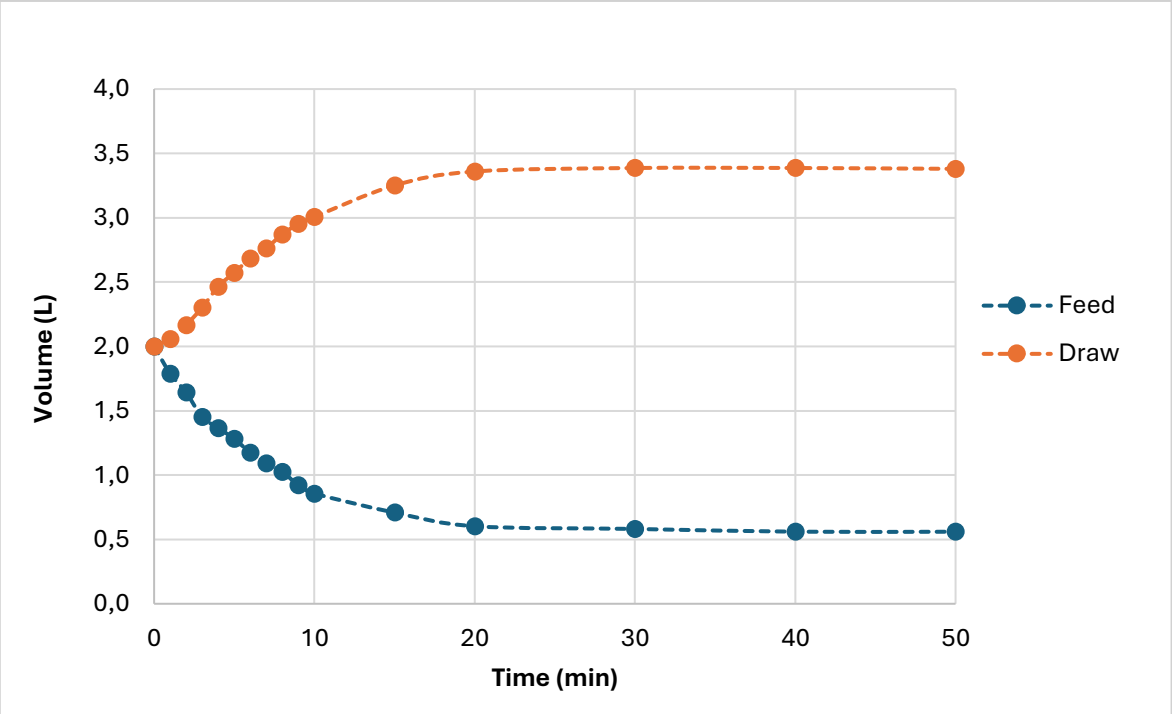

Figure 35: Volume of OFMSW OFMSW fermented liquid and volume of draw solution over time.

The draw solution salinity proved to be an initial key parameter to get high permeation flux and minimized filtration time. The solution salinity of the synthetic draw with concentration of 1.25 M $MgCl_2$ and deionized water allowed a high flux and achieved remarkable WCF value. However, an elevate $MgCl_2$ concentration in the draw solution would lead to higher WCF.

No experimental issues were encountered using OFMSW digestate and fermented for short-term operation of the FO process. The pre-filtered and centrifugated liquid did not cause membrane fouling during the batch or other chemical-physical problems. A simple cleaning procedure with water recirculation allowed to prevent the severe flux decline between batch tests.

Salts accumulation and osmotic backwashing in the layer also could occur, leading to enhance concentration polarization phenomenon and affecting the actual osmotic pressure driving force. The applied cleaning strategy made it possible to avoid these phenomena.

The electric conductivity (EC) of both the feed wastewater and the draw solution, proportional to the inorganic salts content, was recorded to evaluate its impact on the initial permeation flux and the reached WCF. As expected, the salts in the feed solution become concentrated, increasing the EC of the feed and, consequently, the EC of the draw solution decreased until reaching the osmotic equilibrium between both sides of the FO membrane. The conductivity of the feed and draw solution tends to reach the same value in approximately 50 min. A progressive decrease in the draw

solution from 260 mS/cm to 144 mS/cm for the OFMSW digestate (Fig. 36) and from 250 mS/cm to 94 mS/cm for the fermentation liquid from OFMSW (Fig. 37) was monitored, with consequent WCF.

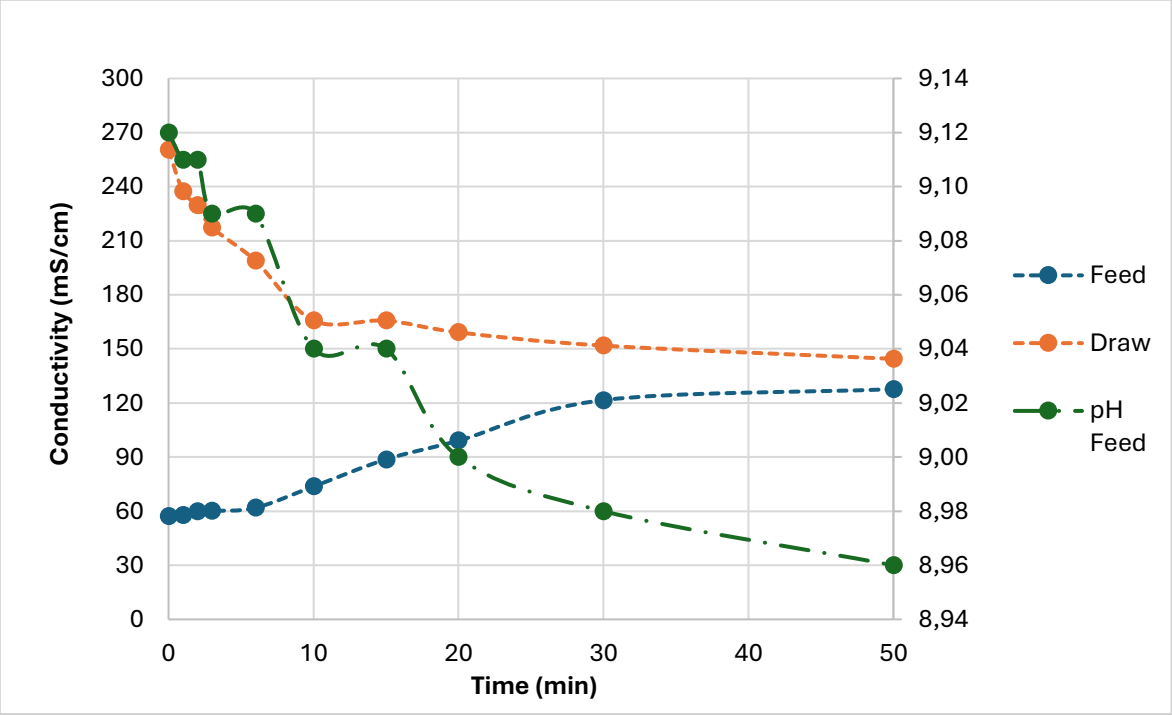

Figure 36: Conductivity of the OFMSW AD supernatant (feed), draw solution and pH of the feed over time.

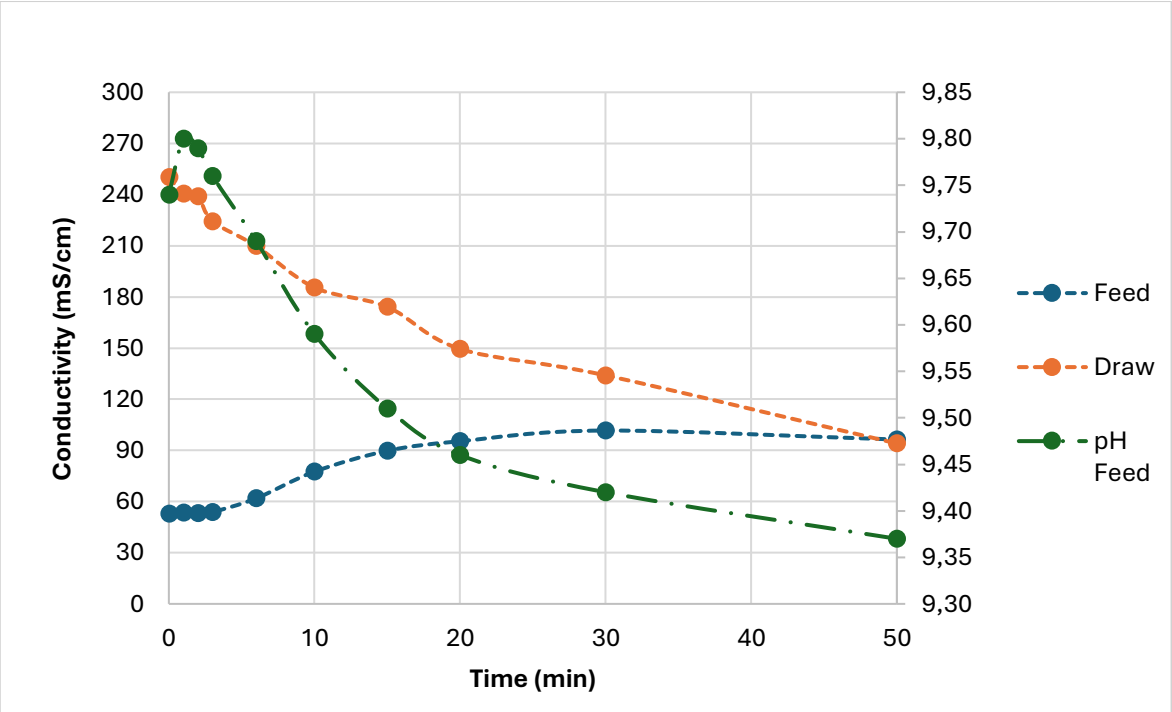

Figure 37: Conductivity of the OFMSW fermented liquid (feed), draw solution and pH of the feed over time.

Another important parameter was the pH of the feed solution, since higher VFA rejection in FO membranes has been observed for alkaline pH values. It was reported that the acetic acid was poorly rejected at acidic pH, which resulted in a passage to the draw solution, thus registering a loss of VFAs as well as a reduction in its concentration potential in the feed (Singh et al., 2019). In that case the rejection is mainly steric dependent where bigger molecules are better rejected. All tested VFAs have a pKa of around 4.8, so at acidic pH values promote the presence of the R-COOH form which could pass through the membrane. For this reason, the basic pH (pH = 9.0) given by the addition of NaOH in the previous stage of TAN recovery contributed to maintain the pH value in alkaline values, thus reaching a high VFAs concentration. Therefore, the rejection is enhanced by electrostatic repulsion with negatively charged FO membrane surface.

VFAs were spiked to feed sample during the concentration and retention has been verified at the beginning and the end of each batch. During the FO process a high-water transfer was observed, with the consequent VFAs concentration up to ~50%. No VFAs were found in the draw solution (below detection limit) demonstrating that the loss of VFAs in the feed solution was not due to a lack of membrane selectivity. The loss of VFAs in the feed, in the range of 5-10%, could only be explained by biodegradation or by a development of biofilm on the membrane.

Further work is required to fully understand the mechanisms in particularly incomplete flux recovery, VFAs rejection, fouling layer and long-term/full scale operation. Deployment of this technology confirms that VFAs concentration by FO could represent a feasible solution, even with real wastewater. Analysis of the draw solution (TOC, metals, cations and anions; *data is not available*) reveal the purity of this stream and the potentiality to produce reuse water during the regeneration of the draw solution.

4.5 Chain elongation (CE) bioprocess

The CE bioprocess results have been evaluated for the fed-batch experiments carried out with OFMSW fermented liquid. All tests performed provided information in terms of reaction kinetics, VFAs and MCFAs productions. The Fig. 38, Fig. 39 and Fig. 40 show the trends for acetic, butyric and caproic acids over time, in the tests performed with ethanol concentration of 100, 250 and 500 gCOD/L respectively.

In Fig. 38 (test T1 and T1') the initial AcOH value was 2.30 gCOD/L; to achieve 1:2 acetic:ethanol molar ratio, 25 mL of ethanol in concertation 100 gCOD/L was added in each of the two replicates. It was decided to set the flow rate supplied by the pumps to achieve a molar ratio of 1:10 in 25 days for the first test and 15 days (the lowest HRT reported in the literature) for the second test.

For each test, an initial increase in acetic acid was observed, followed by a decrease and concomitant increase in the production of caproic acid in day 4, reaching the maximum of 2.18 gCOD/L for T1 and 2.34 gCOD/L for T1'. This was probably due to the occurrence of the first cycle of reverse β-oxidation, which led to the acetic acid elongation to butyric and caproic acid.

After 5 days from the start, and a second increase in acetic acid, all the VFAs started to decline in concentration. The second rise of acetic acids could be simply related to the acidogenic fermentation pathways, which were dominating compared to the reverse β-oxidation reactions. The reasons of this behaviour could be related by the high-fermentation activity of the mixed consortium, which preferred to utilize the higher molecular weight substances for its metabolism rather than the synthesis of MCFA. Consequently, the caproic acid concentration decrease until a stable value of 0.90-0.75 gCOD/L until the end of the test, suggesting that the two investigated conditions were not adequate to stimulate a robust CE process, independently from the reaction time.

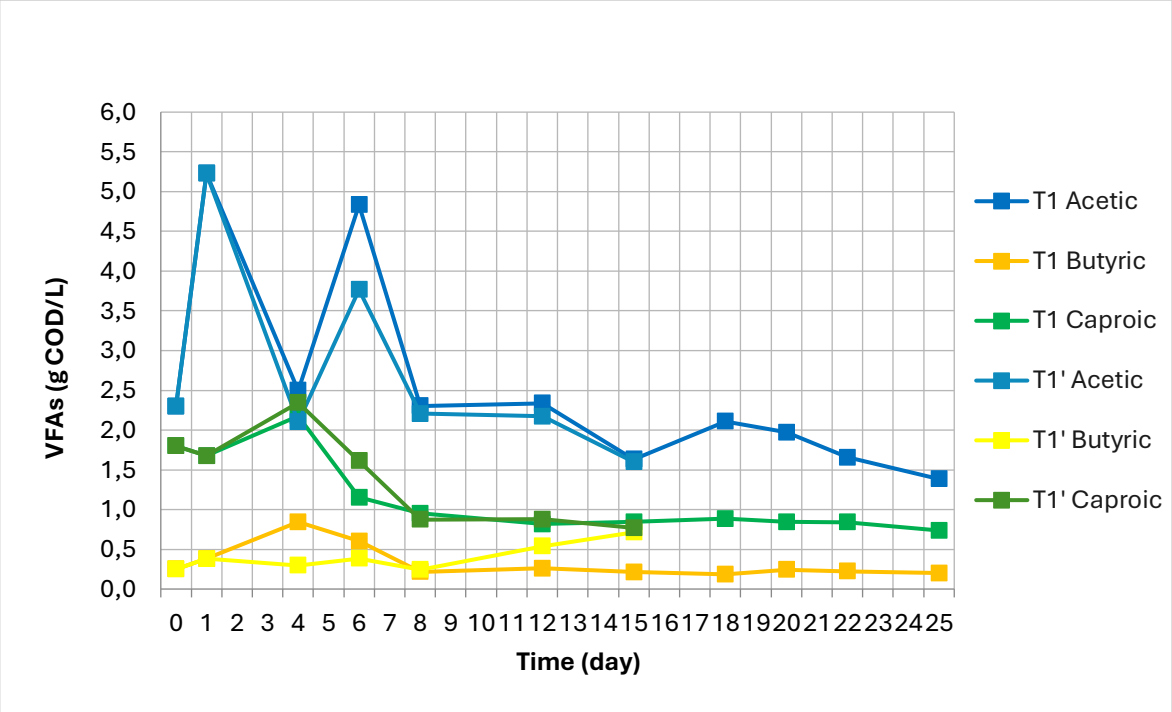

Figure 38: Tests performed showing trends for acetic, butyric and caproic acids (gCOD/L) over time (day) with acetic:ethanol molar ratio 1:2 using ethanol concentration of 100 gCOD/L.

In Fig. 39 (test T2 and T2') the initial AcOH value was 8.91 gCOD/L and to achieve 1:2 acetic:ethanol molar ratio, 46 mL of ethanol in concertation 250 gCOD/L was added in each of the two replicates. In these two tests, it has been decided to set the ethanol flow rate to achieve a molar ratio of 1:10 in 20 and 11 days respectively, decreasing the reaction time compared to the previous tests.

However, the general trend observed in these trials were similar to those observed in previous tests: the sudden initial increase of acetic acid was followed by a decrease in day 4. After 5 days from the start, a significant second acetic acid increase was observed, followed by a general VFAs reduction in concentration. In this case, there was not the reverse β-oxidation cycle since the trend of caproic acid was constantly decreasing.

The second rise of acetic acids concentrations could be connected to the unfair cain elongation reaction equilibrium or with the presence of conditions, microorganisms or factors that promoted the traditional pathways of the acidogenic fermentation process (as previously seen).

The trend of caproic acid concentration decrease until a stable value of 3.10-1.25 gCOD/L, until the end of the tests, considerably lower than the initial concentration at the start of the tests. According to this observation, it can be stated that also these conditions of the fed-batch system were not appropriate for the CE process, but they represented only the natural continuation of the fermentation bioprocesses.

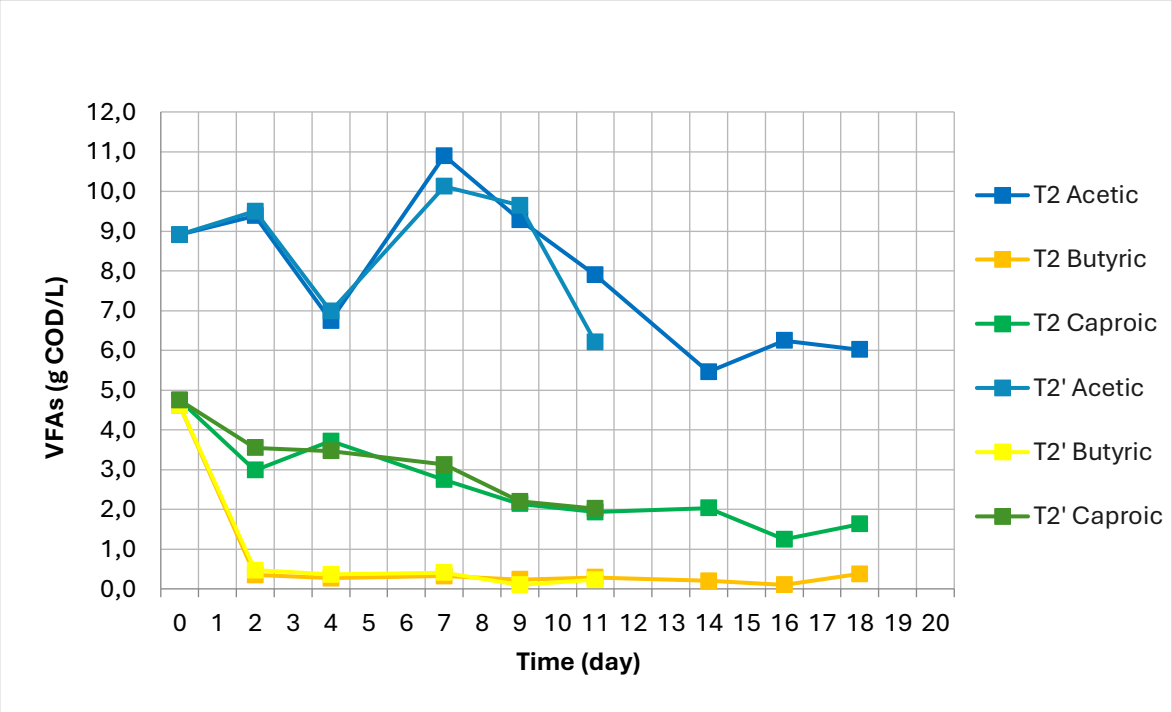

Figure 39: Tests performed showing trends for acetic, butyric and caproic acids (gCOD/L) over time (day) with acetic:ethanol molar ratio 1:2 using ethanol concentration of 250 gCOD/L.

Frome the previous results appear that the initial amount of ethanol was an important factor in the first cycle of the chain elongation reaction; hence, it was decided to make a different initial addition, to check its overall impact in the yield and composition of VFAs.

In Fig. 40 (test T3 and T3') the initial AcOH value was 10.98 gCOD/L. In the test T3 to achieve 1:2 acetic:ethanol molar ratio, 57 mL of ethanol in concertation 500 gCOD/L was added. In the test T3' to achieve 1:4 acetic:ethanol molar ratio, 114 mL of ethanol in concertation 500 gCOD/L was added. For both tests, it was decided to set the pumps' flow rate to achieve a molar ratio of 1:10 in 11 days. In test T3, an immediate initial increase in acetic acid was observed, followed by a slight decrease and concomitant high increase in butyric acid production, in day 4, reaching the maximum of 20.00 gCOD/L (overcoming acetic). In T3' test, in day 4, butyric acid reached the maximum of 17.26 gCOD/L. Similarly, there was an increase in the production of caproic acid, which reached its maximum of 12.07 gCOD/L for T3 and 10.54 gCOD/L for T3'. These values proved the instauration of the first and second cycle of reverse β-oxidation which resulted in acetic acid CE to butyric acid, and butyric acid CE to caproic acid. Most probably, these cycles occurred simultaneously. It was no doubts that the high concentration of ethanol as electron-donor led to the CE reaction by promoting reverse β-oxidation reaction as the main pathway, at the expense of other competing pathways.

All the VFAs started to decline in concentration after 5 days from the beginning of the tests. After its peak, the caproic acid concentration decreased to a stable value of 4.40-3.75 gCOD/L until the end of the test. The initial inclusion of more ethanol for a higher initial acetic:ethanol molar ratio did not greatly affect the kinetics. This factor, however, must be studied for future purposes since a remarkable caproic acid concentration was reached, even though not steadily maintained.

The ethanol concentration adopted in these tests (T3 and T3') was the most suitable for the characteristic of the fed-batch system to boost CE reactions. The advantage given by fed-batch system with this ethanol concentration which increase in acetic, butyric and caproic acid in 4 days is appealing and demonstrates a series of simultaneous active chain elongation cycles.

The OFMSW fermented liquid seemed to be an ideal substrate for the reverse β-oxidation reaction, as it contained both acetic acid and ethanol in concentrations close to a good ratio of 1:5. Consequently, the butyric and caproic acids production started very fast (5^{th} days from the start). However, towards the end of the HRT, a gradual VFAs decrease was detected until a new stable condition at lower values was observed.

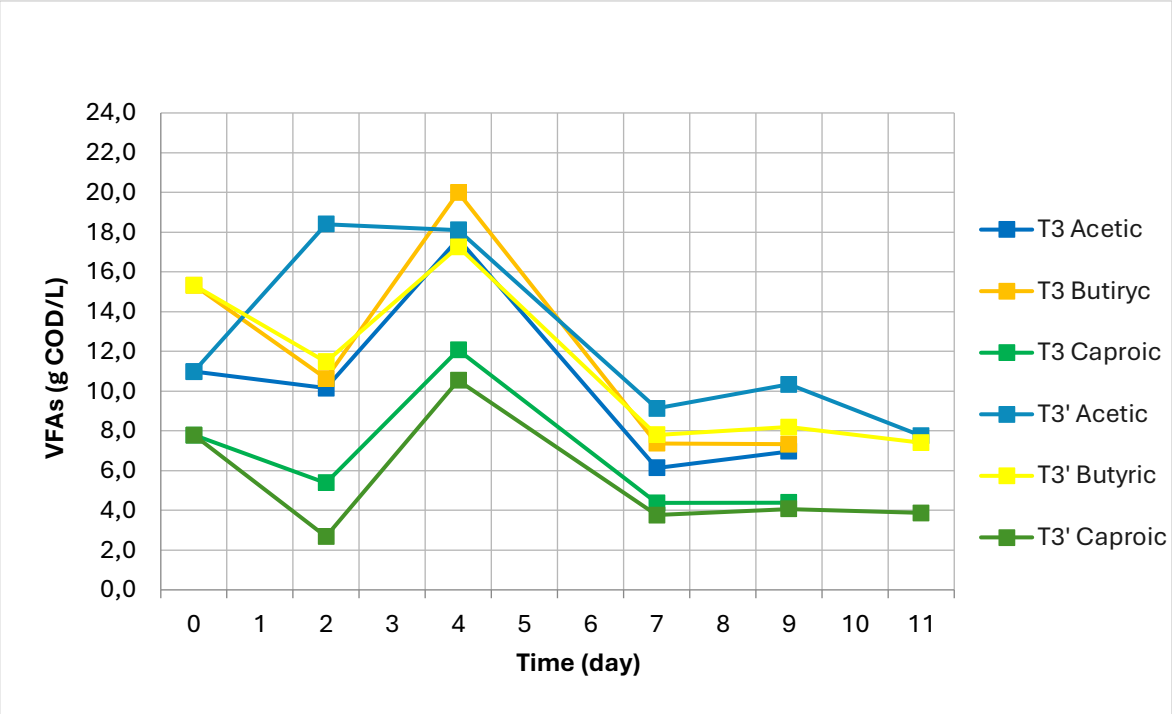

Figure 40: Tests performed showing trends for acetic, butyric and caproic acids (gCOD/L) over time (day) with acetic:ethanol molar ratio 1:2 and 1:4 using ethanol concentration of 500 gCOD/L.

4.5.1 Interpretation of CE processes

To understand how caproic acid production develops in a fed-batch system, it is necessary to follow the values by making them volume-independent and relating them to a theoretical trend affected by dilution. In the following figures, the measured initial concentration of caproic acid (in the fermented OFSMW liquid) was multiplied by the initial volume of 0.50 L. This value was considered the reference parameter affected only by the dilution (volume increase and diluted concentration). Hence, if the actual value of caproic acid follows this trend, it means that its production is equal to the consumption and there is only a decrease of concentration, due to the dilution factor. If the actual value of caproic acid is higher than the theoretical trend, it means that there is a production higher than the consumption, despite the effect of the dilution. If the actual value of caproic acid is lower the theoretical trend, it means that there is a consumption higher than the production, also contributed by the effect given by dilution.

In Fig. 41 the theoretical caproic (T1 and T1') values were calculate from the initial concentration of 1.80 gCOD/L. Initial additions, flow rate, daily ethanol additions and HRT are the same to the above. The theoretical value considers only dilution on production equal to consumption and have final

caproic acid concentration of 1.30 gCOD/L in the T1 and T1' tests, in 25 and 15 days respectively. The real values (R1 and R1') are the same as those previously reported.

It can be noted that on day 4 there is an increase in caproic acid production compared to the theoretical value (24% for R1 and 32% for R1'), reaching the maximum value in both tests.

After the 5th day, there is a decrease in the value until a stable concentration is reached. Although this value is lower than the theoretical value, the real caproic acid trend is slightly constant, an indication that production was still in progress.

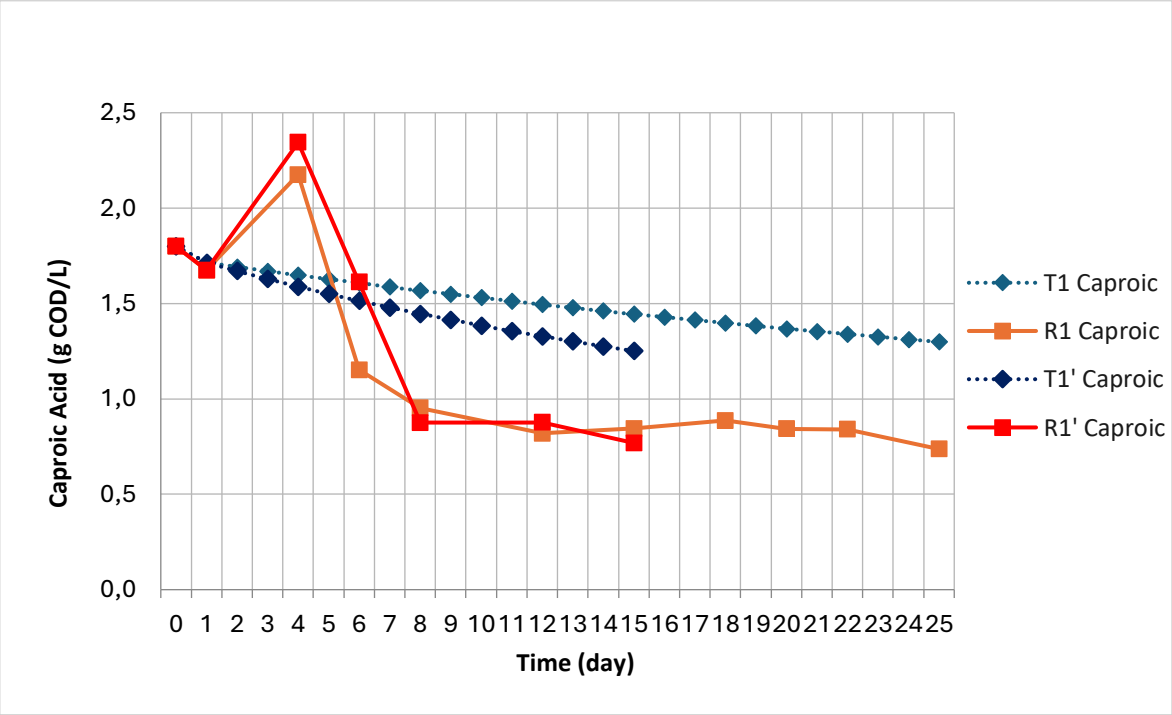

Figure 41: Theoretical value (T1 and T1') and real value (R1 and R1') of caproic acid production over time in fed-batch with initial ethanol of 100 gCOD/L.

In Fig. 42 the theoretical caproic (T2 and T2') values were calculate from the initial concentration of 4.75 gCOD/L. The theoretical value considers only dilution on production equal to consumption and have final caproic acid concentration of 3.15 gCOD/L in the T2 test in 15 days, and in the T2' test in 11 days. The real values (R1 and R1') are the same as those previously reported.

It can be noted that at no time there is more caproic acid production required to compensate its consumption. Around day 4 there is a slight increase, but the values in the two tests were still 10 % below the theoretical value for tests R2, and 12 % for tests R2'.

The quick decrease is an indication that production is completely absent and the caproic acid might have been used as carbon source for fermentative bacteria (in this case the microorganism privileged other metabolic pathways than chain elongation).

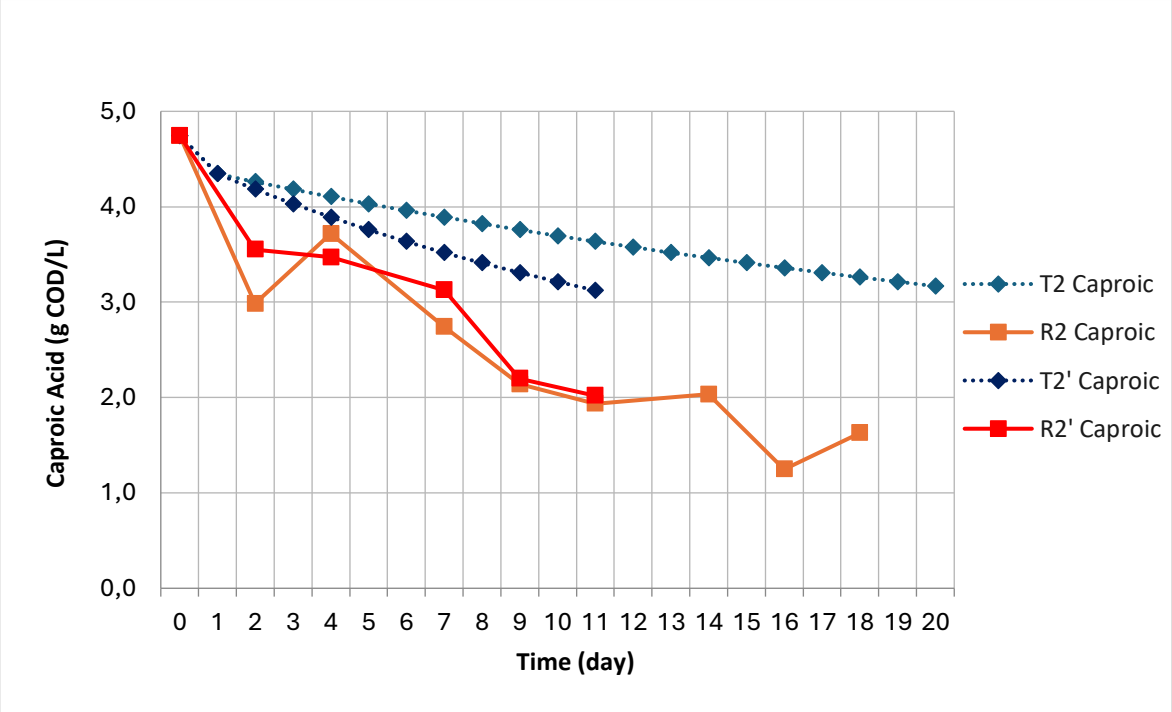

Figure 42: Theoretical value (T2 and T2') and real value (R2 and R2') of caproic acid production over time in fed-batch with initial ethanol of 250 gCOD/L.

In Fig. 43 the theoretical caproic (T3 and T3') values were calculate from the initial concentration of 7.80 gCOD/L. According to the previous considerations, the theoretical values are equal to 5.00 gCOD/L in T3 test and 4.70 gCOD/L in T3', both in 11 days. The real values (R3 and R3') are the same as those previously reported.

It can be noted that on day 4 there is an important increase in caproic acid production compared to the theoretical value (49% and 45% for test R3 and R3' respectively). These tests are the most promising as they achieve higher caproic values with a CE-related increase in a short period of time. Also, a stable caproic acid value was maintained, where production is equal to consumption with a decrease in concentration related only to dilution.

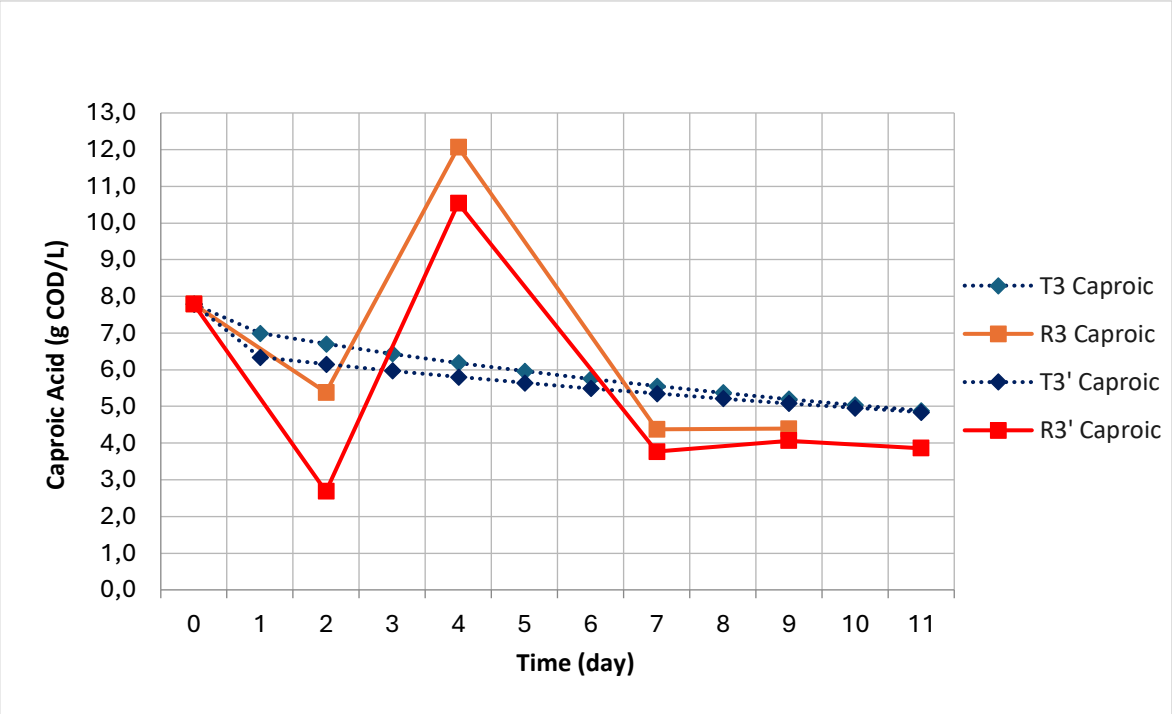

Figure 43: Theoretical value (T3 and T3') and real value (R3 and R3') of caproic acid production over time in fed-batch with initial ethanol of 500 gCOD/L.

The results obtained were considered optimal in light of a possible emerging issue of inhibition of the CE by the Excessive Ethanol Oxidation (EEO). The acetic acetic:ethanol molar ratio higher than 1:10 led to the instauration of the EEO, which can reduce the amount of acetyl-CoA available for VFAs chain elongation, and the acetic acid derived from EEO led to the medium acidification, with the further inhibition of the system (Grootscholten et al., 2013). This result confirmed the importance to have a balanced ratio of the acid to be elongated and electron donor for the instauration of the reverse β-oxidation reactions.

To sum-up, the significant issue related to the fed-batch reactor is that despite a remarkable caproic acid production, the reactor did not accumulate any VFAs as they are redeployed in the biological system. With these results, it is possible to bypass this technical problem, linked to a production and consumption of substates, by achieving high caproic acid revenue in just a few days with the correct addition of ethanol (and low impact due to the dilution).

5. Conclusions

Obtaining added-value commercial products from different wastewater by an integrated process through ammonium nitrogen recovery with gas-permeable membrane and chain elongation bioprocesses was successfully performed.

The suitability and the excellent performance for TAN removal and $(NH_4)_2SO_4$ fertiliser recovery from effluent using a lab-scale gas-permeable membrane (GPM) and has been proven. Tests carried out revealed a correlation between the K_m values with the percentage of NH_3 in TAN, which is related to the acid-base equilibrium. For the treatment of OFMSW AD supernatant, OFMSW fermented liquid and ABPs wastewater using a GPM contactor at 35 °C, TAN recovery of 96.0%, 99.5%, 98.7%, 99.9%, 97.4%, 99.7% were reached controlling the pH in the feed tank. A pH control in the feed tank was considered suitable to diminish the reagent consumption per mass of TAN recovered and to minimise the membrane fouling threat, although higher K_m values could be achieved under more alkaline conditions. Volume ratio modification related to water transfer and the impact in the trapping solution concentration were controlled and a behavioural model was proposed. A high purity commercial quality of concentrated $(NH_4)_2SO_4$ in trapping solution was obtained.

FO membranes for VFAs concentration and clean water recovery was assessed. Draw $MgCl_2$ solution salinity proved to be a key parameter to get high permeation flux and minimized filtration time. Technology was optimised achieved high WCF when osmotic equilibrium was reached. Conductivity and pH have turned out to be important parameter for final concentration of VFAs and verify ssalinity contributes to reduce the achieved WCF.

CE bioprocess results have been evaluated for fed-batch experiments carried out with OFMSW fermented liquid. All tests performed provided information in terms of reaction kinetics, VFAs and MCFAs productions. An overall increase in trends for acetic, butyric and caproic acids over time has been observed at increasing ethanol concentrations from 100 to 250 and 500 gCOD/L. Key parameters turned out to be acetic:ethanol molar ratio and initial ethanol added. Was possible an HRT reduction and pH control. While in the first tests (100 gCOD/L) the VFAs rise could be simply related to the acidogenic fermentation pathways, in the last test (500 gCOD/L) VFAs values proved the instauration of the first and second cycle of reverse β-oxidation which resulted in acetic acid CE to butyric acid, and butyric acid CE to caproic acid. Most probably, these cycles occurred simultaneously. It was no doubts that the high concentration of ethanol as electron-donor led to the CE reaction by promoting reverse β-oxidation reaction as the main pathway, at the expense of other

competing pathways. Caproic acid production in fed-batch system was investigated. Can be noted that on day 4 there is an increase in caproic acid production compared to the theoretical value, reaching the maximum value tests. After the 5^{th} day, there is a decrease in the value until a stable concentration is reached. Although this value is lower than the theoretical value, the real caproic acid trend is slightly constant, an indication that production was still in progress.

In this thesis obtaining high-value product was studied due to development of an integrated process for added-value commercial by TAN removal in the GMP process and $(NH_4)_2SO_4$ fertiliser recovery, concentrate rich VFAs liquid by the FO membrane and water-$MgCl_2$ fertiliser recovery, produce high-value MCFAs fatty acids, particularly caproic acid, through CE in fed-batch bioprocess.

Reference

A Gehring, T., A Cavalcante, W., S Colares, A., Angenent, L. T., T Santaella, S., Lübken, M., & C Leitão, R. (2020). Optimal pH set point for simultaneous production and pertraction of n-caproic acid: an experimental and simulation study. *Journal of Chemical Technology and Biotechnology*, *95*(12), 3105–3116. https://doi.org/10.1002/jctb.6486

A. K, P., M, M., Rajamanickam, S., Sivarethinamohan, S., Gaddam, M. K. R., Velusamy, P., R, G., Ravindiran, G., Gurugubelli, T. R., & Muniasamy, S. K. (2023). Impact of climate change and anthropogenic activities on aquatic ecosystem – A review. In *Environmental Research* (Vol. 238). Academic Press Inc. https://doi.org/10.1016/j.envres.2023.117233

ABPs Regulation EU Parliament. (2009). *THE EUROPEAN PARLIAMENT AND THE COUNCIL laying down health rules as regards animal by-products and derived products not intended for human consumption and repealing Regulation (EC) No 1774/2002 (Animal by-products Regulation)*.

Aguilar-Pozo, V. B., Chimenos, J. M., Elduayen-Echave, B., Olaciregui-Arizmendi, K., López, A., Gómez, J., Guembe, M., García, I., Ayesa, E., & Astals, S. (2023). Struvite precipitation in wastewater treatment plants anaerobic digestion supernatants using a magnesium oxide by-product. *Science of the Total Environment*, *890*. https://doi.org/10.1016/j.scitotenv.2023.164084

Al-Juboori, R. A., Al-Shaeli, M., Aani, S. Al, Johnson, D., & Hilal, N. (2023). Membrane Technologies for Nitrogen Recovery from Waste Streams: Scientometrics and Technical Analysis. In *Membranes* (Vol. 13, Issue 1). MDPI. https://doi.org/10.3390/membranes13010015

APHA Standard Methods. (2017). *Preparation of Common Types of Desk Reagents Specified in Standard Methods*. https://doi.org/10.2105/SMWW.2882.216

Astals, S., Martínez-Martorell, M., Huete-Hernández, S., Aguilar-Pozo, V. B., Dosta, J., & Chimenos, J. M. (2021). Nitrogen recovery from pig slurry by struvite precipitation using a low-cost magnesium oxide. *Science of the Total Environment*, *768*. https://doi.org/10.1016/j.scitotenv.2020.144284

Bartels, J. R. (2008). *A feasibility study of implementing an Ammonia Economy*.

Battista, F., Zeni, A., Andreolli, M., Salvetti, E., Rizzioli, F., Lampis, S., & Bolzonella, D. (2024). Treatment of food processing wastes for the production of medium chain fatty acids via chain elongation. *Environmental Technology and Innovation*, *33*. https://doi.org/10.1016/j.eti.2023.103453

Beckinghausen, A., Odlare, M., Thorin, E., & Schwede, S. (2020). From removal to recovery: An evaluation of nitrogen recovery techniques from wastewater. In *Applied Energy* (Vol. 263). Elsevier Ltd. https://doi.org/10.1016/j.apenergy.2020.114616

Bertasini, D., Battista, F., Rizzioli, F., Frison, N., & Bolzonella, D. (2023). Decarbonization of the European natural gas grid using hydrogen and methane biologically produced from organic waste: A critical overview. *Renewable Energy*, *206*, 386–396. https://doi.org/10.1016/j.renene.2023.02.029

Blandin, G., Ferrari, F., Lesage, G., Le-Clech, P., Héran, M., & Martinez-Lladó, X. (2020). Forward osmosis as concentration process: Review of opportunities and challenges. In *Membranes* (Vol. 10, Issue 10, pp. 1–40). MDPI AG. https://doi.org/10.3390/membranes10100284

Blandin, G., Rosselló, B., Monsalvo, V. M., Batlle-Vilanova, P., Viñas, J. M., Rogalla, F., & Comas, J. (2019). Volatile fatty acids concentration in real wastewater by forward osmosis. *Journal of Membrane Science*, *575*, 60–70. https://doi.org/10.1016/j.memsci.2019.01.006

Candry, P., Radić, L., Favere, J., Carvajal-Arroyo, J. M., Rabaey, K., & Ganigué, R. (2020). Mildly acidic pH selects for chain elongation to caproic acid over alternative pathways during lactic acid fermentation. *Water Research*, *186*. https://doi.org/10.1016/j.watres.2020.116396

Chen, C., Dai, Z., Li, Y., Zeng, Q., Yu, Y., Wang, X., Zhang, C., & Han, L. (2023). Fouling-free membrane stripping for ammonia recovery from real biogas slurry. *Water Research*, *229*. https://doi.org/10.1016/j.watres.2022.119453

Coma, M., Vilchez-Vargas, R., Roume, H., Jauregui, R., Pieper, D. H., & Rabaey, K. (2016). Product Diversity Linked to Substrate Usage in Chain Elongation by Mixed-Culture Fermentation. *Environmental Science and Technology*, *50*(12), 6467–6476. https://doi.org/10.1021/acs.est.5b06021

Darestani, M., Haigh, V., Couperthwaite, S. J., Millar, G. J., & Nghiem, L. D. (2017). Hollow fibre membrane contactors for ammonia recovery: Current status and future developments. In *Journal of Environmental Chemical Engineering* (Vol. 5, Issue 2, pp. 1349–1359). Elsevier Ltd. https://doi.org/10.1016/j.jece.2017.02.016

Dutta, A., Kalam, S., & Lee, J. (2022). Elucidating the inherent fouling tolerance of membrane contactors for ammonia recovery from wastewater. *Journal of Membrane Science*, *645*. https://doi.org/10.1016/j.memsci.2021.120197

Ferby, M., & He, Z. (2024). Recovery of both volatile fatty acids and ammonium from simulated wastewater: Performance of membrane contactor and understanding the effects of osmotic distillation. *Journal of Environmental Chemical Engineering*, *12*(5). https://doi.org/10.1016/j.jece.2024.113760

Fernández-Domínguez, D., Astals, S., Peces, M., Frison, N., Bolzonella, D., Mata-Alvarez, J., & Dosta, J. (2020). Volatile fatty acids production from biowaste at mechanical-biological treatment plants: Focusing on fermentation temperature. *Bioresource Technology*, *314*. https://doi.org/10.1016/j.biortech.2020.123729

Fernando-Foncillas, C., & Varrone, C. (2021). Effect of reactor operating conditions on carboxylate production and chain elongation from co-fermented sludge and food waste. *Journal of Cleaner Production*, *292*. https://doi.org/10.1016/j.jclepro.2021.126009

Garcia-González, M. C., & Vanotti, M. B. (2015). Recovery of ammonia from swine manure using gas-permeable membranes: Effect of waste strength and pH. *Waste Management*, *38*(1), 455–461. https://doi.org/10.1016/j.wasman.2015.01.021

Gottardo, M., Adele Tuci, G., Pavan, P., Dosta, J., & Valentino, F. (2024). Short and medium chain organic acids production from hydrolyzed food waste: technical–economic evaluation and insight into the product's quality. *Chemical Engineering Science*, *284*. https://doi.org/10.1016/j.ces.2023.119539

Gottardo, M., Dosta, J., Cavinato, C., Crognale, S., Tonanzi, B., Rossetti, S., Bolzonella, D., Pavan, P., & Valentino, F. (2023). Boosting butyrate and hydrogen production in acidogenic fermentation of food waste and sewage sludge mixture: a pilot scale demonstration. *Journal of Cleaner Production*, *404*. https://doi.org/10.1016/j.jclepro.2023.136919

Grootscholten, T. I. M., Steinbusch, K. J. J., Hamelers, H. V. M., & Buisman, C. J. N. (2013). Improving medium chain fatty acid productivity using chain elongation by reducing the hydraulic retention time in an upflow anaerobic filter. *Bioresource Technology*, *136*, 735–738. https://doi.org/10.1016/j.biortech.2013.02.114

He, L., Wang, Y., Zhou, T., & Zhao, Y. (2020). Enhanced ammonia resource recovery from wastewater using a novel flat sheet gas-permeable membrane. *Chemical Engineering Journal*, *400*. https://doi.org/10.1016/j.cej.2020.125338

IEA Emissions Factors. (2023). *IEA Emissions Factors*.

Kanchanamala Delanka-Pedige, H. M., Munasinghe-Arachchige, S. P., Abeysiriwardana-Arachchige, I. S. A., & Nirmalakhandan, N. (2021). Evaluating wastewater treatment infrastructure systems based on UN Sustainable Development Goals and targets. *Journal of Cleaner Production*, *298*. https://doi.org/10.1016/j.jclepro.2021.126795

Ladewig, B., & Al-Shaeli, M. N. Z. (2017). *Fundamentals of Membrane Processes* (pp. 13–37). https://doi.org/10.1007/978-981-10-2014-8_2

Lee, W. S., Chua, A. S. M., Yeoh, H. K., & Ngoh, G. C. (2014). A review of the production and applications of waste-derived volatile fatty acids. In *Chemical Engineering Journal* (Vol. 235, pp. 83–99). https://doi.org/10.1016/j.cej.2013.09.002

Licon Bernal, E. E., Maya, C., Valderrama, C., & Cortina, J. L. (2016). Valorization of ammonia concentrates from treated urban wastewater using liquid-liquid membrane contactors. *Chemical Engineering Journal*, *302*, 641–649. https://doi.org/10.1016/j.cej.2016.05.094

Lidén, G. (2002). Understanding the bioreactor. *Bioprocess and Biosystems Engineering*, *24*(5), 273–279. https://doi.org/10.1007/s004490100263

Liu, D., Wang, W., Liu, D., Gao, Z., & Wang, W. (2024). Bubble Turbulent Gas-Permeable Membrane for Ammonia Recovery from Swine Wastewater: Mass Transfer Enhancement and Antifouling Mechanisms. *Environmental Science and Technology*, *58*(13), 6019–6029. https://doi.org/10.1021/acs.est.3c07903

Micolucci, F., Gottardo, M., Bolzonella, D., Pavan, P., Majone, M., & Valentino, F. (2020). Pilot-scale multi-purposes approach for volatile fatty acid production, hydrogen and methane from an automatic controlled anaerobic process. *Journal of Cleaner Production*, *277*. https://doi.org/10.1016/j.jclepro.2020.124297

Morrow, C. P., Furtaw, N. M., Murphy, J. R., Achilli, A., Marchand, E. A., Hiibel, S. R., & Childress, A. E. (2018). Integrating an aerobic/anoxic osmotic membrane bioreactor with membrane distillation for potable reuse. *Desalination*, *432*, 46–54. https://doi.org/10.1016/j.desal.2017.12.047

Narisetty, V., Reshmy, R., Maitra, S., Tarafdar, A., Alphy, M. P., Kumar, A. N., Madhavan, A., Sirohi, R., Awasthi, M. K., Sindhu, R., Varjani, S., & Binod, P. (2023). Waste-Derived Fuels and Renewable Chemicals for Bioeconomy Promotion: A Sustainable Approach. *Bioenergy Research*, *16*(1), 16–32. https://doi.org/10.1007/s12155-022-10428-y

Noriega-Hevia, G., Serralta, J., Seco, A., & Ferrer, J. (2023). A pH-based control system for nitrogen recovery using hollow fibre membrane contactors. *Journal of Environmental Chemical Engineering*, *11*(5). https://doi.org/10.1016/j.jece.2023.110519

Peña-Picola, S., Serra-Toro, A., Da Silva, C., Peces, M., Jordán, M., Vila, J., Grifoll, M., Valentino, F., Astals, S., & Dosta, J. (2024). Acidogenic fermentation of biowaste coupled with nitrogen recovery using selective membranes to produce a VFA-rich liquid with a high C/N ratio. *Journal of Environmental Chemical Engineering*, *12*(2). https://doi.org/10.1016/j.jece.2024.112352

Perdigão-Lima, T., Diaz De Tuesta, J. L., Feliciano, M., Furst, L. C., Roman, F. F., Silva, A. S., Pereira Wilken, A. A., Silva, A. M. T., & Gomes, H. T. (2024). Removal of gaseous ammonia released from leachate by adsorption on carbon-based adsorbents prepared from agro-industrial wastes. *Global Nest Journal*, *26*(4). https://doi.org/10.30955/gnj.004862

Piadeh, F., Offie, I., Behzadian, K., Rizzuto, J. P., Bywater, A., Córdoba-Pachón, J. R., & Walker, M. (2024). A critical review for the impact of anaerobic digestion on the sustainable development goals. In *Journal of Environmental Management* (Vol. 349). Academic Press. https://doi.org/10.1016/j.jenvman.2023.119458

Quintela, C., Peshkepia, E., Grimalt-Alemany, A., Nygård, Y., Olsson, L., Skiadas, I. V., & Gavala, H. N. (2024). Excessive Ethanol Oxidation Versus Efficient Chain Elongation Processes. *Waste and Biomass Valorization*, *15*(4), 2545–2558. https://doi.org/10.1007/s12649-023-02323-0

Ramos-Suarez, M., Zhang, Y., & Outram, V. (2021). Current perspectives on acidogenic fermentation to produce volatile fatty acids from waste. In *Reviews in Environmental Science and Biotechnology* (Vol. 20, Issue 2, pp. 439–478). Springer Science and Business Media B.V. https://doi.org/10.1007/s11157-021-09566-0

Rci. (2022). *Renewable Carbon as a Guiding Principle for Sustainable Carbon Cycles*. www.renewable-carbon-initiative.com

Ren, W., He, P., Zhang, H., & Lü, F. (2024). Temperature is an underestimated parameter to regulate the start-up of enhanced carbon chain elongation. *Renewable Energy*, *234*. https://doi.org/10.1016/j.renene.2024.121221

Research and Markets. (2023). *Caproic Acid - Global Strategic Business Report- Product Image Caproic Acid - Global Strategic Business Report*.

Rezaei, M., Warsinger, D. M., Lienhard V, J. H., Duke, M. C., Matsuura, T., & Samhaber, W. M. (2018). Wetting phenomena in membrane distillation: Mechanisms, reversal, and prevention. In *Water Research* (Vol. 139, pp. 329–352). Elsevier Ltd. https://doi.org/10.1016/j.watres.2018.03.058

Riaño, B., Molinuevo-Salces, B., Vanotti, M. B., & García-González, M. C. (2021). Ammonia recovery from digestate using gas-permeable membranes: A pilot-scale study. *Environments - MDPI*, *8*(12). https://doi.org/10.3390/environments8120133

Rizzioli, F., Bertasini, D., Bolzonella, D., Frison, N., & Battista, F. (2023). A critical review on the techno-economic feasibility of nutrients recovery from anaerobic digestate in the agricultural sector. In *Separation and Purification Technology* (Vol. 306). Elsevier B.V. https://doi.org/10.1016/j.seppur.2022.122690

Roghair, M., Liu, Y., Strik, D. P. B. T. B., Weusthuis, R. A., Bruins, M. E., & Buisman, C. J. N. (2018). Development of an effective chain elongation process from acidified food waste and ethanol into n-Caproate. *Frontiers in Bioengineering and Biotechnology*, *6*(APR). https://doi.org/10.3389/fbioe.2018.00050

Ronan, E., Aqeel, H., Wolfaardt, G. M., & Liss, S. N. (2021). Recent advancements in the biological treatment of high strength ammonia wastewater. In *World Journal of Microbiology and Biotechnology* (Vol. 37, Issue 9). Springer Science and Business Media B.V. https://doi.org/10.1007/s11274-021-03124-0

Rongwong, W., & Sairiam, S. (2020). A modeling study on the effects of pH and partial wetting on the removal of ammonia nitrogen from wastewater by membrane contactors. *Journal of Environmental Chemical Engineering*, *8*(5). https://doi.org/10.1016/j.jece.2020.104240

San-Valero, P., Abubackar, H. N., Veiga, M. C., & Kennes, C. (2020). Effect of pH, yeast extract and inorganic carbon on chain elongation for hexanoic acid production. *Bioresource Technology*, *300*. https://doi.org/10.1016/j.biortech.2019.122659

Serra-Toro, A., Abboud, Y. B. H., Cardete-Garcia, M. A., Astals, S., Valentino, F., Mas, F., & Dosta, J. (2024). Ammoniacal nitrogen recovery from swine slurry using a gas-permeable membrane: pH control strategies and feed-to-trapping volume ratio. *Environmental Science and Pollution Research*. https://doi.org/10.1007/s11356-024-32193-5

Serra-Toro, A., Astals, S., Madurga, S., Mata-Álvarez, J., Mas, F., & Dosta, J. (2022). Ammoniacal nitrogen recovery from pig slurry using a novel hydrophobic/hydrophilic selective membrane. *Journal of Environmental Chemical Engineering*, *10*(5). https://doi.org/10.1016/j.jece.2022.108434

Serra-Toro, A., Vinardell, S., Astals, S., Madurga, S., Llorens, J., Mata-Álvarez, J., Mas, F., & Dosta, J. (2022). Ammonia recovery from acidogenic fermentation effluents using a gas-permeable membrane contactor. *Bioresource Technology*, *356*. https://doi.org/10.1016/j.biortech.2022.127273

She, Q., Wang, R., Fane, A. G., & Tang, C. Y. (2016). Membrane fouling in osmotically driven membrane processes: A review. In *Journal of Membrane Science* (Vol. 499, pp. 201–233). Elsevier. https://doi.org/10.1016/j.memsci.2015.10.040

Sheikh, M., Lopez, J., Reig, M., Vecino, X., Rezakazemi, M., Valderrama, C. A., & Cortina, J. L. (2023). Ammonia recovery from municipal wastewater using hybrid NaOH closed-loop membrane contactor and ion exchange system. *Chemical Engineering Journal*, *465*. https://doi.org/10.1016/j.cej.2023.142859

Shrestha, R. K., Strahm, B. D., & Sucre, E. B. (2015). Greenhouse gas emissions in response to nitrogen fertilization in managed forest ecosystems. In *New Forests* (Vol. 46, Issue 2, pp. 167–193). Kluwer Academic Publishers. https://doi.org/10.1007/s11056-014-9454-4

Singh, N., Dhiman, S., Basu, S., Balakrishnan, M., Petrinic, I., & Helix-Nielsen, C. (2019). Dewatering of sewage for nutrients and water recovery by Forward Osmosis (FO)using divalent draw solution. *Journal of Water Process Engineering*, *31*. https://doi.org/10.1016/j.jwpe.2019.100853

Spirito, C. M., Marzilli, A. M., & Angenent, L. T. (2018). Higher Substrate Ratios of Ethanol to Acetate Steered Chain Elongation toward n-Caprylate in a Bioreactor with Product Extraction. *Environmental Science and Technology*, *52*(22), 13438–13447. https://doi.org/10.1021/acs.est.8b03856

Sürmeli, R. Ö., Bayrakdar, A., & Çalli, B. (2018). Ammonia recovery from chicken manure digestate using polydimethylsiloxane membrane contactor. *Journal of Cleaner Production*, *191*, 99–104. https://doi.org/10.1016/j.jclepro.2018.04.138

Tarasava, K., Lee, S. H., Chen, J., Köpke, M., Jewett, M. C., & Gonzalez, R. (2022). Reverse β-oxidation pathways for efficient chemical production. In *Journal of Industrial Microbiology and Biotechnology* (Vol. 49, Issue 2). Oxford University Press. https://doi.org/10.1093/jimb/kuac003

UN 2030 Agenda. (2015). *TRANSFORMING OUR WORLD: THE 2030 AGENDA FOR SUSTAINABLE DEVELOPMENT UNITED NATIONS UNITED NATIONS TRANSFORMING OUR WORLD: THE 2030 AGENDA FOR SUSTAINABLE DEVELOPMENT*.

Valentino, F., Munarin, G., Biasiolo, M., Cavinato, C., Bolzonella, D., & Pavan, P. (2021). Enhancing volatile fatty acids (VFA) production from food waste in a two-phases pilot-scale anaerobic digestion process. *Journal of Environmental Chemical Engineering*, *9*(5). https://doi.org/10.1016/j.jece.2021.106062

Vecino, X., Reig, M., Bhushan, B., Gibert, O., Valderrama, C., & Cortina, J. L. (2019). Liquid fertilizer production by ammonia recovery from treated ammonia-rich regenerated streams using liquid-liquid membrane contactors. *Chemical Engineering Journal*, *360*, 890–899. https://doi.org/10.1016/j.cej.2018.12.004

Vom Berg, C., Carus, M., Stratmann, M., & Dammer, L. (2022). *Renewable Carbon as a Guiding Principle for Sustainable Carbon Cycles*. www.renewable-carbon-initiative.com

Wang, J., & Yin, Y. (2022). Biological production of medium-chain carboxylates through chain elongation: An overview. In *Biotechnology Advances* (Vol. 55). Elsevier Inc. https://doi.org/10.1016/j.biotechadv.2021.107882

Wang, Z., Ma, J., Tang, C. Y., Kimura, K., Wang, Q., & Han, X. (2014). Membrane cleaning in membrane bioreactors: A review. In *Journal of Membrane Science* (Vol. 468, pp. 276–307). Elsevier. https://doi.org/10.1016/j.memsci.2014.05.060

Wei, Y., Ren, B., Zheng, S., Feng, X., He, Y., Zhu, X., Zhou, L., & Li, D. (2021). Effect of high concentration of ammonium on production of n-caproate: Recovery of a high-value biochemical from food waste via lactate-driven chain elongation. *Waste Management*, *128*, 25–35. https://doi.org/10.1016/j.wasman.2021.04.015

Wu, Q., Jiang, Y., Chen, Y., Liu, M., Bao, X., & Guo, W. (2021). Opportunities and challenges in microbial medium chain fatty acids production from waste biomass. In *Bioresource Technology* (Vol. 340). Elsevier Ltd. https://doi.org/10.1016/j.biortech.2021.125633

Xiang, S., Liu, Y., Zhang, G., Ruan, R., Wang, Y., Wu, X., Zheng, H., Zhang, Q., & Cao, L. (2020). New progress of ammonia recovery during ammonia nitrogen removal from various wastewaters. In *World Journal of Microbiology and Biotechnology* (Vol. 36, Issue 10). Springer. https://doi.org/10.1007/s11274-020-02921-3

Yao, M., Tijing, L. D., Naidu, G., Kim, S. H., Matsuyama, H., Fane, A. G., & Shon, H. K. (2020). A review of membrane wettability for the treatment of saline water deploying membrane

distillation. In *Desalination* (Vol. 479). Elsevier B.V. https://doi.org/10.1016/j.desal.2020.114312

Ye, B., Liang, T., Nong, Z., Qin, C., Lin, S., Lin, W., Liu, H., & Li, H. (2021). Simultaneous desalination and ammonia recovery using microbial electrolysis desalination and chemical-production cell: A feasibility study of alkaline soil washing wastewater. *Desalination*, *520*. https://doi.org/10.1016/j.desal.2021.115372

Zarebska, A., Nieto, D. R., Christensen, K. V., & Norddahl, B. (2014). Ammonia recovery from agricultural wastes by membrane distillation: Fouling characterization and mechanism. *Water Research*, *56*, 1–10. https://doi.org/10.1016/j.watres.2014.02.037

Zhang, X., & Liu, Y. (2021). Circular economy-driven ammonium recovery from municipal wastewater: State of the art, challenges and solutions forward. In *Bioresource Technology* (Vol. 334). Elsevier Ltd. https://doi.org/10.1016/j.biortech.2021.125231

Zhang, Y., Bai, J., & Zuo, J. (2022). Production of medium chain fatty acids through co-fermentation of food waste and sewage sludge without external electron donors. *Journal of Environmental Chemical Engineering*, *10*(6). https://doi.org/10.1016/j.jece.2022.108688

Ringraziamenti

Desidero vivamente ringraziare il Prof. Francesco Valentino, supervisore di questa tesi, per avermi trasmesso la passione della ricerca in questo meraviglioso ambito delle Scienze Ambientali e per essere sempre stato d'aiuto e appoggio in ogni momento, per il tirocinio e per questo lavoro di tesi.

Ringrazio il Prof. Joan Dosta, correlatore di questa tesi, per avermi accolto con orgoglio nel suo gruppo di ricerca e per avermi trasmesso la sua conoscenza con chiarezza e interesse, coltivando tra noi un vero rapporto professionale e personale.

Ringrazio il Prof. Marco Gottardo, correlatore di questa tesi, per avermi assistito nel periodo di permanenza in laboratorio, donando il suo tempo per aiutarmi con la sua esperienza e professionalità in qualsiasi aspetto teorico e pratico.

Desidero poi ringraziare il Dott. Andreu Serra-Toro per avermi aiutato nel tirocinio e di aver dato vita ad un importante rapporto di amicizia facendomi appassionare una città ed un'altra cultura che non dimenticherò mai.

Desidero ringraziare con tutto il cuore le persone a me più care, quali la mia Famiglia in particolare i miei genitori Andrea e Roberta e mio fratello Valerio, che con la loro gioia mi hanno incoraggiato in ogni singolo istante e per essermi stati vicini in ogni momento.

Ringrazio i miei amici, tra tutti Francesco, Lorenzo, Matteo, Marco e Margherita, che sono sempre stati al mio fianco e hanno condiviso come me momenti importanti ed emozioni.

Ringrazio i miei amici Alba, Braulio, Fabrizio e Tomás con i quali ho instaurato un bellissimo rapporto di amicizia che è andato aldilà del tirocinio.

Ultimi, ma sicuramente non meno importanti, saluto i tanti amici conosciuti durate il mio stage all'estero e le mie compagne di corso, che hanno fatto parte di questi anni indimenticabili.

Sono veramente grato di aver vissuto un'esperienza incredibile che mi ha fatto appassionare e mi ha dato la possibilità di esprimermi e fare un percorso di crescita che porterò con me per tutta la mia vita.

Voglio inoltre ricordare i miei nonni, i miei angeli custodi che, hanno sempre vegliato su di me in questo lungo percorso e dedicare questa tesi a mia nonna che, con la sua dolcezza, è la luce della mia strada.

- Vittorio -